Doctoral Dissertation

In silico and *in vitro* investigations on the molecular mechanism of steroid hormone response of elephant shark, *Callorhinchus milii*, progesterone receptor

(*In silico* 及び *in vitro* 解析を用いたゾウギンザメの

プロゲステロン受容体のホルモン応答性の分子基盤解明)

林　暁智（Xiaozhi LIN）

Graduate School of Life Science

Hokkaido University

March, 2022

CONTENTS

Abbreviations

17,20-DP, 17α,20β-dihydroxy-4-pregnen-3-one

17OH-P4, 17α-hydroxyprogesterone

17OH-Preg, 17α-hydroxy-pregnenolone

19nor-DOC, 19nor-deoxycorticosterone

19nor-P4, 19nor-progesterone

20β-S, 17α,20β,21-trihydroxy-4-pregnen-3-one

20β-P, 4-pregnen-20β-ol-3-one

5α-DHP, 5α-dihydroprogesterone

a.a., amino acid(s)

AF-1, activation function-1

AF-2, activation function-2

AR, androgen receptor

B, corticosterone

CHO-K1, Chinese hamster ovary cell line

COS-7, African green monkey cell line

CR, corticoid receptor

Cyp, cytochrome P450

DBD, DNA-binding domain

DHT, dehydrotestosterone

DMSO, dimethylsulfoxide

DOC, 11-deoxycorticosterone

E, cortisone

EC_{50}, half maximal effective concentration

ER, estrogen receptor

F, cortisol

FPKM, fragments per kilobase of transcript per million mapped reads

GR, glucocorticoid receptor

H3-H5 interaction, helix 3-helix 5 interaction

HEK293, human embryonic kidney 293 cell line

HepG2, human hepatoma cell line

HRE, hormone-response element

HSD, hydroxysteroid dehydrogenase

LBD, ligand-binding domain

MAPK, mitogen-activated protein kinase

MD simulation, molecular dynamic simulation

MMTV, mouse mammary tumor virus

MR, mineralocorticoid receptor

ns, nanosecond(s)

NTD, N-terminal domain

P4, progesterone

PCOS, polycystic ovary syndrome

PCR, polymerase chain reaction

PEI, polyethylenimine

PI3K, phosphoinositide 3-kinases

PR, progesterone receptor

Preg, pregnenolone

RMSD, root mean square deviation

RNA-seq, RNA sequencing

RU486, mifepristone

S, 11-deoxycortisol

SAE, *Squalus acanthias* embryo cell line

SD, standard deviation

SEM, standard error of the mean

SHR, steroid hormone receptor

SRD5α, 5α-reductase

General Abstract

Progesterone receptor (PR) is a ligand-dependent transcriptional factor which plays important roles in the reproductive biology of vertebrates [1]. A recent study on genome of a cartilaginous fish, elephant shark, has provided an interesting insight into the evolution of gnathostome [2], which makes this fish an ideal model for the comparative analysis and evolutionary study of steroid hormone receptors (SHRs).

In the first chapter, I analyzed the amino acid sequence of elephant shark PR which is cloned in our laboratory and compared with PRs of other vertebrates. Results showed that the DNA-binding domain and ligand-binding domain are highly conserved during evolution. The gene expression analysis of synthetic enzymes of steroid hormones indicates the possibility that progesterone, 17OH-progesterone and 5α-dihydro-progesterone is the physiological ligand for elephant shark PR.

The ligand responses of full-length and truncated elephant shark PR were investigated and compared with human and zebrafish PRs. The results showed that full-length elephant shark PR can be stimulated by more steroids than human and zebrafish. Elephant shark and human PRs still showed transactivation after the removal of A/B domain while truncated zebrafish PR almost lost the response ability to steroids. Chapter 1 provides an insight into the endocrine system of elephant shark as well as the ligand-dependent transcriptional function of elephant shark PR.

In chapter 2, the effects of mifepristone (RU486), a widely used clinical antagonist of human PR, was examined on elephant shark PR. Results showed that RU486 did not inhibit the progesterone-induced activation of elephant shark PR. Gly-722 in human PR corresponding to Cys-528 in elephant shark PR, which is on the helix 3, is considered essential for the antagonistic effects of RU486 [3]. Mutant PRs with cysteine/glycine substitution on helix 3 were constructed to confirm the relevance of this amino acid to the

antagonistic effect of RU486 after mutation was recorded. A decline in steroid response of elephant shark PR-Gly528 by 11-deoxycortisol and an increase in activation of human PR-Cys722 were observed. To understand the molecular mechanism of this phenomenon, I investigated the ligand-receptor interactions between PR and 11-deoxycortisol using *in silico* methods including docking simulation and molecular dynamic (MD) simulation. The simulations provided a possibility that the interaction with cysteine on helix 3 and methionine on helix 7, Met-607 in elephant shark PR corresponding to Met-801 in human PR, is crucial for 11-deoxycortisol binding stability of PR. To confirm the role of the methionine residue, mutant PRs with methionine to glycine mutation on helix 7 were constructed and their steroid-induced activation were tested. The mutant PRs did not show any steroid response, which indicated the loss of interaction between methionine on helix 7 can lead to the loss of steroid hormone response for PR.

In order to further understand the actual role of the methionine on helix 7 to PR-11-deoxycortisol interaction, methionine to leucine mutant PRs were constructed and evaluated by *in silico* analysis. The simulations indicated that methionine to leucine mutation on helix 7 is comparatively stable than methionine to glycine mutation, suggesting that the steroid-induced activation of PRs are maintained after mutation. Chapter 2 provides us with some further understanding into the role of the interaction between ligand and helices in the ligand-binding stability of PR, which has never been described previously.

Key words: progesterone receptor, elephant shark, cartilaginous fish, steroid hormone, mutation, in silico analysis, MD simulation.

General Introduction

Steroid hormones, derived from cholesterol, play an important role in a variety of physiological life processes from fetal to adult. Steroid hormones are involved in the regulation of multiple physiological processes including reproduction, growth, immunity and metabolism [4,5]. Although the discovery and investigation on steroid hormones has started in 1930s [6], it took about 5 decades until the first molecular cloning of steroid hormone receptors (SHRs) in 1980s [7]. The isolation of SHR is a key step for the characterization of steroid hormone-induced activation of gene transcription.

Before discussing the SHRs, we should have a clear view on how the steroid hormones are synthesized, which is called steroidogenesis. Steroidogenesis is a complex process of biosynthesizing steroid hormones from a common precursor, cholesterol. The cholesterol in cells will be firstly transported to mitochondria and converted into pregnenolone, the first steroid, under the effect of the enzyme cytochrome P450 side-chain cleavase (Cyp11A1) [8,9]. After that, the cell-specific enzymatic chain reactions will allow the biosynthesis of steroid hormones by adrenal gland (mineralocorticoids, glucocorticoids and androgen) [10], testis (androgens) [11], ovary (estrogens and progestins) [12,13], etc.

Two enzyme families play a major role in the steroidogenesis, cytochrome P450 (Cyp) and hydroxysteroid dehydrogenase (HSD) [4,8]. Despite these two, the enzyme 5α-reductase (SRD-5α), mainly the isoform 2, is also involved in the conversion of steroid hormones, for example, the production of dihydrotestosterone, which is the active form of testosterone [14].

SHRs belong to the nuclear receptor super family and exhibit high conservation in structure between species. They consist of N-terminal domain (NTD) containing the ligand-independent activation function 1 (AF-1) domain, DNA-binding domain (DBD) composed of two zinc fingers, hinge domain, and ligand-binding domain (LBD)

containing the ligand-dependent activation function 2 (AF-2) domain on the C-terminal [15-17].

In the absence of ligand, SHRs are localized in the cytoplasm and complexed with chaperone proteins (also called heat-shock proteins) which help the receptor to maintain the three-dimensional structure prior to the binding with its ligand. Once a ligand binds to the receptor, some of the chaperone proteins will be released and a conformational change in AF-2 domain occurs [18-21]. The receptor-ligand complexes will form homodimers and translocate to the nucleus and then bind to the hormone-response elements (HREs) on gene regulatory regions to initiate gene transcription [13]. In addition, when the receptor-ligand complexes form heterodimers, they do not bind to HREs [22].

Steroid hormones normally work through a genomic way, as known as the classical pathway. On the other side, there is another non-genomic mode of steroid activation which is relied on the intracellular signaling transduction following the pathway of protein kinases (PI3K, MAPK) [13,23-26].

Mutations and deletions in steroid hormone receptor are the most general reason for hormonal insensitivity syndromes. Previously, the clinical syndromes caused by steroid hormone resistance have been well-described by large amounts of studies [27-35]. To date, the progesterone resistant syndrome has not been well-described. Some previous studies considered that the resistance to progesterone is involved in endometriosis and polycystic ovary syndrome (PCOS) [36,37].

In previous studies, large number of mutations on estrogen receptor (ER) [27,28,38], glucocorticoid receptor (GR) [31,39], mineralocorticoid receptor (MR) [40] and androgen receptor (AR) [41] have been identified. However, no mutation of progesterone receptor linked to clinical syndromes has been described to date. As a result, it is not available to

study the role of any typical amino acids based on the report from clinical cases. While studying the characterization of amino acids in PR, previous studies more tended to rely on analyzing the amino acid substitution during the molecular evolution of PRs. In recent years, using computational analytic method to predict the function of proteins has been more and more popular. For nuclear receptors like PR, the combination of *in vitro* and *in silico* methods is undoubtedly a good way to understand the functional meaning of amino acid substitution during evolution.

Cartilaginous fishes, the most primitive group of jawed vertebrates (gnathostomes), diverged from bony vertebrates about 450 million years ago [2]. Although cartilaginous fishes only occupy a small part of modern jawed vertebrates' diversity comparing to the bony vertebrates [42], their special evolutionary position makes a key contribution to the understanding of the evolution of jawed vertebrates. Cartilaginous fishes (Chondrichthyes) consist of two subclasses, elasmobranches and holocephalans. The model animal of this study, elephant shark (*Callorhinchus milii*), belongs to the order Chimaeriformes which is the only living group of holocephalans. The whole-genome analysis of elephant shark was published in 2014 [2], which elucidated its genome is the slowest evolving of all known vertebrates. This finding makes elephant shark an ideal model species for evolutionary studies to gain an interesting insight into the ancestral state of physiological system of vertebrates.

In the first chapter of this thesis, I will analyze the gene expression of progesterone receptor, as well as the common enzymes involved in the biosynthesis of steroid hormones, using public RNA-seq data of elephant shark and other species. These investigations could provide us some theoretical evidence to understand the endocrine system of elephant shark. I will also introduce the basic information of the elephant shark

PR and estimate its steroid response ability comparing with other species.

In chapter 2, I will try to investigate the evolutionary meaning of the cysteine to glycine substitution on helix 3, Gly-722 in human PR corresponding to Cys-528 in elephant shark PR, using *in silico* and *in vitro* methods. Constructs with mutation on the corresponding residues will be estimated by computer simulations and *in vitro* experiments.

This study aims to gain a better understanding of the endocrine system of cartilaginous fishes. Meanwhile, through investigating the role of specific amino acid residues of PR, we can expand and deepen our insight into the functional meaning of molecular evolution in PR.

Chapter 1

Isolation and functional characterization of elephant shark, *Callorhinchus milii*, progesterone receptor

Abstract

Progesterone receptor (PR) plays important roles in the reproductive biology of all vertebrates studied to date. A recent study on genomes from elephant shark has provided an interesting insight into the gnathostome evolution [2], which makes this shark a good model for comparative analysis of steroid hormone receptor. However, elephant shark PR has not been isolated or studied yet.

In this chapter, I analyzed the amino acid sequence of elephant shark PR. The comparison and similarity analysis with other vertebrate PRs show that the DNA-binding domain and ligand-binding domain are highly conserved during evolution. The gene expression analysis revealed that elephant shark PR is mainly expressed in muscle, ovary and testis, and that the expression level is lower than that of human and zebrafish PRs. I also predicted that progestins and corticoids are synthesized in elephant shark through investigating the expression of their synthetic enzymes, indicating the possibility that progesterone, 17OH-progesterone and 5α-DHP is the physiological ligand for elephant shark PR. Further, I have studied the ligand responses of full-length and truncated PRs from elephant shark, human, and zebrafish to 9 common progestin and corticoids. The results showed that PR from elephant shark can be stimulated by all these 9 steroids while 8 for human and 4 for zebrafish. Transcriptional activation of the truncated PRs, lacking A/B domain and containing a GAL4-DBD instead of the PR-DBD, revealed that truncated elephant shark and human PRs still can be stimulated by part of the steroids, while truncated zebrafish PR almost lost the response ability to steroids. These findings showed that the allosteric interaction between the NTD and the hinge-LBD domain of full-length PRs is important in the ligand-dependent transcriptional activation.

Key words: progesterone receptor evolution, elephant shark, cartilaginous fish, steroid hormone, ligand-dependent regulation.

Introduction

Progesterone is a crucial steroid hormone in the endocrine regulation of female reproductive system in mammals. Its corresponding receptor, progesterone receptor (PR), is a ligand-dependent transcription factor belonging to the nuclear receptor super family, which also includes receptors for steroids such as androgens, estrogens, mineralocorticoids, glucocorticoids, thyroid hormone, and retinoids. PR plays a fundamental role in the physiological regulation of gene expression networks to initiate the development, differentiation and proliferation of target tissues, especially in reproduction system, as well as the pathological processes in endocrine-based cancers, mainly reported in breast cancer but also prostate cancer in males [43,44], in response to the binding with progesterone and other steroid hormones [1].

Two well-described signaling pathways have been proposed to activate PR-mediated hormone responses. One is the classical pathway, in which the liganded PR directly binds to the hormone-response elements (HREs) on gene regulatory regions to initiate gene transcription [45]. The other one is the non-classical pathway, which relies on various of second messengers and pathways of intracellular signal transduction [23-26].

The basic structure of PR, which is similar to other members in the SHR super family, consists of NTD, DBD, hinge domain, and LBD on the C-terminal. The NTD contains the region of ligand-independent transactivation AF-1 domain while LBD contains a ligand-dependent AF-2 domain. The DBD consists of two zinc fingers which make the receptor available to bind to target DNA [15-17]. Previous studies showed truncated SHRs, lacking NTD and/or DBD exhibited altered response to steroid hormones [46-48].

Elephant shark (*Callorhinchus milii*) belongs to the Holocephali, which is one of two subclasses of Chondrichthyes, while the other one is Elasmobranchii that contains sharks,

rays, and skates. In 2014, the whole-genome analysis of elephant shark executed by Venkatesh *et al.* revealed that the genome of *C.milii* is the slowest evolving of all known vertebrates [2]. The genome size of elephant shark is comparatively small, 0.937 gigabases, which is about 1/3 of human genome. In contrast, these characteristics make elephant shark a good model for comparative analysis of SHRs. Furthermore, most of the SHRs from elephant shark, including PR, have not been isolated and their characteristics have not been studied to date.

In this chapter, I will describe the amino acid sequence of elephant shark PR deduced from its cDNA cloned in our lab, which has an additional 159 a.a. on N-terminal compared with the sequences on NCBI database [2]. I then investigated the expression level and steroid hormone response of elephant shark PR and compared with PRs from other species. Further, I also examined the allosteric role of the N-terminal domain in the ligand response using PRs lacking this domain. The results in this chapter will provide a basic understanding of the ligand response function of elephant shark PR.

Materials & Methods

Chemical reagents

Pregnenolone (Preg), progesterone (P4), 17α-hydroxypregnenolone (17OH-Preg),17α-hydroxy-progesterone (17OH-P4), deoxycorticosterone (DOC), 11-deoxycortisol (S), cortisol (F), cortisone (E), corticosterone (B), and aldosterone were purchased from Sigma-Aldrich. For reporter gene assays, all hormones were dissolved in dimethylsulfoxide (DMSO), and the final concentration of DMSO in culture medium of cells did not exceed 0.1% (v/v).

Molecular cloning of PRs

To isolate full-length cDNAs of elephant shark, human and zebrafish PR, the first strand cDNA was synthesized using total RNA isolated from ovary. Specific primer sets were designed based on the sequence information in Genbank database. DNA fragments were amplified using specific primer set and amplified DNAs were subcloned with pCR-Blunt II-TOPO vector (Invitrogen, Carlsbad, CA). Sequencing was performed using a BigDye Terminator Cycle Sequencing-kit (Applied Biosystems, Forster City, CA), and analyzed on the ABI PRISM 377 automatic sequencer (Applied Biosystems).

Construction of plasmid vectors

The full-coding regions of PRs from elephant shark, human and zebrafish were amplified by polymerase chain reaction (PCR) with KOD DNA polymerase (Toyobo Co., Ltd.), and the D/E domains of PRs were amplified with Blend Taq DNA polymerase (Toyobo Co., Ltd.). PCR products were purified from TAE gel and ligated into pcDNA3.1 plasmid (at *Bam* HI-*Not* I site for elephant shark PR, *Kpn* I-*Not* I site for human PR, and

Not I-*Hind* III site for zebrafish PR) (Life Technologies, Carlsbad, CA) for full-coding regions or into pBind vector (at *Mlu* I-*Not* I site for elephant shark, human and zebrafish PR) for D/E domains.

Transactivation assay and statistical analysis

Human embryonic kidney 293 (HEK293) cells (for full-length PRs) and Chinese hamster ovary (CHO-K1) cells (for truncated PRs) were used in the reporter gene assay. For HEK293 or CHO-K1, cells were seeded in 24-well plates at 5×10^4 cells per well in phenol red-free DMEM (High Glucose) (Wako Pure Chemical Corp.) for HEK293 cells or DMEM (Ham's F-12) (Nacalai tesque Inc.) for CHO-K1 supplemented with 10% chacoal/dextran-treated fetal bovine serum (Hyclone, South Logan, UT).

For the luciferase assay of full-length PRs, the HEK293 cells were transfected with 2 kinds of plasmid, MMTV-Luc (200 ng per well) (as reporter construct) and pRL-tk (50 ng per well) (as an internal control to normalize the variation in transfection efficiency; contains the *Renilla riniformis* luciferase gene with the herpes simplex virus thymidine kinase promoter) (Promega), as well as 100 ng of pcDNA3.1-PR construct using PEI-max transfection reagent (Polyscience Inc.). After 4 hours of incubation, steroids were applied to the medium at various concentrations. After an additional 44 hours, the cells were collected and used in the measurement of luciferase activity by a chemiluminescence assay using the Dual-Luciferase Reporter Assay System (Promega).

For the luciferase assay of PR-LBDs, the CHO-K1 cells were transfected with 200 ng of pG5-luc reporter vector (contains a Gal-4 binding site) and 50 ng of pBind-PR-LBD construct each well using PEI-max transfection reagent. After 4 hours of incubation, several steroid hormones were applied to the medium at various concentrations. After an

additional 44 hours, the cells were collected and used in the measurement of luciferase activity by a chemiluminescence assay using the Dual-Luciferase Reporter Assay System. The luminescence was measured by a Turner Designs Luminometer TD-20/20 (Promega). The promoter activity was calculated as the ratio of firefly (*Photinus pyralis*) luciferase activity to sea pansy (*Renilla riniformis*) luciferase activity. All transfections were performed for at least 3 times with triplicate sample points in each experiment. The results were presented mean ± SEM from 3 separate experiments. The comparison between 2 groups were analyzed with multiple *t*-test. The dose-response data and EC_{50} values were analyzed using GraphPad Prism (version 8.0.1 (145), GraphPad Software, Inc.). $P < 0.05$ was considered to have statistical significance. Statistical significance was shown as: $P < 0.05$, *; $P < 0.01$, **; $P < 0.001$, ***.

Phylogenetic analysis

The phylogenetic relationship was constructed with neighbor-joining method [49] using alignment of amino acid sequences by ClustalW implemented in MEGA7 (https://www.megasoftware.net/) [50]. The evolutionary distances were computed using Jones-Taylor-Thornton (JTT) model [51], with 1000 bootstrap tests [52]. Amino acid sequence of elephant shark PR is deduced from the nucleotide sequence determined in our laboratory. The full-coding amino acid sequences of PRs from other species used in this study were obtained from NCBI protein database.

Similarity analysis

Amino acid sequences of domains A/B (NTD), C (DBD), D (hinge), and E (LBD) of PRs from 6 species were compared with elephant shark PR using Geneious Prime

2021.1.0 (https://www.geneious.com). The full-coding amino acid sequences of PRs from other species used in this study were obtained from NCBI protein database. GenBank accession numbers are as follows: human PR (AAD01587.1), mouse PR (NP_032855.2), Florida redbelly turtle PR (BAF91193.1), Japanese quail PR (XP_015707740.1), African clawed frog PR (AAG42362.1), zebrafish PR (NP_001159807.1).

Protein expression analysis

I downloaded paired-end RNA-seq reads of elephant shark for the brain, gills, heart, intestine, kidney, liver, muscle, ovary, spleen, testis and thymus from database of NCBI (accession number: SRP013772), and reference genome assembly and gene annotation from Ensembl (accession ID: GCA_000165045.2).

Paired-end RNA-seq reads of human for 16 tissues (adipose, adrenal, brain, breast, colon, heart, kidney, liver, lung, lymph node, ovary, prostate, skeletal muscle, testis, thyroid and white blood cell) from database of NCBI (accession number: PRJEB2445), and reference genome assembly and gene annotation from Ensembl (accession ID: GCA_000001405.28) were used for protein expression analysis of human PR.

Paired-end RNA-seq reads of zebrafish for 12 tissues (bones, brain, embryo, gills, heart, intestine, kidney, liver, muscle, ovary, testis and unfertilized egg) from database of National Center for Biotechnology Information (accession number: SRP044781), and reference genome assembly and gene annotation from Ensembl (accession ID: GCA_000002035.4) were used for protein expression analysis of zebrafish PR.

RNA-seq reads of various tissues were independently aligned to the reference sequences using RSEM (v1.3.3) [53], which uses Bowtie2 (v2.4.1) for alignment [54]. The relative measure of transcript abundance is fragments per kilobase of transcript per million

mapped reads (FPKM).

Results

Comparison of elephant shark PR with vertebrate PRs.

The full-coding region of elephant shark PR that I used in this study contains 2217 base pairs of nucleotides which correspond to 739 amino acids (Fig. 1-1). The two predicted isoforms of elephant shark PR on NCBI protein database, X1 (accession: XP_007900068.1) and X2 (accession: XP_007900077.1), have 580 and 541 amino acids, respectively. The elephant shark PR cloned in our lab has an additional 159 amino acids on the N-terminal, comparing to the longer predicted isoform X1. Like other SHRs, elephant shark PR is also divided into 4 domains, N-terminal domain, DNA-binding domain, hinge domain, and ligand-binding domain. The NTD of elephant shark PR is from residue 1 to 370 (370 a.a.), DBD is 371 to 448 (78 a.a.), hinge is 449 to 491 (43 a.a.), LBD is 492 to 739 (248 a.a.). The 91 a.a. AF-1 region of elephant shark PR is predicted based on the alignment with human PR (data not shown). However, the similarity of the amino acid sequence of this region is too low. Unfortunately, there is little information about the AF-1 domain of PR from non-mammalian species. It is thus premature to describe the correct AF-1 region of elephant shark PR.

I show the phylogenetic relationship of PRs from elephant shark and other species including cartilaginous fish, bony fish, amphibian, reptile, bird, rodent and human (Figure 1-2). The elephant shark PR can be considered at a similar evolutionary position with little skate, which belongs to another subclass Elasmobranchii of Chondrichthyes.

Comparison of elephant shark PR with six other species (zebrafish, human, quail, turtle, mouse, and frog) for the overall and partial regions showed that these phylogenetically diverse PRs have strong conservation on the C domain (85 to 89%) and comparatively strong conservation on the E domain (64 to 75%), but with weak conservation on the A/B

domain (11 to 18%) and the D domain (18 to 25%) (Fig. 1-3). The high similarity on DBDs among PRs suggests that PRs in different species might bind to similar target DNA regions.

The relative expression analysis showed that the elephant shark PR is predominantly expressed in muscle, ovary, and testis (Fig. 1-4), which is comparatively similar to the expression pattern of human and zebrafish PRs.

Prediction of biosynthesis pathway of progestins and corticoids in elephant shark

Figure 1-5 demonstrates the biosynthesis pathway from cholesterol to progestins, mineralocorticoids and glucocorticoids in physiological system. The cytochrome P450c21A2 is a key enzyme for the synthesis of common corticoids such as 11-deoxycorticosterone, corticosterone, 11-deoxycortisol and cortisol. This enzyme has already been identified in some cartilaginous fishes which belong to Elasmobrachii such as sharks and rays [55,56,87], but not in any holocephalans including elephant shark [57]. Therefore, the synthesis of corticoids may stop at 21-deoxycorticosterone and 21-deoxycortisol. On the other side, 20β-HSD is an enzyme involved in the synthesis of progestins that play a crucial role in teleost fishes such as 17α,20β-DP, 20β-S and 20β-P. 20β-HSD is not expressed in cartilaginous fish like elephant shark. Therefore, these 3 steroids could be considered to be absent in *C.milii*. Another one is 19nor-progesterone, which is normally considered as an artificial synthetic hormone. In previous studies, however, researchers have identified 19nor-steroids such as 19nor-DOC in rodents [58,59], providing the possibility that some animals may have the ability to synthesize 19nor-steroids. Nevertheless, the enzymes involved in the synthesis of this kind of steroids still remain unknown. These results indicate the possibility that progesterone,

17OH-progesterone and 5α-DHP is the physiological ligand for elephant shark PR.

Expression levels of enzymes involved in the biosynthesis of steroid hormone

The enzymes that synthesize progestins, P450 side-chain cleavase (P450scc) and P450c17A1, are mainly expressed in kidney, ovary and testis in elephant shark while also expressed in liver and thyroid in human (Fig. 1-6 A-D). P450c11B1 is the enzyme that converts progestin to corticoid. In elephant shark, P450c11B1 is highly expressed in kidney (Fig. 1-6E). Although the expression levels of P450c11B1 in human were very low, RNA-seq read set showed that P450c11B1 was mainly expressed in adrenal of human [90].

3β-HSD is a key enzyme to synthesize progesterone, which is the most common progestin. 3β-HSD is mainly expressed in kidney, ovary, and testis in elephant shark (Fig. 1-7A). Comparing with the expression of 3 isoforms of 3β-HSD in human (Fig. 1-7B-D), the expression pattern of elephant shark 3β-HSD is similar to the second isoform of human 3β-HSD.

Both elephant shark and human have 3 isoforms of 5α-reductase. Figure 1-8 shows the relative expression of 3 isoforms of 5α-reductase in elephant shark and human. Although 5α-reductase 1 and 2 are considered to be similar and mainly involved in the biosynthesis of steroids, their expression levels in different tissues are diverged (Fig. 1-8 A-D). Both of the third isoforms of 5α-reductase in elephant shark and human are highly expressed in all tissues examined, providing an interesting insight into the physiological role of this isoform in the synthesis of steroid hormone.

Transcriptional activation of full-length and truncated elephant shark PR by steroid hormones.

I compared the transcriptional activation of full-length and truncated PRs from elephant shark, human and zebrafish in response to nine steroid hormones at 100 nM concentration (Fig. 1-9). The responses were compared to the activity of cells expressing the same vectors (expressing vector, reporter vector and control vector) that were treated with vehicle (DMSO) alone.

Full-length PR from elephant shark can be stimulated by all these nine steroids (Fig. 1-9, A, left), in contrast to eight in human (all except cortisone), and four in zebrafish (progesterone, 17α-hydroxyprogesterone, deoxycorticosterone, 11-deoxycortisol) (Fig. 1-9, B and C, left).

The analysis of the truncated PRs, lacking the A/B domain and containing GAL4-DBD instead of PR-DBD, revealed that the truncated elephant shark PR can only respond to five of the steroids (pregnenolone, progesterone, 17α-hydroxyprogesterone, deoxycorticosterone, and 11-deoxycortisol) (Fig. 1-9, A, right), while four to human (pregnenolone, 17α-hydroxyprogesterone, deoxycorticosterone, but with cortisone). Truncated zebrafish PR has no obvious response to all nine steroids except for a weak response to deoxycorticosterone.

The results suggested that the ligand dependent response of elephant shark PR is functionally more similar to human PR than zebrafish. The differences of activation level and ligand specificities between full-length and truncated PRs exhibited high dependency on the NTD and DBD for the regulation of transactivation by steroids.

EC_{50} values for steroid hormone activation of full-length and truncated elephant shark PR.

To understand the sensitivity of elephant shark PR to steroids, I examined the concentration-dependency of hormone response with both full-length (Fig. 1-10 and Table 1-1) and truncated PRs (Fig. 1-11 and Table 1-2). Elephant shark PR showed high sensitivities to progesterone and deoxycorticosterone with EC_{50} values lower than 1 nM. In comparison to elephant shark PR, human PR showed lowest EC_{50} value to progesterone, and zebrafish PR is the most sensitive to deoxycorticosterone, but none of the steroids show EC_{50} value lower than 1 nM. In contrast, elephant shark PR exhibited the greatest response to aldosterone, while human PR respond to aldosterone and corticosterone, zebrafish PR to deoxycorticosterone (Table 1-1).

In parallel, truncated elephant shark PR and human PR both of which lacking NTD and DBD showed lowest EC_{50} value to progesterone in similar level, although it is higher than 1 nM (Table 1-2).

Various hormone responses of PRs in different cell lines.

The hormone responses of full-length and truncated PRs from elephant shark and other vertebrates were examined in cell lines including HEK293, CHO-K1, COS-7, and HepG2 (Table 1-3). All three full-length PRs can be stimulated by steroid hormones in HEK293, COS-7, and HepG2 cells but not CHO-K1 cells. In contrast, truncated PRs only showed hormone response in CHO-K1 cells. Unfortunately, none of these cell lines is available to examine the transactivation of full-length and truncated PRs. As a result, the ligand responses of full-length PRs were examined with HEK293 cells while the truncated PRs were examined with CHO-K1 cells in this study.

Discussion

Elephant shark belongs to the order Chimaeriformes, which is the only living group of Holocephali. Holocephali is one of two subclasses of cartilaginous fishes. All living holocephalans are chimaeras, whereas another subclass of cartilaginous fish is Elasmobranchii that includes sharks, rays and skates. Cartilaginous fishes occupy a special position in the evolution of vertebrates [42]. Further, the whole-genome study indicated that the genome of elephant shark is evolving slowest in all known vertebrates [2], making this fish an ideal model for evolutionary study.

In this chapter, basic information about elephant shark PR has been reported from its amino acid sequence to its expression in different tissues. Unlike human and zebrafish, elephant shark PR is mainly expressed in ovary and testis, indicating that PR might be mostly involved in the reproduction system in elephant shark.

The analysis of hormone synthetic enzymes also provides us an interesting insight into the endocrine system of elephant shark. Previous study has detected the existence and concentration of steroid hormones in elephant shark, such as progesterone, E2 and testosterone [60]. However, the existence of other progestins and corticoids remains to be elucidated. I examined the expression of P450scc, P450c17A1, 5α-reductase and 3β-HSD in elephant shark and clarified the existence of common progestins such as progesterone, 17OH-progesterone, 5α-DHP. Even though there is an enzyme that converts progestins to corticoids, P450c11B1 is confirmed to be expressed in elephant shark. However, P450c21A2, the enzyme that synthesizes common corticoids, such as 11-deoxycorticosterone, corticosterone, 11-deoxycortisol and cortisol, still remains unknown [57]. This would be indirect evidence for the existence of cytochrome P450c21A2 if any of these corticoids can be detected from elephant shark samples.

Further, although PR is mainly expressed in tissues from the reproductive system, it is also slightly expressed in muscle. The expression of synthetic enzymes revealed that two of three isoforms of 5α-reductase are also expressed in the muscle of elephant shark. In addition, I found that elephant shark PR showed about 8-fold activation with 4 nM of EC_{50} value to 5α-DHP, which is synthesized by 5α-reductase from progesterone (data not shown). These results indicated the possibility that the binding of PR to 5α-DHP plays a physiological role in the muscle of elephant shark.

In this chapter, I also investigated the steroid hormone response ability of elephant shark PR, compared to human and zebrafish. The results exhibited strong response of elephant shark PR to progesterone (EC_{50} 0.15 nM), 17OH-progesterone (EC_{50} 0.49 nM), 11-deoxycorticosterone (EC_{50} 0.15 nM) and 11-deoxycortisol (EC_{50} 0.45 nM) (Fig. 1-10 & Table 1-1). On the contrary, human PR only showed a strong response to progesterone (EC_{50} 0.08 nM) and 11-deoxycorticosterone (EC_{50} 1.13 nM), while zebrafish PR did not show any strong response to the steroids used in this experiment. A possible explanation for the comparatively weak responses of zebrafish PR is that the progestins synthesized by 20β-HSD, which are considered as the main physiological progestins for bony fishes, were not used in this study. The physiological meaning of elephant shark PR's strong response to 17OH-progesterone and 11-deoxycortisol, which is not observed in human PR is still unknown. Further investigations are needed.

In addition, after the loss of the N-terminal domain, the response of PRs to steroid hormones is largely reduced (Fig. 1-9, 11 & Table 1-2). These findings elucidated the allosteric importance of NTD in steroid activation of PR. However, making this conclusion based on the comparison of steroid hormone responsiveness derived from 2 different cell lines may be controversial. Unfortunately, I can't find a cell line that can be

used for both full-length and truncated PR at this moment.

Furthermore, I have used HEK293 cells, a cell line derived from mammalian, to investigate the ligand response of PRs from elephant shark, a cartilaginous fish. These results obtained in this study may not reflect the actual physiological role of elephant shark PR. It would be more reliable if cell lines derived from cartilaginous can be used for reporter gene assay. In fact, previous studies have established two cell lines derived from cartilaginous fish, one is *Squalus acanthias* embryo (SAE) cell from embryo of spiny dogfish shark [88] and the other one is silky shark brain (SSB) cell from brain of silky shark [90]. There is no information on the potential of SSB cell line, while the SAE cell line has been proved available to be transfected by plasmids. Although the SAE cells have been maintatined in a continuously proliferative state for 3 years [40], this cell line have to be cultured at a temperature about 18℃, which is difficult for our laboratory to achieve. On the other hand, the SSB cell line can grow well at a higher temperature around 29-30℃ and even at 37℃ [89]. However, further studies are required to clarify whether the cell line can be used for plasmid transfection for luciferase assay. Taken together, using common cell lines is a more reasonable choice at this stage.

Table 1-1

EC_{50} (nM)	Preg	17OH-P4	P4	DOC	S
Elephant	28.9	0.5	0.2	0.2	0.5
shark PR	31%	95%	100%	108%	92%
Human PR	59.9	162.2	0.1	1.1	65.1
	77%	95%	100%	105%	103%
Zebrafish	-	65.4	13.9	6.3	118.5
PR	-	94%	100%	140%	45%

EC_{50} (nM)	Aldo	B	F	E
Elephant	41.6	9.5	73.0	58.1
shark PR	127%	92%	103%	67%
Human PR	34.6	9.3	-	-
	114%	114%	-	-
Zebrafish	-	-	-	-
PR	-	-	-	-

Table 1-1. EC_{50} values for concentration-dependent transcriptional activation of full-length elephant shark, human and zebrafish PRs.

The percentage relative induction is compared with the maximal response of full-length PRs to progesterone (P4). "-" refers to the EC_{50} value is unable to calculate. EC_{50} values near 1 nM or lower are underlined.

*Preg: pregnenolone; 17OH-P4: 17-OH-progesterone; P4: progesterone; DOC: 11-deoxycorticosteronel; S: 11-deoxycortisol; Aldo: aldosterone; B: corticosterone; F: cortisol; E: cortisone.

Table 1-2

EC_{50} (nM)	Preg	17OH-P4	P4	DOC	S
Elephant	4.3	43.2	4.2	7.5	14.1
shark PR	103%	135%	100%	118%	125%
Human PR	7.7	184.5	4.0	84.5	-
	105%	38%	100%	96%	-
Zebrafish	438.2	723.3	213.3	42.3	268.0
PR	63%	116%	100%	99%	67%

EC_{50} (nM)	Aldo	B	F	E
Elephant	-	77.2	456.1	-
shark PR	-	90%	76%	-
Human PR	-	84.8	-	-
	-	85%	-	-
Zebrafish	-	0.3	50.9	-
PR	-	40%	51%	-

Table 1-2. EC_{50} values for concentration-dependent transcriptional activation of truncated elephant shark, human and zebrafish PRs.

The percentage relative induction is compared with the maximal response of truncated PRs to progesterone (P4). "-" refers to the EC_{50} value is unable to calculate.

*Preg: pregnenolone; 17OH-P4: 17-OH-progesterone; P4: progesterone; DOC: 11-deoxycorticosteronel; S: 11-deoxycortisol; Aldo: aldosterone; B: corticosterone; F: cortisol; E: cortisone.)

Table 1-3.

		HEK293	CHO-K1	COS-7	HepG2
Elephant shark	full	↑	↓	↑	↑
	LBD	-	↑	±	-
Human	full	↑	-	↑	↑
	LBD	↑(low)	↑	±	-
Zebrafish	full	↑	↑	↑	↑
	LBD	-	-	±	-

Table 1-3. Hormone response of vertebrate PRs in different cells.

The hormone response activities of plasmids with full-coding region of PRs and truncated PRs were measured in 4 different types of cells. All cells were treated with the indicated concentration (10^{-7} M) of steroid hormones or vehicle alone (DMSO) for 44 hours before the reporter gene activity was measured. "↑" refers to the plasmid shows statistically higher response to steroids compared to the activity of cells expressing the same vectors (expressing vector, reporter vector and control vector) that treated with vehicle (DMSO) alone. "↓" refers to the plasmid shows statistically lower response to steroids compared to the activity of cells expressing the same vectors that treated with vehicle (DMSO) alone. "-" refers to the construct shows no statistical significance of ligand response compared to the activity of cells expressing the same vectors that treated with vehicle (DMSO) alone. Data that is unstable in replicating experiments or the result is uncalculatable shows in "±".

Table 1-4. GenBank accession ID.

human PR	AAD01587.1
mouse PR	NP_032855.2
Chinese hamster PR	XP_003496188.1
golden hamster PR	XP_005077381.1
Florida redbelly turtle PR	BAF91193.1
chicken PR	AAA49013.1
Japanese quail PR	XP_015707740.1
African clawed frog PR	AAG42362.1
medaka PR	XP_023816983.1
zebrafish PR	NP_001159807.1
coelacanth PR	XP_014345729.1
spotted gar PR	XP_006628126.2
Atlantic hagfish SR2	ABD46743.1
sea lamprey PR	APA19935.1

Figure 1-1

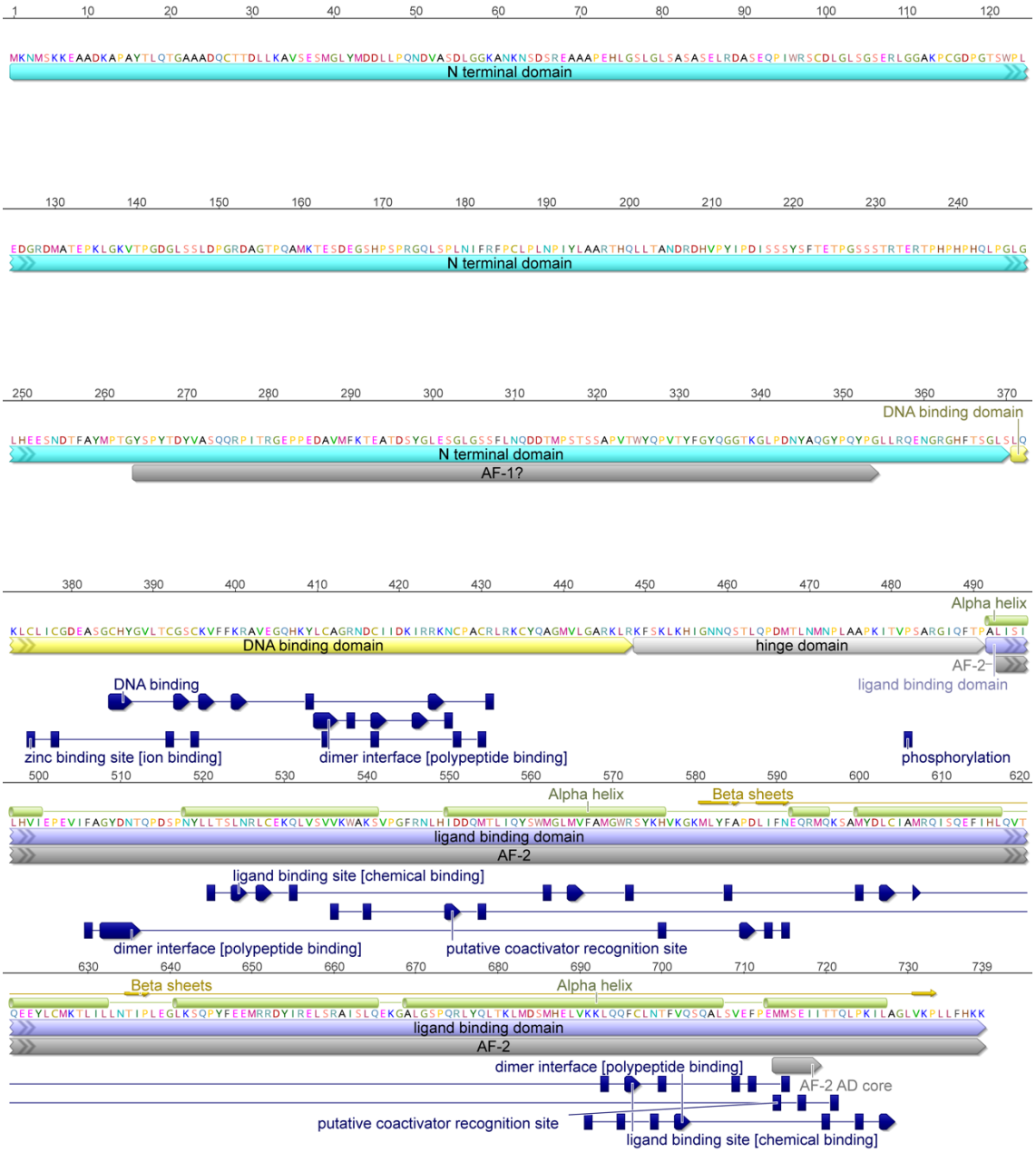
N terminal domain
N terminal domain
DNA binding domain
N terminal domain
AF-1?
Alpha helix
DNA binding domain
hinge domain
AF-2
ligand binding domain
DNA binding
zinc binding site [ion binding]
dimer interface [polypeptide binding]
phosphorylation
Alpha helix
Beta sheets
ligand binding domain
AF-2
ligand binding site [chemical binding]
dimer interface [polypeptide binding]
putative coactivator recognition site
Beta sheets
Alpha helix
ligand binding domain
AF-2
dimer interface [polypeptide binding]
AF-2 AD core
putative coactivator recognition site
ligand binding site [chemical binding]

Figure 1-1. The full sequence of elephant shark progesterone receptor.

The full-coding amino acid sequence of elephant shark PR, which was deduced from its cDNA sequenced in our laboratory. The full-coding region contains 2217 base pairs of nucleotides which corresponding to 739 amino acids. N-terminal domain is in cyan, DNA-binding domain is light yellow, hinge domain is light grey and ligand-binding domain is purple. Two activation function regions (AF-1 & AF-2) are in dark grey with AD core of AF-2 indicated. Secondary-structural elements of the PR-LBD are indicated above the sequence; alpha-helices are light green and beta-sheets are yellow. The DNA-binding sites and zinc-binding sites are spotted on DNA-binding domain. The dimer interfaces range from DBD to LBD. The ligand-binding sites and coactivator recognition sites are indicated on LBD.

Figure 1-2

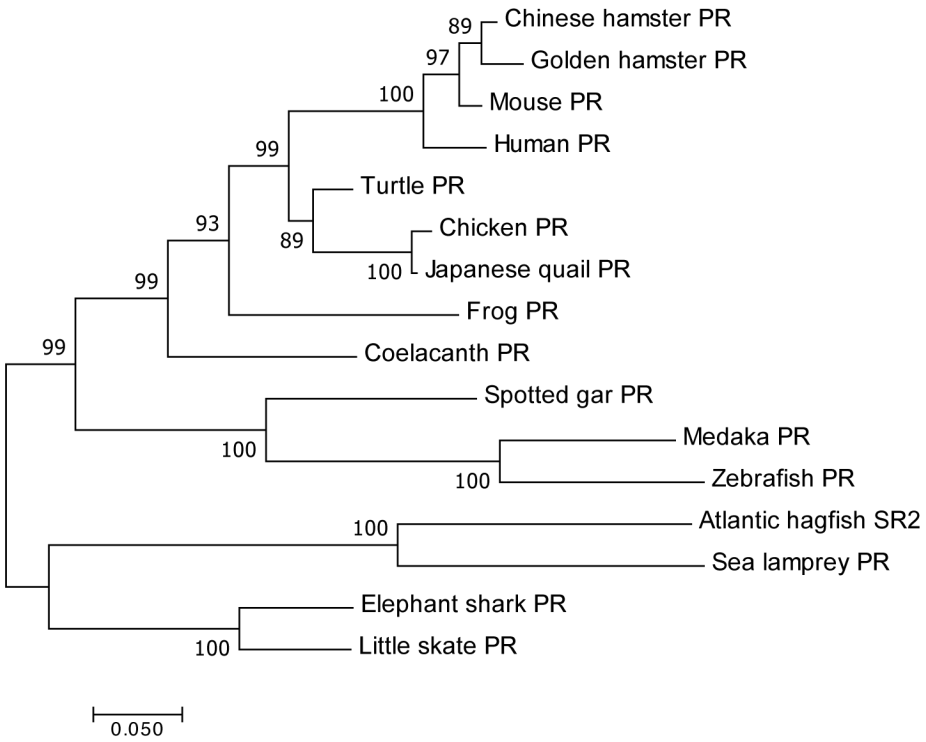

Figure 1-2. Phylogenetic relationship of vertebrate PRs.

The phylogenetic relationship was constructed with neighbor-joining method [49] after amino acid sequences of ligand-binding domains from PRs aligned by ClustalW [50]. The values next to the branches represent the percentage of replicate trees in which the associated taxa clustered together in 1000 bootstrap tests.

Figure 1-3

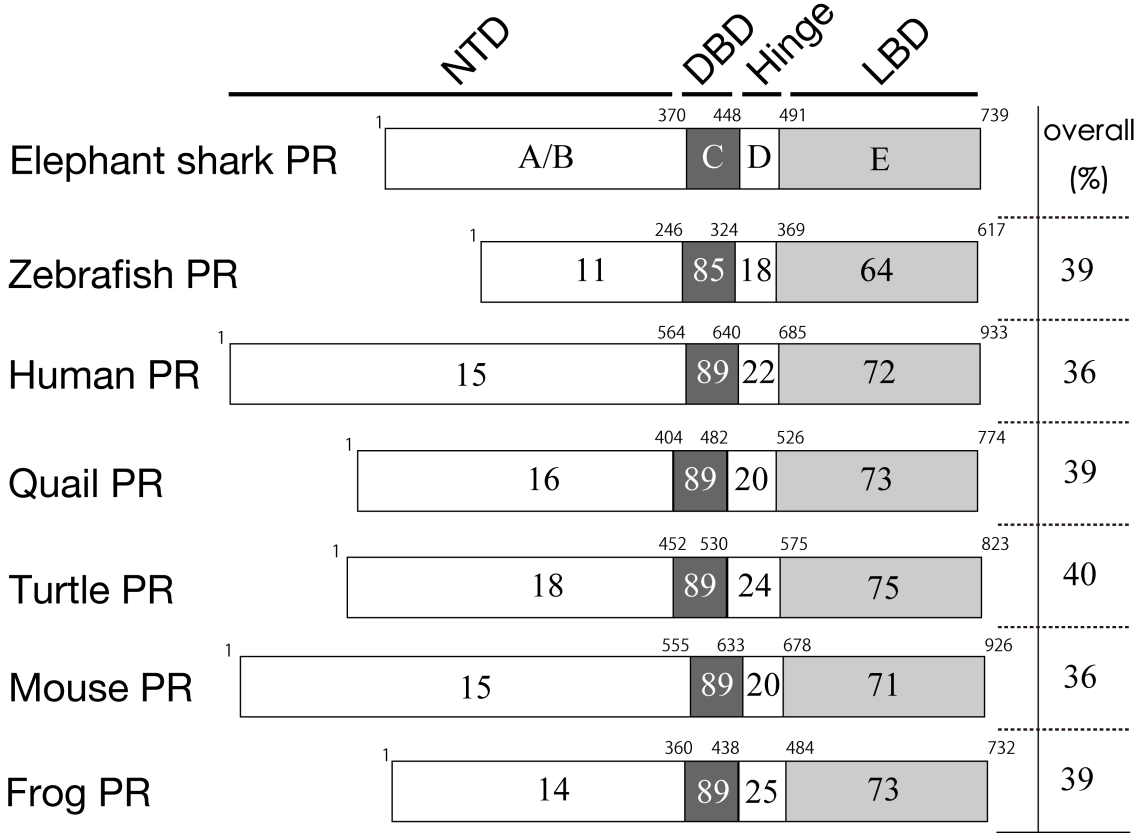

Figure 1-3. Comparison of A to E domains from vertebrate PRs.

The domains A/B (NTD), C (DBD), D (hinge), and E (LBD) on PRs of 6 common species were compared with elephant shark PR. Values in each domain show the percentage of identical amino acids in other species compared to elephant shark PR. Values on the right side represent the overall identity of PRs of these 6 species compared to elephant shark.

Figure 1-4

A.

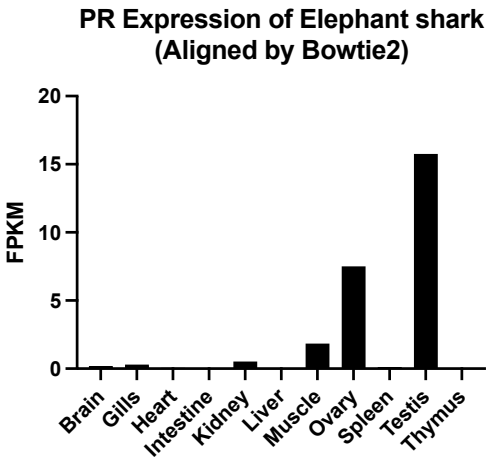

B.

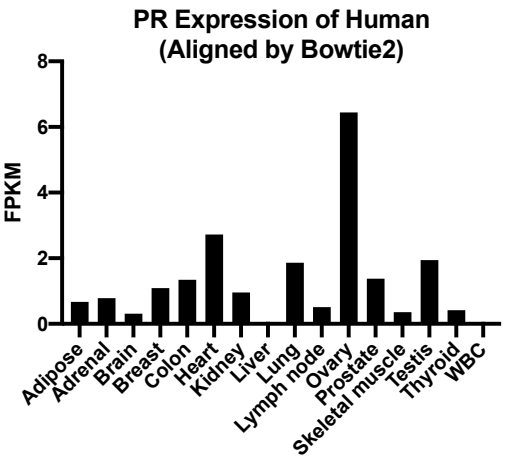

C.

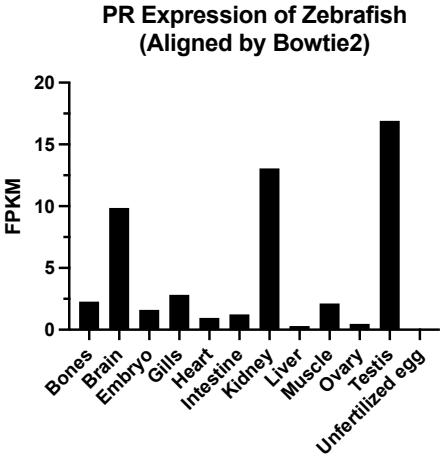

Figure 1-4. PR expression levels of different tissues in elephant shark, human and zebrafish.

Relative expression of elephant shark PR (A), human PR (B) and zebrafish PR (C) were calculated based on RNA-seq data. Transcript abundances are shown in normalized counts called fragments per kilobase of exon per million fragments mapped (FPKM). FPKM values were estimated by normalizing gene length, followed by normalizing for sequencing depth.

Figure 1-5

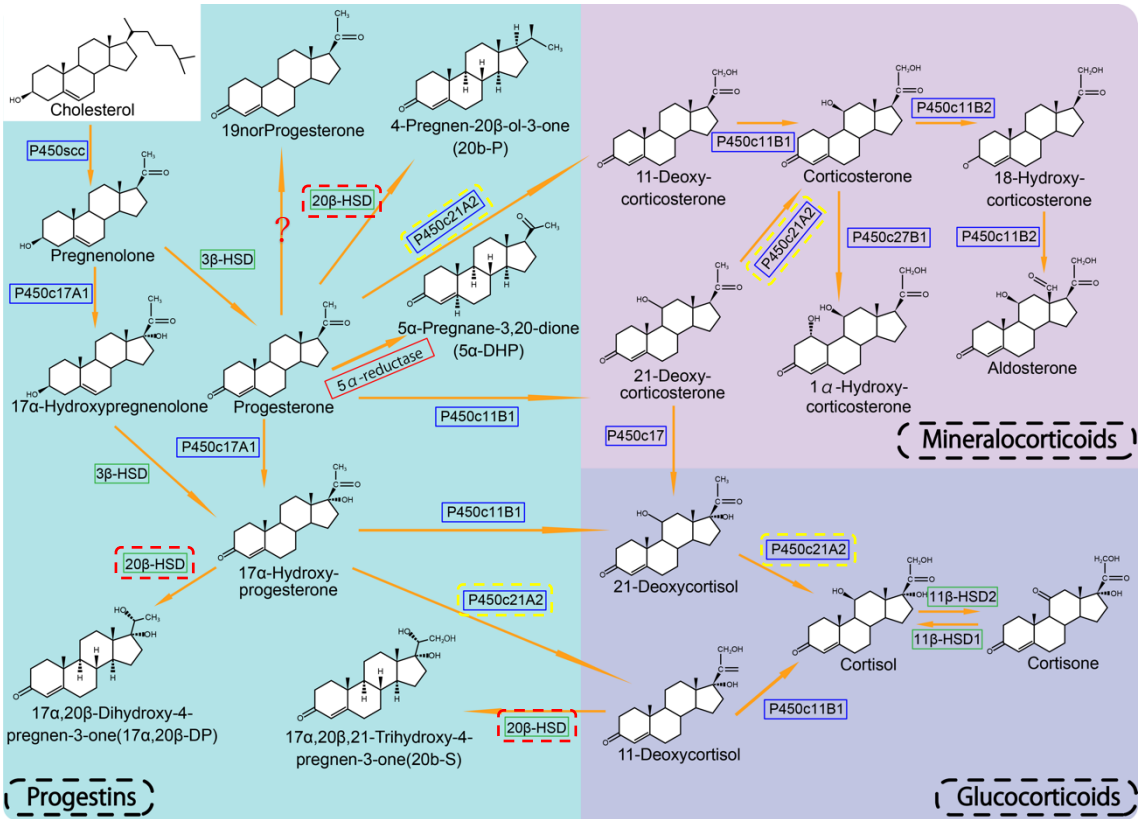

Figure 1-5. The synthesis pathway of progestins and corticoids.

The structures and synthesis pathways of the steroid hormones including progestins, mineralocorticoids and glucocorticoids are shown. Labels next to the arrows represent the enzymes that are involved in the synthesis of hormones. Blue labels are enzymes that belong to cytochrome P450 family. The yellow labels are in the hydroxysteroid dehydrogenase (HSD) family. The enzymes that cannot be found in the genome database of elephant shark are framed in yellow (cytochrome P450) and red (HSD), respectively.

Figure 1-6

A.

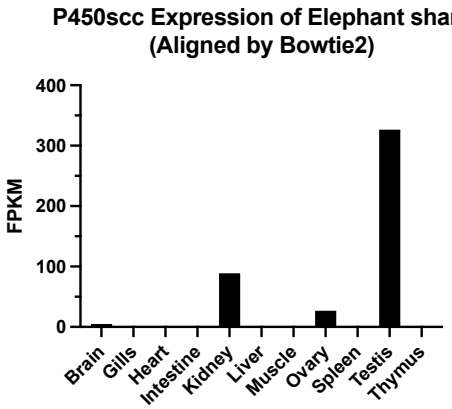

B.

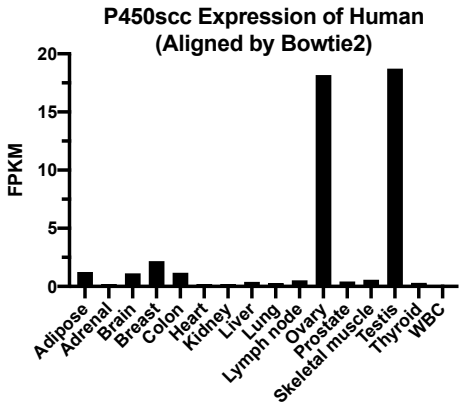

C.

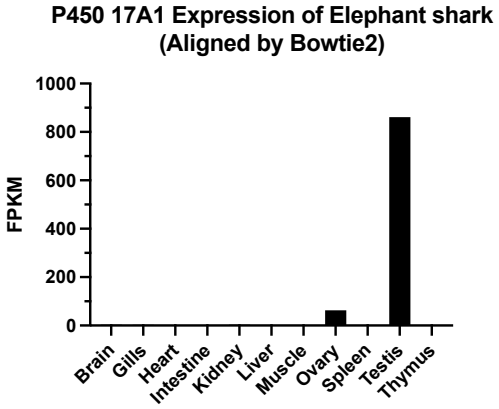

D.

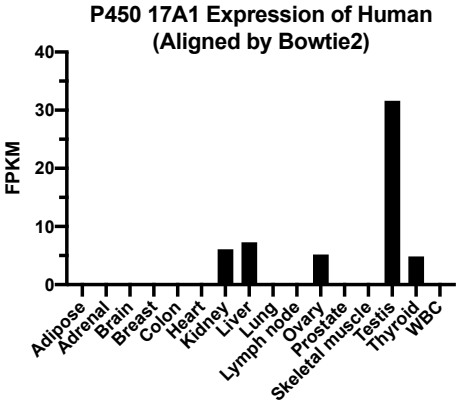

E.

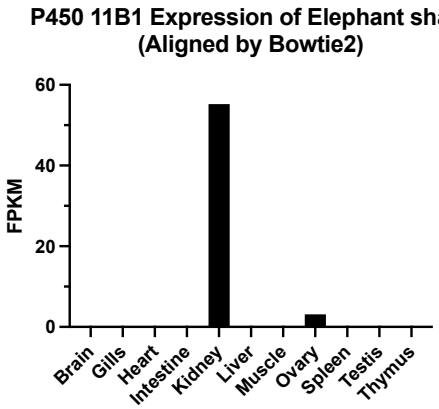

F.

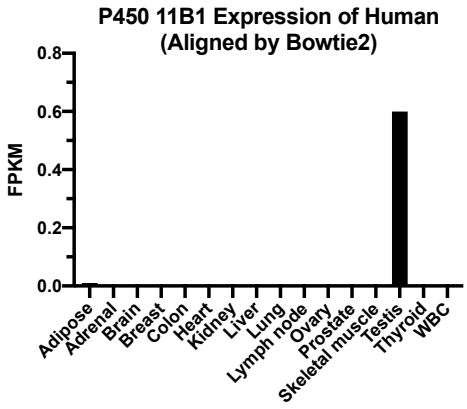

Figure 1-6. Expression levels of cytochrome P450 in different tissues in elephant shark and human.

Relative expression of cytochrome P450 in elephant shark (A, C, D) and human (B, D, F) were calculated based on RNA-seq data. The transcript abundances are shown in normalized counts called fragments per kilobase of exon per million fragments mapped (FPKM) in the dataset. For sequencing depth, FPKM values were estimated by normalizing gene length.

Figure 1-7

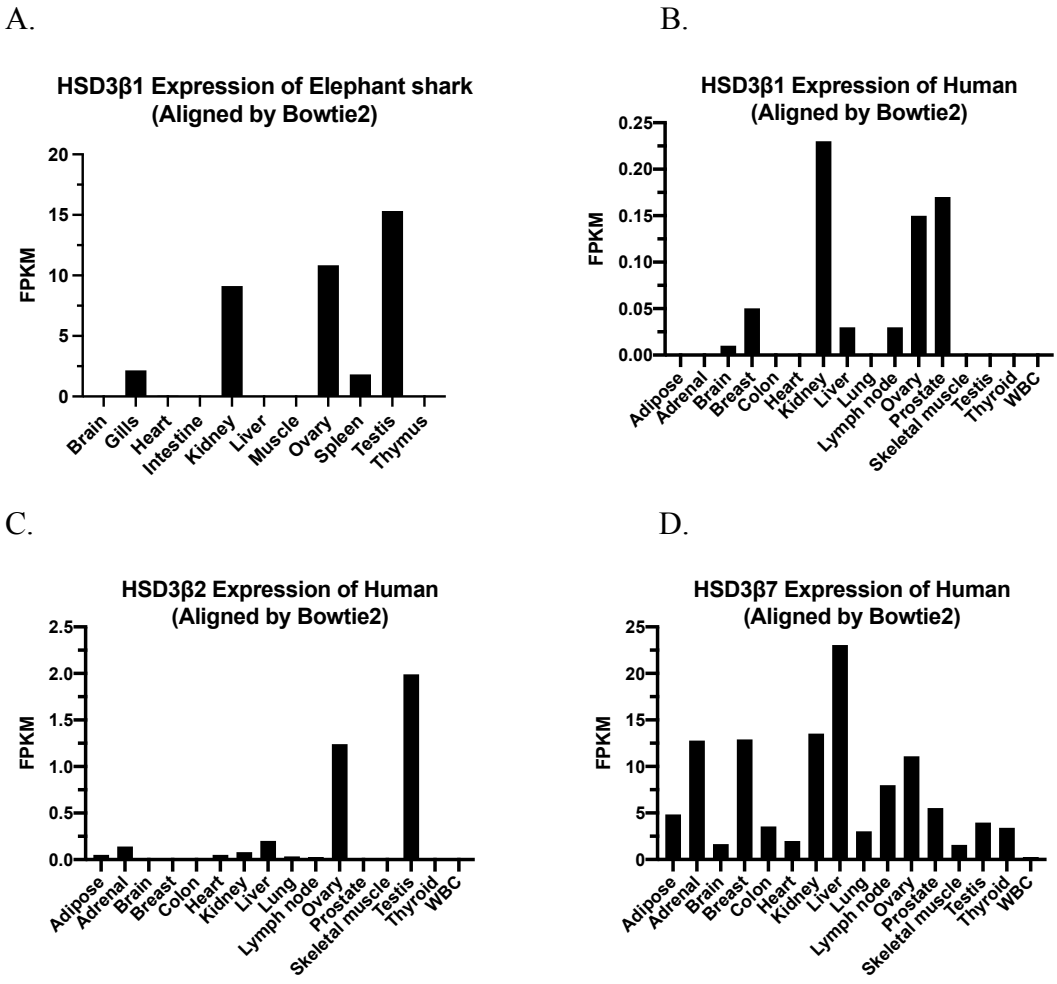

Figure 1-7. Expression levels of hydroxysteroid dehydrogenases (HSD) in different tissues in elephant shark and human.

Relative expression of HSD3β in elephant shark (A, C, D) and human (B, D, F) were calculated based on RNA-seq data. The abundances of transcripts are shown in normalized counts called fragments per kilobase of exon per million fragments mapped (FPKM). For sequencing depth, FPKM values were estimated by normalizing gene length.

Figure 1-8

A.

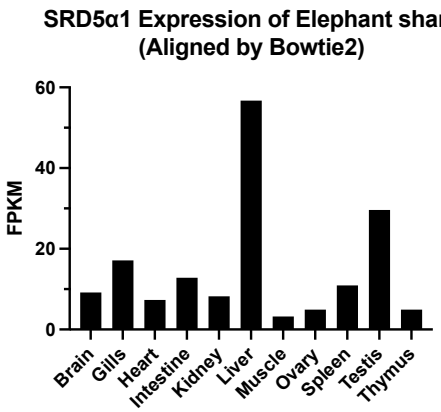

B.

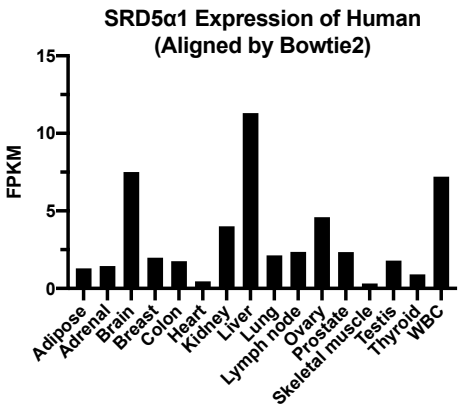

C.

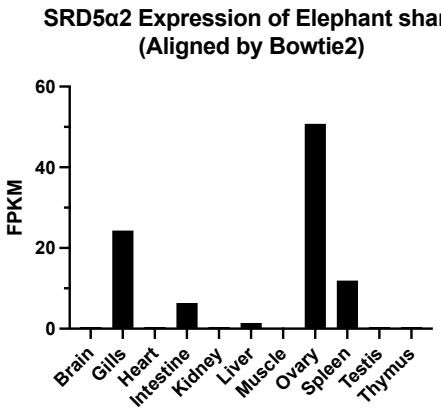

D.

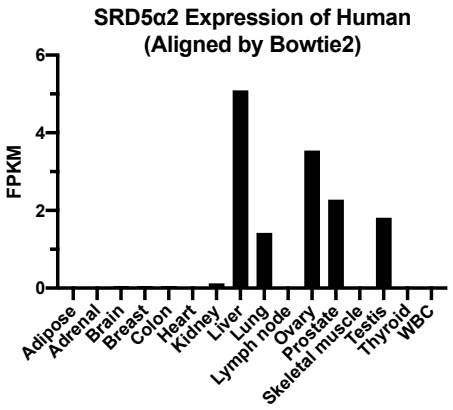

E.

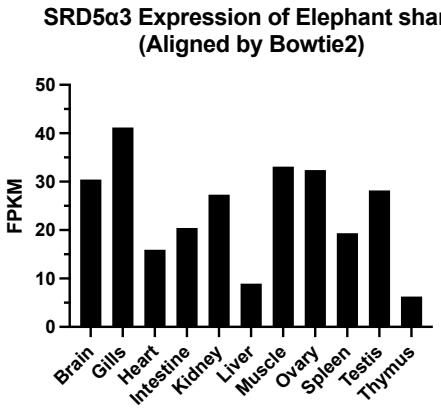

F.

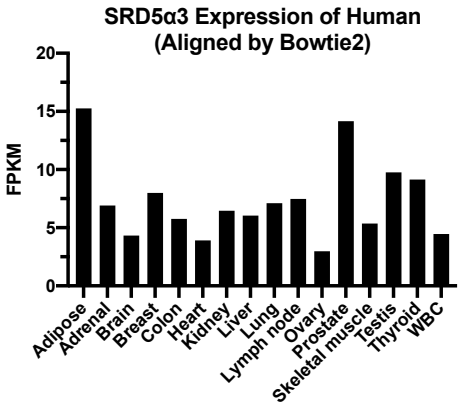

Figure 1-8. Expression levels of 5α-reductase in different tissues in elephant shark and human.

Relative expression of 5α-reductase in elephant shark (A, C, D) and human (B, D, F) were calculated based on RNA-seq data. The abundances of transcripts are shown in normalized counts called fragments per kilobase of exon per million fragments mapped (FPKM). For sequencing depth, FPKM values were estimated by normalizing gene length.

Figure 1-9

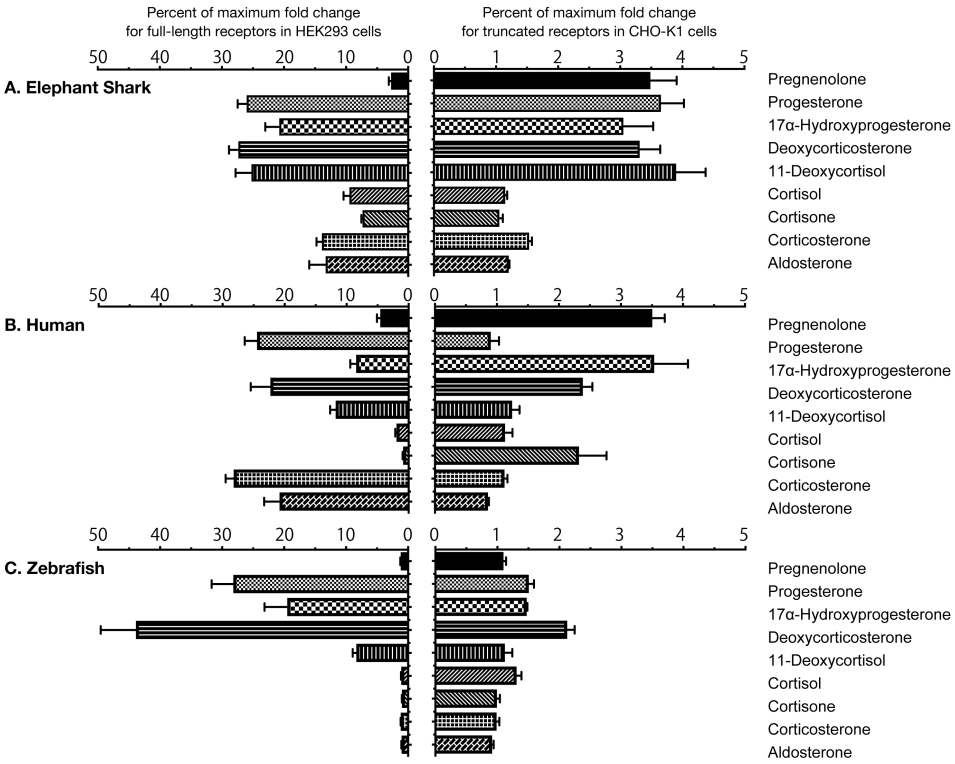

Figure 1-9. Steroid hormone responses of full-length and truncated (lack of N-terminal domain) PRs from elephant shark, human and zebrafish.

Full-length (left) and truncated (right) elephant shark (A), human (B), and zebrafish (C) PRs. Constructs with full-length PRs were coexpressed in HEK293 cells with an MMTV-luc reporter vector. The constructs for truncated PRs, which contain the D and E domains, are fused to a GAL4-DBD and coexpressed in CHO-K1 cells with a luciferase reporter vector containing a GAL4 protein binding cite. Both of the cells were treated with the indicated concentration (10^{-7} M) of steroid hormones or vehicle alone (DMSO) for 44 hours before the reporter gene activity was measured. Each column represents the means ± SEM of 3 independent experiments and expressed as fold activation compared to the activity of cells expressing the same vectors (expressing vector, reporter vector and control vector) that treated with vehicle (DMSO) alone, which was set as 1.

Figure 1-10

A.

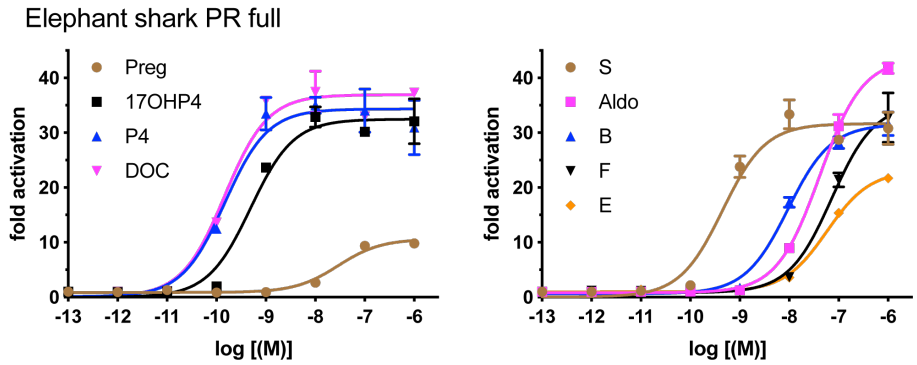

B.

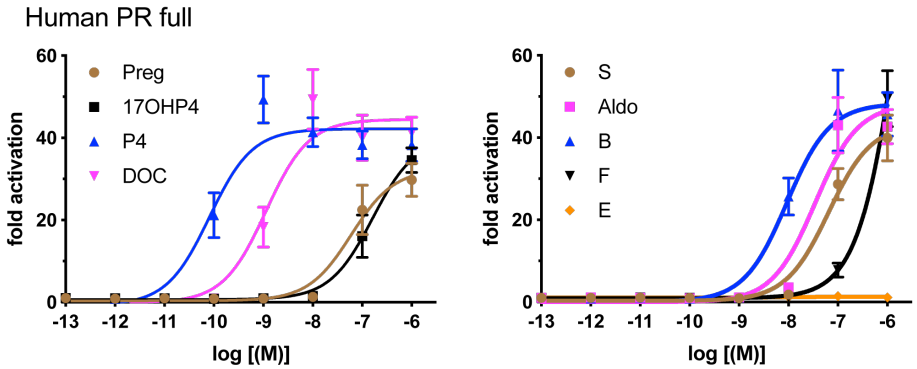

C.

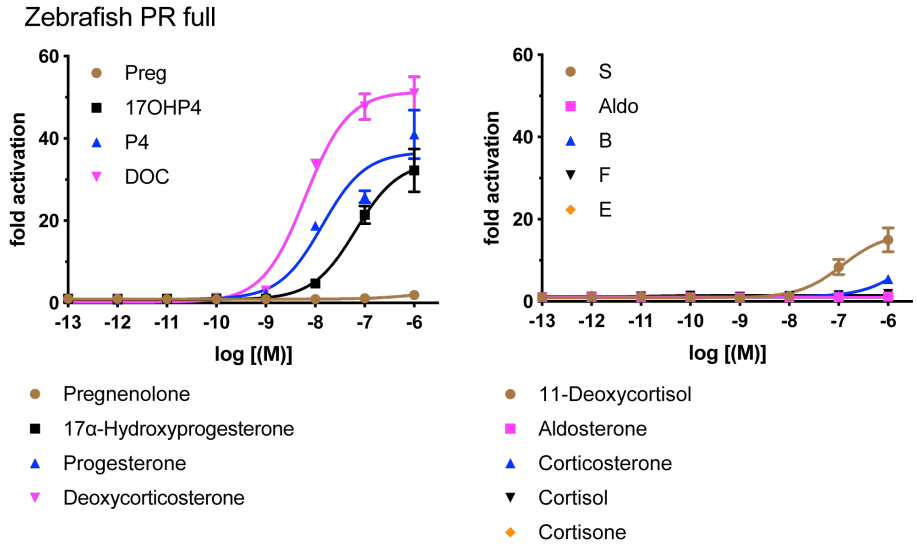

Figure 1-10. Concentration-dependent transcriptional activation by steroids of full-length elephant shark (A), human (B), zebrafish PRs (C).

Plasmids with full-coding region of PRs from elephant shark (A), human (B), and zebrafish (C) were transfected to HEK293 cells with an MMTV-luc reporter vector. The cells were treated with increasing concentrations (10^{-13} M to 10^{-6} M) of indicated steroids or with vehicle (DMSO) alone before reporter gene activity was measured. Data are means ± SEM of 3 independent experiments and expressed as fold activation compared to the activity of cells expressing the same vectors (expressing vector, reporter vector and control vector) that treated with vehicle (DMSO) alone, which was set as 1.

Figure 1-11

A.

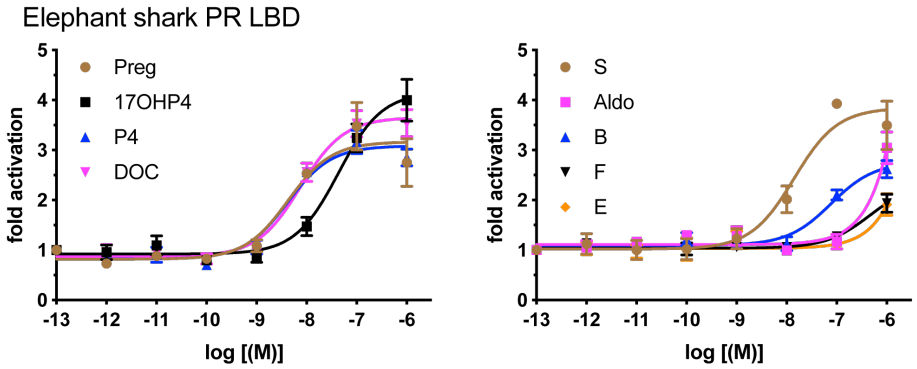

B.

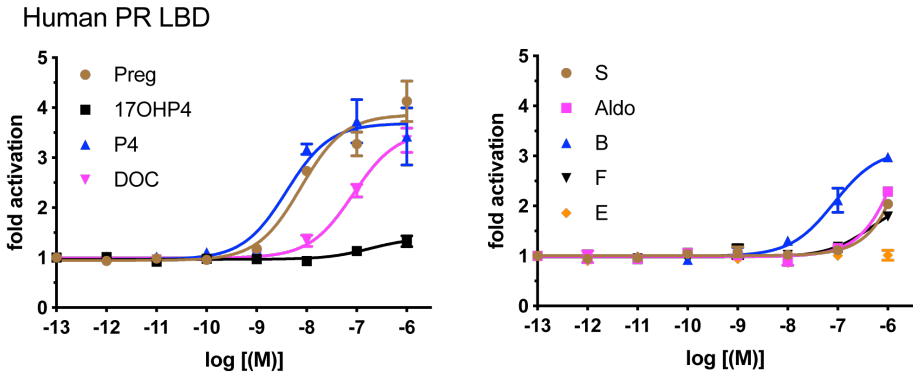

C.

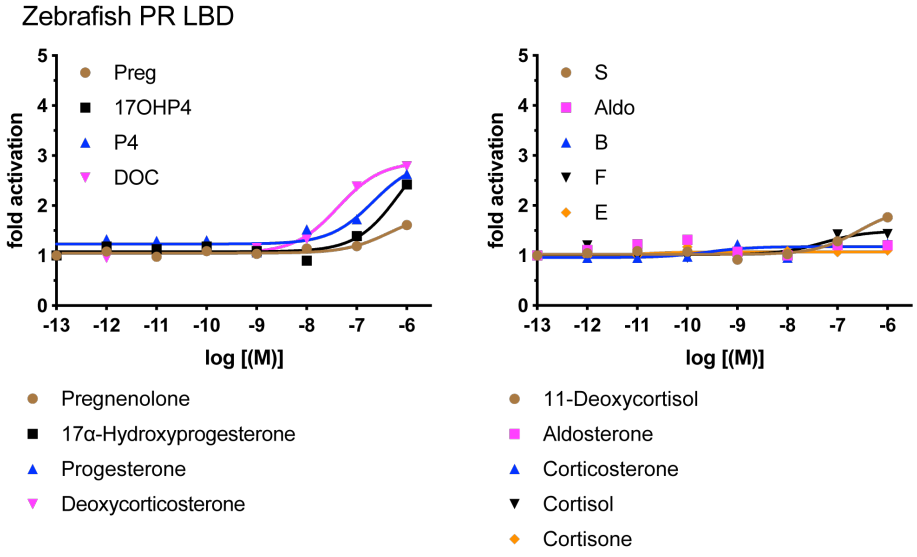

Figure 1-11. Concentration-dependent transcriptional activation by steroids of truncated elephant shark (A), human (B), zebrafish PRs (C).

Plasmids encoding the D and E domains of the indicated PRs and fused to the GAL4-DBD were co transfected to CHO-K1 cells with a luciferase reporter vector containing a GAL4 protein binding site. The cells were treated with increasing concentrations (10^{-13} M to 10^{-6} M) of indicated steroids or with vehicle (DMSO) alone before measuring of reporter gene activity. Data are means ± SEM of 3 independent experiments and expressed as fold activation compared to the activity of cells expressing the same vectors (expressing vector, reporter vector and control vector) that treated with vehicle (DMSO) alone, which was set as 1.

Chapter 2

In silico and *in vitro* analysis of 11-deoxycortisol binding of progesterone receptor

Abstract

Mifepristone (RU486) has antagonistic effects on the hormone-dependent transactivation of human PR and is widely used in clinical practice. In this chapter, I examined the effects of RU486 of elephant shark PR. Results showed that RU486 did not inhibit the progesterone-induced activation of elephant shark PR. Gly-722 in human PR corresponding to Cys-528 in elephant shark PR, which is on the helix 3, is considered essential for the antagonistic effects of RU486 [61]. To confirm the relevance of this amino acid residue, mutant PRs were constructed. Interestingly, RU486 inhibited progesterone-induced activation of the mutant elephant shark PR-Gly528, but not the mutant human PR-Cys722.

Further, I found a decline in steroid response of elephant shark PR-Gly528 by 11-deoxycortisol and an increase in activation of human PR-Cys722. To understand the molecular mechanism of this phenomenon, I investigated the interaction of PR-11-deoxycortisol with *in silico* methods including docking simulation and molecular dynamic (MD) simulation. The simulations indicated the cysteine on helix 3 and methionine on helix 7, Met-607 in elephant shark PR corresponding to Met-801 in human PR, may be crucial for the binding stability of PR with 11-deoxycortisol.

Confirming the importance of the methionine on helix 7, methionine to glycine mutant PRs were made and used to test the steroid activation. Unexpectedly, all the mutants with glycine on the typical position of helix 7 did not show any steroid-induced activation. These results elucidated that the loss of interaction with methionine on helix 7 can lead to the loss of steroid hormone response for PR.

To further investigate the role of the methionine on helix 7 in PR-11-deoxycortisol interaction, methionine to leucine mutant PRs were constructed and evaluated by *in silico*

analysis. Docking simulations indicated the cysteine/glycine switch on helix 3 did not affect the ligand-leucine interaction on helix 7. The results of MD simulation showed that methionine to leucine mutation on helix 7 can lead to a less decrease of binding stability comparing to methionine to glycine mutants.

This chapter provides us with some further understanding into the role of the interaction between ligand and helices in the ligand-binding stability of PR, which has never been described previously.

Key words: progesterone receptor, elephant shark, interhelix interaction, mutation, *in silico* analysis, MD simulation.

Introduction

In the first chapter, the gene expression results have provided me a basic insight into the endocrine system of elephant shark. By comparing the hormone response of elephant shark PR with human and zebrafish, we can gain further understanding on the evolution of steroid activation of PRs as well as the allosteric role of N-terminal domain in the ligand response.

In recent years, studies have focused on an amino acid, Gly-722 in human PR corresponding to Cys-528 in elephant shark PR, which is on the helix 3 of PRs. On this position, PRs of non-mammalians are mainly cysteine while those of mammalians are glycine (Fig. 2-1). The indicated amino acid has been found to play a key role in the antagonistic effect of mifepristone (RU486), a widely used artificial synthetic GR and PR antagonist [61]. It is also considered to be critical in the evolution of mammals [62]. In addition, the crystal structure data of human PR suggested that the replacement of glycine by cysteine in this position could sterically change the binding pocket [63]. Previous study also showed that van der Waals contact between the indicated amino acid and another amino acid, Met-759 in human PR corresponding to Met-565 in elephant shark PR on the helix 5, can be critical in the helix 3-helix 5 (H3-H5) interaction which can affect the ligand response of PR [64]. In contrast, the mutation of these two amino acids in human PR and their corresponding amino acids in human mineralocorticoid receptor (MR) and glucocorticoid receptor (GR) have been proved available to alter the hormone response [65-67]. In addition, this kind of amino acid switch on this position cannot be observed in the same position of other SHRs while CR is cysteine, GR and AR are glycine, MR and ER are alanine. Studies on the role of this amino acid could provide an insight into the evolution of ligand response selectivity of PR. Further, the potential of H3-H5

interaction in the steroid response of cartilaginous fish SHRs has not been studied to date.

In this chapter, I will make several mutated PR constructs to investigate the change of steroid hormone response after the glycine/cysteine switch on the corresponding residue on helix 3 through luciferase assay. Thus, *in silico* methods will be used to investigate the mechanism of the changes of ligand response after the single amino acid mutation.

The information at the molecular level in this chapter can provide an insight into the meaning of the evolution of progesterone receptors from non-mammalian (cysteine) to mammalian (glycine). This research can further provide a deeper insight into the role of typical amino acids within the ligand-binding domain of PR, which has not been well-studied before.

Materials & Methods

Construction of plasmid vectors

With KOD-Plus- Mutagenesis Kit (Toyobo Co., Ltd.), the single amino acid mutagenesis on PRs from elephant shark and human PR was carried out. Primer sets were designed for mutagenesis PCR (Table 2-3). The PCR products were gel-purified and ligated into pcDNA3.1 plasmid (at *Bam* HI-*Not* I site for elephant shark PR, *Kpn* I-*Not* I site for human PR). All DNA sequences of mutant PRs were verified by sequencing.

Homology modelling and molecular docking

For homology modeling, the crystal structure of human progesterone receptor (PDB ID: 1E3K) was used as a template. The target sequence information of ligand-binding domain from human PR-Cys722, wild-type elephant shark PR, and elephant shark PR-Gly528 were submitted to SWISS-MODEL server [68-73] (https://swissmodel.expasy.org/). The output of homology modeling was visualized and analyzed using SAMSON software platform (OneAngstrom. (2020). https://www.samson-connect.net/). The protein-only structure of wild-type human PR was isolated from the template structure for homology modeling by Swiss-PdbViewer [68] (http://www.expasy.org/spdbv/).

The 3D conformer Spatial Data File (SDF) of 11-deoxycortisol was downloaded from PubChem (PubChem CID: 440707. https://pubchem.ncbi.nlm.nih.gov/) and converted to Protein Data Bank (PDB) file using Swiss-PdbViewer. The extension of Autodock Vina Extended [74] on SAMSON software platform was used to predict the ligand-binding poses for 11-deoxycortisol in wild-type and mutant PRs from elephant shark and human. During the docking simulation, 23 side-chains of amino acids around the binding-pocket of the PRs were set to be flexible.

Protein-ligand interaction was analyzed by Discovery Studio Visualizer (BIOVIA, Dassault Systèmes. (2021). https://3ds.com/products-services/biovia/).

Molecular dynamics

In molecular dynamic (MD) simulation, the binding conformations with the lowest binding energy retrieved from docking simulations were used. As PDB files, each PRs and its ligand (11-deoxycortisol) were saved separately.

All MD simulations were performed to evaluate the binding stability of the PR-ligand docked complex using the GROMACS [75-81] (version: 2020.6. https://www.gromacs.org/) with CHARMM36 all-atom force field [82-84] (version: July 2020). The protein-ligand complex was solvated in TIP3P water molecules. The solvated system was neutralized by placing counter ions, Na^+ or Cl^-. After that, the system was energy minimized for 50,000 steps followed by equilibration using the NVT and NPT ensemble for 100 picoseconds (ps) each. To maintain a constant temperature at 300 K with standard pressure of 1.0 bar, Berendsen thermostat was used, and each MD simulation was performed for 10 nanoseconds (ns). The Coulombic interaction energy and Lennard-Jones potential energy between ligand and receptor, and the RMSD of ligand was calculated using GROMACS. The fluctuation of values during the 10 ns MD simulation was visualized by Gnuplot (version: 5.4. http://www.gnuplot.info/).

Results

Antagonized transcriptional activation of full-length and truncated PRs by RU486.

To analyze the effects of RU486, a PR antagonist, I examined antagonized transactivation of both full-length and truncated PRs from elephant shark and human, as well as full-length PRs from zebrafish and turtle (Fig. 2-2). The results revealed that only human PR can be antagonized by RU486. Further, I found that truncated human PR also decreased progesterone-stimulated transactivation by RU486.

Effects of single amino acid mutation on helix 3 to steroid activation of PR.

The amino acid, Gly-722 of human PR is a key of the antagonistic effect by RU486 to PR [61]. I found that elephant shark PR possesses cysteine residue at the position corresponding to Gly-722 of human PR.

To understand the role of amino acids in this position, I introduced a single amino acid mutation of Cys528 to Gly (C528G) on elephant shark PR and Gly-722 to Cys (G722C) on human PR, and examined their ligand response using luciferase assay. The antagonistic effect of RU486 showed a reverse result compared to the wild type ones (Fig. 2-3). In contrast, the ligand specificities were also changed after the mutation on this position (Fig. 2-4). Cysteine to glycine mutation on elephant shark PR results in reduction of progesterone-, 17α-hydroxyprogesterone-, deoxycorticosterone-, 11-deoxycortisol-, and cortisone-stimulated transactivation, as well as the increase of responsiveness to aldosterone (Fig. 2-4, A). In parallel, glycine to cysteine mutation on human PR leads to reduction of responsiveness to progesterone, 17,20-DP, 11-deoxycorticosterone, aldosterone, and corticosterone, meanwhile an increased responsiveness towards 11-deoxycortisol was observed (Fig. 2-4, B).

In addition, I also examined the concentration-dependency of 11-deoxycortisol response of these two mutant PRs with 2 different reporter vectors, MMTV-luc and TAT3 (Fig. 2-5 and Table 2-1). The results indicated that human PR-Cys722 and wild-type elephant shark, both of which have a cysteine on helix 3, showed a higher response and lower EC_{50} values, and the result was not affected by the reporter vector used in the luciferase assay.

I investigated PR-11-deoxycortisol interaction through docking simulation and molecular dynamic (MD) simulation to further understand the structural basis of the steroid activation of wild-type and mutant PRs from human and elephant shark.

Interaction with cysteine on helix 3 and methionine on helix 7 may be crucial for 11-deoxycortisol binding stability of PR.

Docking simulation results showed that only PRs with cysteine on helix 3, showed alkyl interaction between 11-deoxycortisol and 2 residues, Cys528 and Met607 in elephant shark PR, corresponding to Cys722 and Met801 in human PR-Cys722 (Fig. 2-6 A, D). When interacting with PRs with glycine on helix 3, 11-deoxycortisol only have van der Waal's contact with Gly528 and Met607 in elephant shark PR-Gly528, which corresponds to Gly722 and Met801 in human PR (Fig. 2-6 B, C). Furthermore, MD simulation results (Fig. 2-7 A, F) elucidated that in comparison with other PRs, wild-type elephant shark PR and human PR-Cys722 bound to 11-deoxycortisol showed lower Coulombic interaction potential which reflects electrical binding, suggesting that wild-type elephant shark PR and human PR-Cys722 have higher binding stability with 11-deoxycortisol than those with glycine on helix 3.

However, the average values of Lennard-Jones potential which reflects the van der Waal's contact, and RMSD values which represent the conformational fluctuations of the

ligand during the 10 ns simulation (Fig. 2-7 B, C, G, H) did not show a significant difference.

The average value of hydrogen bond increased obviously after glycine to cysteine mutation in human PR, while not having much difference in elephant shark PR (Fig. 2-7 D). Percentages of different hydrogen numbers were centralized, reflecting that the binding pose is comparatively stable during the 10 ns simulation (Fig. 2-7 E). Whether changes of hydrogen bond numbers can lead to the difference of steroid activation remains to be elucidated. Further investigation is necessary.

These results raise the possibility that the interaction between 11-deoxycortisol with cysteine on helix 3 and methionine on helix 7 in PRs is crucial for the binding stability, which may lead to a change of ligand response.

Loss of interaction with methionine on helix 7 can lead to the loss of steroid hormone response for PR.

To verify the hypothesis that the interaction of 11-deoxycortisol with the cysteine on helix 3 and methionine on helix 7 in PRs is crucial for binding stability, I created 4 constructs with methionine to glycine mutation on helix 7, based on wild-type elephant shark PR and human PR constructs, elephant shark PR-Gly528 and human PR-Cys722. The mutation implies a loss of the side-chain of methionine residue. Then, I investigated receptor-ligand interaction of these mutant constructs with docking simulation and MD simulation.

Docking simulation results showed that binding poses did not change largely after methionine to glycine switch on helix 7 (Fig. 2-8). Also, the residues that interact with 11-deoxycortisol were similar to the previous results, whereas the correspondent residue

on helix 7 did not interact with the ligand anymore after methionine to glycine mutation as the distance between the residue and the ligand becomes too far away to have interaction (＞8Å, data not showed).

Although both of the average values of Coulombic interaction and Lennard-Jones potential showed comparatively low levels (Fig. 2-9 A, B), the fluctuations of Lennard-Jones potential were unstable during the 10 ns simulation (Fig. 2-9 G), implying that the receptor-ligand interaction is unstable during the 10 ns simulation. On the other hand, the fluctuations of Coulombic interaction and RMSD were stable compared to the Lennard-Jones potential (Fig. 2-9 F, H).

While the average number of hydrogen bonds of all 4 constructs was low (Fig. 2-9 D), the percentage of different hydrogen numbers was decentralized compared to previous results (Fig. 2-9 E). This reflects that the binding pose is comparatively unstable during the 10 ns simulation.

To further confirm the effect of methionine to glycine mutation on helix 7 to the steroid activation of PR, I introduced a single amino acid mutation of Met607 to Gly (M607G) on elephant shark PR and elephant shark PR- Gly528, and of Met801 to Gly (M801G) on human PR and human PR-Cys722, and examined their ligand response with a luciferase assay.

All 4 constructs, elephant shark PR-Gly607, elephant shark PR-Gly528Gly607, human PR-Gly801, human PR-Cys722Gly801, showed no response to progestins and corticoids (Fig. 2-10). These results elucidated that the loss of interaction with methionine on helix 7 might lead to steroid hormone response loss for PR. Unfortunately, these results cannot confirm the importance of interaction between 11-deoxycortisol and cysteine on helix 3 and methionine on helix 7 in PRs.

Effects of methionine to leucine mutation on helix 7 on PR-11-deoxycortisol interaction.

As previous results showed that the loss of interaction with methionine on helix 7 can lead to the loss of steroid hormone response, it is important to construct another mutant that will not lead to the loss of steroid activation. I examined the amino acid sequence of residues around helix 7 in steroid hormone receptors, including PR, MR, GR, AR, and ER, from 6 species (Fig. 2-11). All ERs have a leucine on the corresponding Met607 position of elephant shark PR, indicating a new orientation to study the role of this residue in steroid hormone activation of PR.

As before, I created 4 constructs with methionine to leucine mutation on helix 7 based on constructs of wild-type elephant shark PR and human PR, elephant shark PR-Gly528, and human PR-Cys722, and investigated receptor-ligand interaction of the new constructs with docking simulation and MD simulation.

Interestingly, docking simulation results showed that the cysteine/glycine switch did not obviously affect the interaction between the ligand and the residues on helix 7, Met-600, Leu-603, and Leu-607 in elephant shark PR-M607L and elephant shark PR-C528G-M607L corresponding to Phe-794, Leu-797, and Leu-801 in human PR-M801L and human PR-G722C-M801L (Fig. 2-12). Only Leu-607 in elephant shark PR-C528G-M607L did interact with the D-ring of 11-deoxycortisol instead of the B-ring. These findings provide an interesting insight into the role of the methionine on helix 7 in steroid activation of PR.

MD simulations revealed that the average values of Coulombic interaction and RMSD (Fig. 2-13 A&C) exhibit a reversed result compared with the results shown in figure 2-7

A and C. Interestingly, although the average level of Lennard-Jones potential (Fig. 2-13 B) is similar to the previous results, the fluctuations (Fig. 2-13 G) are comparatively stable comparing the results of methionine to glycine switch on helix 7 (Fig. 2-9 G). However, the analysis of hydrogen bond interaction displayed a similar result to mutants with glycine on helix 7 (Fig. 2-13 D&E), indicating that the binding pose could still be unstable compared to helix 7 non-mutated constructs.

I examined the average values of the standard deviation of the observed receptor-ligand interaction indexes (Fig. 2-14, Table 2-2). When the methionine on helix 7 was replaced by glycine, the standard deviation of all observed indexes, Coulombic interaction energy, Lennard-Jones potential energy, RMSD and hydrogen-bond number, were increased. These changes also suggest that the receptor-ligand interaction has become unstable during the 10 ns MD simulation. On the other side, when the methionine on helix 7 was replaced by leucine, the standard deviations of Coulombic interaction energy, Lennard-Jones potential energy and RMSD were comparatively closer to the wild-type methionine than the glycine mutant.

Discussion

It is considered that Cys-528 in elephant shark PR and Gly-722 in human PR, both are on helix 3, can directly affect the antagonistic effect of RU486 and artificial synthetic ligands [61]. Although the role of these residues of PR was recognized by its responsibility for a non-physiological ligand, investigating the characteristic and evolutionary meaning of the cysteine to glycine switch is still intriguing. In particular, PR has this kind of amino acid switch on this position, while other SHRs are highly conserved. Furthermore, PRs that has cysteine at this position is the only group shares the same amino acid (cysteine) as CR, the ancestral type of MR and GR. Understanding the two ways of evolution of this residue, from cysteine to alanine (MR & ER), from cysteine to glycine (GR & AR), can provide much useful information for the molecular evolution of steroid hormone receptors.

In chapter 2, I observed the inversion of the antagonistic effect of RU486 on PRs after the glycine/cysteine switch on helix 3, which is similar to previous studies [61]. The diminished 11-deoxycortisol activation of elephant shark PR-Gly528 and increased response of human PR-Cys722 were observed in parallel (Fig. 2-4, 5 & Table 2-1). To further understand the molecular mechanism of this phenomenon, I used *in silico* methods to analyze receptor-ligand interaction differences. Interestingly, I found that methionine on helix 7, Met-607 in elephant shark PR corresponding to Met-801 in human PR, may play an important role in binding of PR to 11-deoxycortisol (Fig. 2-6 & 2-15).

To confirm this hypothesis, the *in silico* and *in vitro* methods were applied. In molecular simulations, the loss of interaction between steroid and methionine on helix 7 could result in destabilizing 11-deoxycortisol binding for PRs (Fig. 2-8, 9). The i*n vitro* experiments also confirmed this. All 4 PR constructs with methionine to glycine mutation on helix 7

showed complete loss of response to the progestins and corticoids but not to 11-deoxycortisol (Fig. 2-10). These results elucidated the crucial role of this residue and the interaction of the ligand with helix 7 in the steroid activation of PR. Despite further investigations are needed, I considered that the decrease of interaction between helix 7 and the B-ring of steroid hormones may result in destabilization of ligand-binding.

Further, it is important to clarify that the PRs with methionine to glycine mutation on helix 7 still can bind to ligands. My MD simulation results (Fig. 2-9) provide the possibility that PRs with methionine to glycine mutation, are still able to bind to 11-deoxycortisol. Unfortunately, it is difficult to evaluate if ligand-binding occurs, while receptors do not exhibit an obvious response to all steroid hormones used in my experiments.

It is not enough to explain the reason for the loss of ligand response after methionine to glycine mutation on helix 7. To know the role of this residue, therefore, I choose to introduce another type of mutation, methionine to leucine mutation, at the same position. Sequence alignment indicated that this methionine is highly conserved through PR, GR, MR, CR, and AR, except for ER, which has a leucine at this position (Fig. 2-11). In contrast to methionine to glycine mutation, docking simulations show that methionine to leucine mutation can maintain interaction of 11-deoxycortisol with 3 residues on helix 7, residue 600, 603, and 607 in elephant shark PR, corresponding to residue 794, 797, and 801 in human PR, respectively. The interaction with helix 7 also reflected as lower standard deviations (Table 2-2), which means that these mutants show higher stability than methionine to glycine mutants during the 10 ns MD simulations.

These results indicated that methionine to leucine mutation on helix 7 may be able to prevent the loss of steroid activation after mutation. However, this prediction should be

validated through *in-vitro* experiments.

Furthermore, the S-S interaction between cysteine on helix 3 and other residues should also be considered. Although there is no report about the role of disulfide bond in PR to date. However, intramolecular disulfide bond is reported to involve in the DNA-binding of GR [91]. Intermolecular S-S interaction is reported to be the connecting form of GR dimerization [92]. When it is a cysteine on helix 3 of PR, the intramolecular S-S interaction with other cysteine may form the binding pocket into a shape that is easier and more stable for 11-deoxycortisol to bind to it, but also harder for some of the steroid hormones. It is also reported that the glycine to cysteine mutation on helix 3 of human PR can result in an additional connect of this residue with Met-909, which is in the AF-2 region [62]. This may also change the structure of binding pocket.

In addition, to evaluate the relationship between *in silico* results and *in vitro* results, we need to obtain large amounts of data to analyze it.

Table 2-1. EC_{50} values for 11-deoxycortisol response transcriptional activation of wild-type elephant shark, wild-type human PR, elephant shark PR-Cys528Gly and human PR-Gly722Cys.

11-deoxycortisol	ElePR_WT	ElePR_C528G	HuPR_WT	HuPR_G722C
EC_{50} (nM) (MMTV)	0.5	5.2	51.6	6.7
95% confidence intervals	0.3-0.7	4.2-6.5	39.5-67.0	5.0-8.9
EC_{50} (nM) (TAT3)	0.5	5.7	24.5	7.2
95% confidence intervals	0.4-0.6	5.0-6.6	20.1-29.7	5.7-9.1

Table 2-2. Average values of standard deviations of MD simulation results.

Amino acid on helix 7	Methionine	Glycine	Leucine
Coulombic energy [kJ/mol]	14.6	19.5	16.5
Lennard-Jones energy [kJ/mol]	9.7	11.1	10.1
RMSD [nm]	0.023	0.032	0.027
hydrogen-bond number	0.59	0.84	0.85

Table 2-3. PCR primers used for mutagenesis.

	Forward	Reverse
elephant shark PR-C528G	5’-GGC GAG AAA CAA CTA GTC TCT GTT GTG-3’	5’-CAG CCT GTT CAG ACT GGT TAG CAG-3’
human PR-G722C	5’-TGC GAG AGG CAA CTT CTT TCA GTA GTC-3’	5’-TAG TTG ATT AAG ACT TGT CAG CAA AG-3’
elephant shark PR-M607G	5’-GGG CGG CAG ATC TCT CAA GAA TTC ATT-3’	5’-TGC TAT GCA CAG ATC ATA CAT CGC AGA-3’
human PR-M801G	5’-TGG CAG ATC CCA CAG GAG TTT GTC-3’	5’-CCC GGT AAG GCA TAA TGA ATA GAA TGA TGA-3’
elephant shark PR-M607L	5’-TTG CGG CAG ATC TCT CAA GAA TTC ATT CAT-3’	5’-TGC TAT GCA CAG ATC ATA CAT CGC AGA-3’
human PR-M801L	5’-TGG CAG ATC CCA CAG GAG TTT GTC-3’	5’-CAA GGT AAG GCA TAA TGA ATA GAA TGA TGA TTC-3’

Figure 2-1

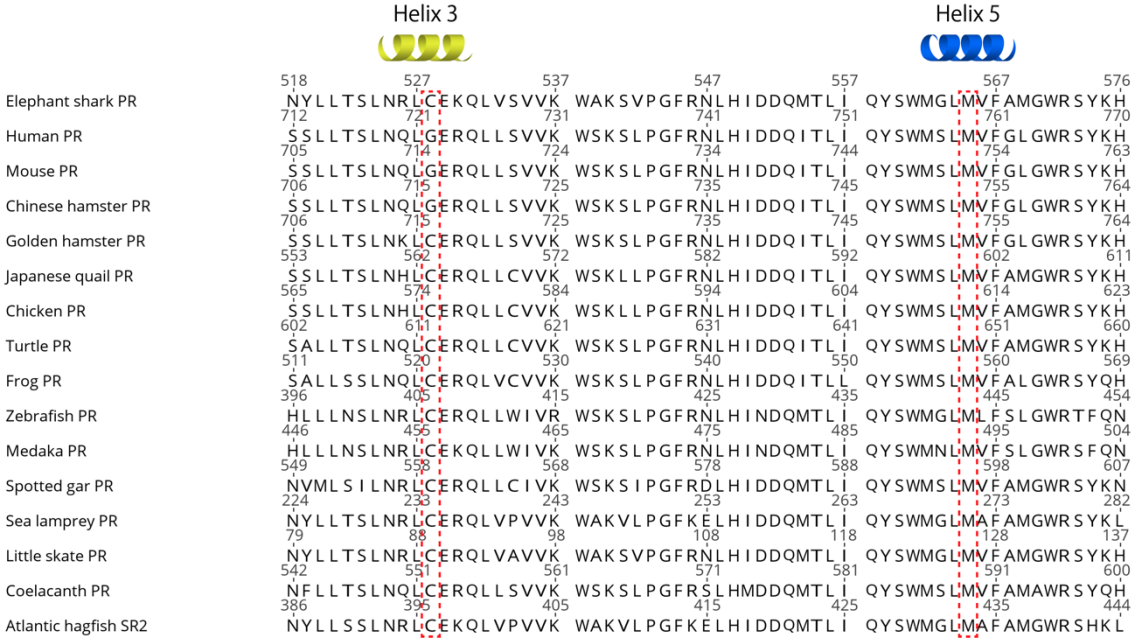

Figure 2-1. Alignment of helix 3 through helix 5 in vertebrate PRs.

Alignment of amino acid sequences from elephant shark PR and various vertebrate PRs. Gly-722 in human PR corresponding to Cys-528 in elephant shark PR is on helix 3 within ligand-binding domain. Met-759 in human PR corresponding to Met-565 in elephant shark PR is on helix 5 of LBD.

Figure 2-2

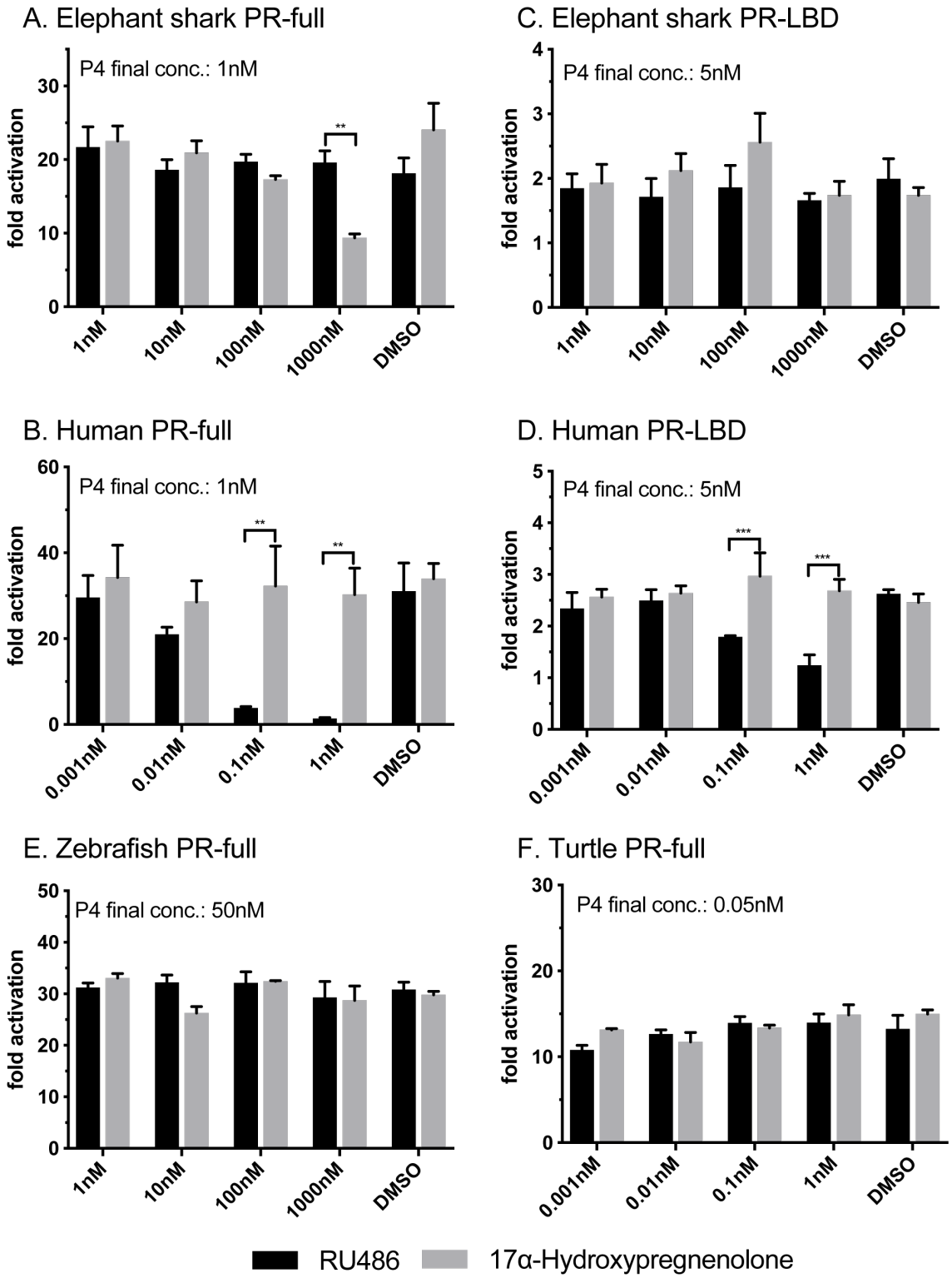
A. Elephant shark PR-full
P4 final conc.: 1nM
fold activation
1nM
10nM
100nM
1000nM
DMSO
C. Elephant shark PR-LBD
P4 final conc.: 5nM
B. Human PR-full
P4 final conc.: 1nM
0.001nM
0.01nM
0.1nM
1nM
DMSO
D. Human PR-LBD
P4 final conc.: 5nM
E. Zebrafish PR-full
P4 final conc.: 50nM
F. Turtle PR-full
P4 final conc.: 0.05nM
RU486
17α-Hydroxypregnenolone

Figure 2-2. Antagonized transactivation of full-length and truncated vertebrate PRs by RU486.

Plasmids with the full-coding region of PRs from elephant shark, human, zebrafish, and turtle were transfected to HEK293 cells with an MMTV-luc reporter vector (A to B, E to F). Constructs encoding the D and E domains of the elephant shark and human PRs fused to the GAL4-DBD were co-transfected to CHO-K1 cells with a luciferase reporter vector containing a GAL4 protein binding cite (C to D). The cells were treated with the indicated concentration of progesterone (P4), with addition increasing concentrations (10^{-12} M to 10^{-6} M) of PR antagonist (RU486) /control steroid (17α-hydroxypregnenolone) /vehicle (DMSO), or with vehicle (DMSO) alone before measuring of reporter gene activity. Data are means ± SEM of 3 independent experiments and expressed as fold activation compared to the activity of cells expressing the same vectors (expressing vector, reporter vector, and control vector) that treated with vehicle (DMSO) alone, which was set as 1.

Figure 2-3

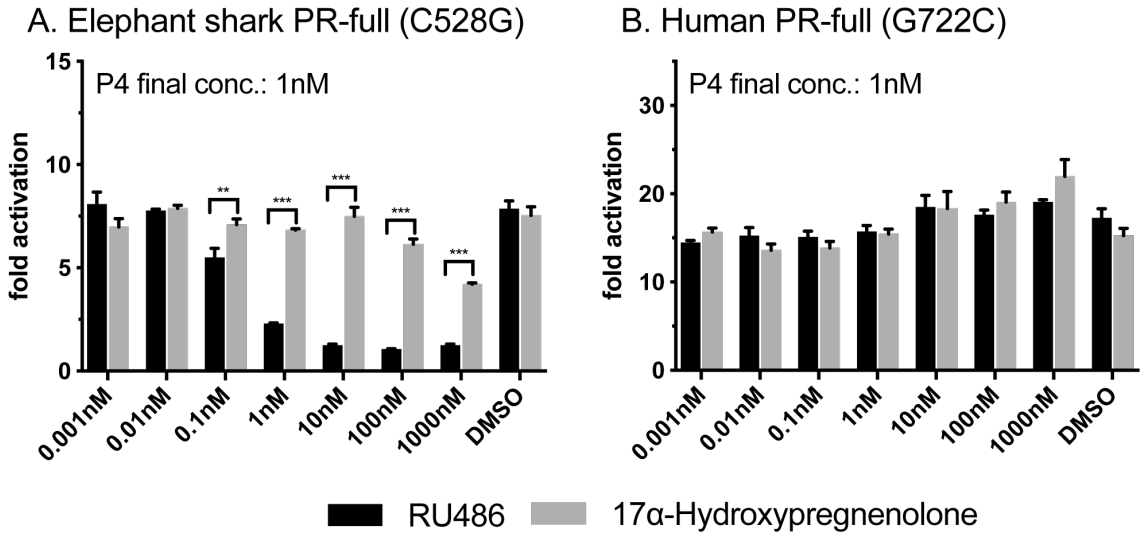

Figure 2-3. Comparison of antagonized transactivation of full-length PRs by RU486 after a glycine/cysteine switch on helix 3 in elephant shark and human PR.

Plasmids encoding the full region of PRs from elephant shark, human, zebrafish, and turtle were transfected to HEK293 cells with an MMTV-luc reporter vector. The cells were treated with the indicated concentration of progesterone (P4), with addition concentrations (10^{-12} M to 10^{-6} M) of PR antagonist (RU486) /control steroid (17α-hydroxy-pregnenolone) /vehicle (DMSO), or with vehicle (DMSO) alone before the activity of the reporter gene was measured. Data are means ± SEM of 3 independent experiments and expressed as fold activation compared to the activity of cells expressing the same vectors (expressing vector, reporter vector, and control vector) that treated with vehicle (DMSO) alone, which was set as 1.

Figure 2-4

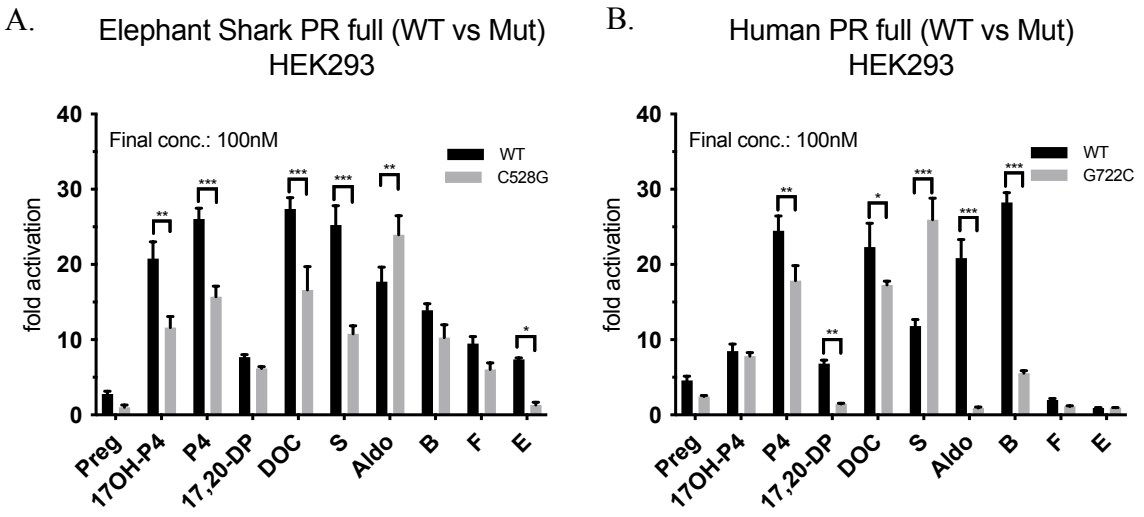

Figure 2-4. Comparison of ligand response after a glycine/cysteine switch on helix 3 in elephant shark and human PR.

Plasmids with the full coding region of PRs with a single amino acid mutation from elephant shark and human were transfected to HEK293 cells with an MMTV-luc reporter vector. Cells were treated with the indicated concentration (10^{-7} M) of steroid hormones or vehicle alone (DMSO) for 44 hours before the activity of the reporter gene was measured. Data are means ± SEM of 3 independent experiments and expressed as fold activation compared to the activity of cells expressing the same vectors (expressing vector, reporter vector, and control vector) that treated with vehicle (DMSO) alone, which was set as 1. The results were compared to the results shown in Fig. 1-9 (**A** and **B**, left). The comparison between 2 groups was analyzed with multiple *t*-test. Statistical significance was shown as: $P < 0.05$, *; $P < 0.01$, **; $P < 0.001$, ***.

Preg: pregnenolone; 17OH-P4: 17-OH-progesterone; P4: progesterone; 17,20-DP: 17α,20β-Dihydroxy-4-pregnen-3-one; DOC: 11-deoxycorticosteronel; S: 11-deoxycortisol; Aldo: aldosterone; B: corticosterone; F: cortisol; E: cortisone.

Figure 2-5

A.

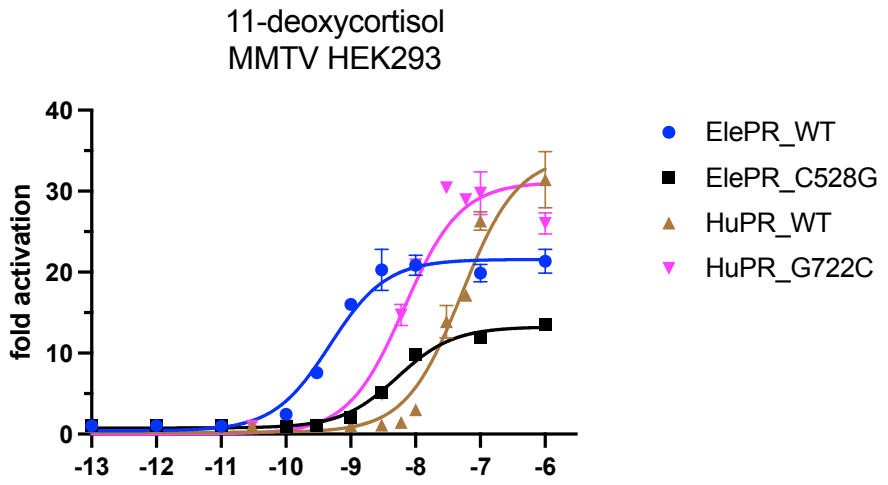
11-deoxycortisol
MMTV HEK293
fold activation
40
30
20
10
0
-13
-12
-11
-10
-9
-8
-7
-6
ElePR_WT
ElePR_C528G
HuPR_WT
HuPR_G722C

B.

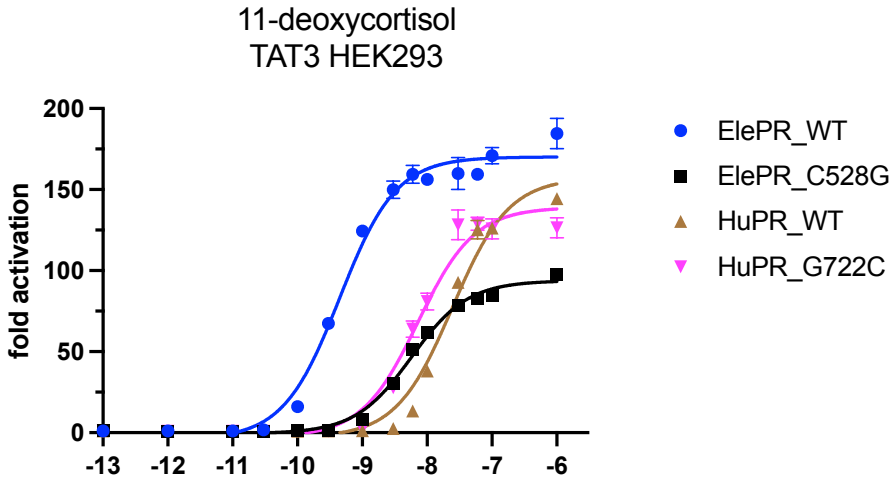
11-deoxycortisol
TAT3 HEK293
fold activation
200
150
100
50
0
-13
-12
-11
-10
-9
-8
-7
-6
ElePR_WT
ElePR_C528G
HuPR_WT
HuPR_G722C

Figure 2-5. Comparison of ligand-dependent response to 11-deoxycortisol after glycine/cysteine switch on helix 3 in elephant shark and human PR.

Plasmids encoding full-length PRs with a single amino acid mutation from elephant shark and human were transfected to HEK293 cells with an MMTV-luc or TAT3 reporter vector. The cells were treated with increasing concentrations (10^{-13} M to 10^{-6} M) of 11-deoxycortisol or with vehicle (DMSO) alone before the measurement of reporter gene activity. Data are means ± SEM of 3 independent experiments and expressed as fold activation compared to the activity of cells expressing the same vectors (expressing vector, reporter vector, and control vector) that treated with vehicle (DMSO) alone, which was set as 1.

Figure 2-6

A.

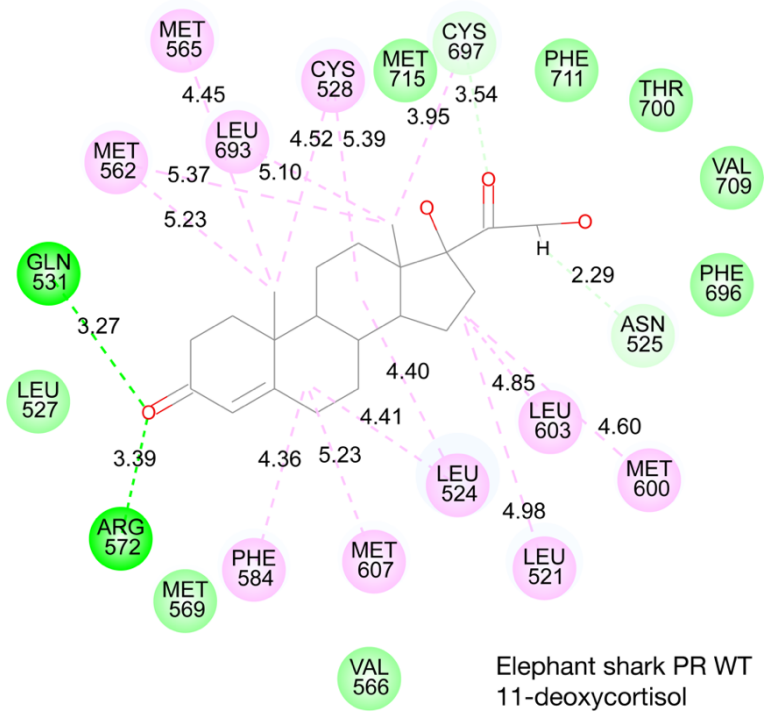
MET 565
CYS 528
MET 715
CYS 697
PHE 711
THR 700
VAL 709
PHE 696
ASN 525
LEU 603
MET 600
LEU 524
LEU 521
MET 607
PHE 584
MET 569
ARG 572
LEU 527
GLN 531
MET 562
LEU 693
VAL 566
4.45
4.52
5.39
3.95
3.54
5.37
5.10
5.23
H
2.29
3.27
4.40
4.85
4.41
4.60
3.39
4.36
5.23
4.98
Elephant shark PR WT
11-deoxycortisol

B.

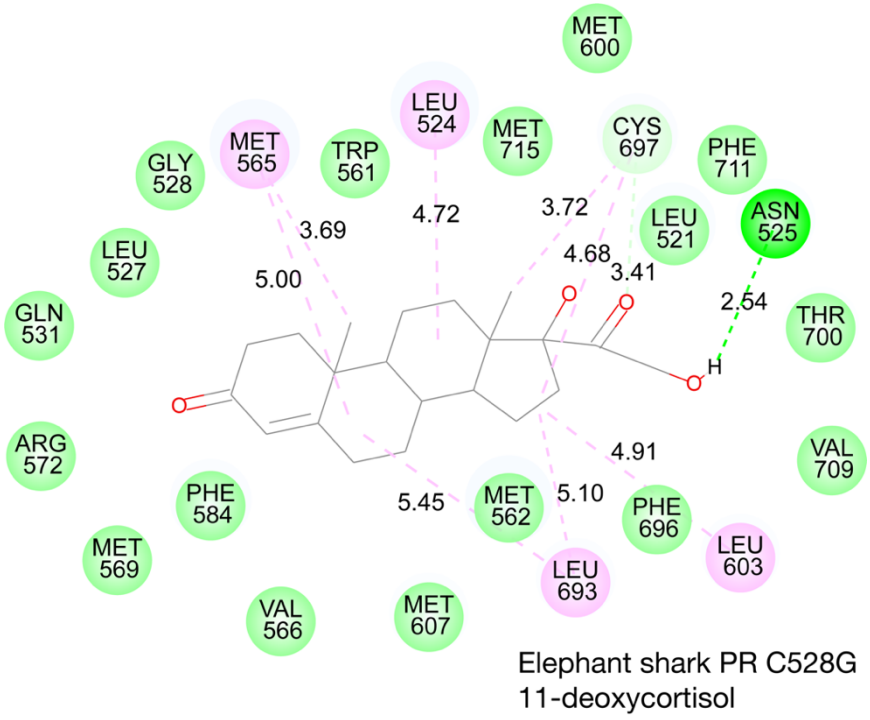
MET 600
LEU 524
MET 715
CYS 697
PHE 711
MET 565
TRP 561
GLY 528
LEU 527
GLN 531
ARG 572
PHE 584
MET 569
VAL 566
MET 607
LEU 693
MET 562
PHE 696
LEU 603
LEU 521
ASN 525
THR 700
VAL 709
3.69
4.72
3.72
5.00
4.68
3.41
2.54
H
4.91
5.45
5.10
Elephant shark PR C528G
11-deoxycortisol

C.

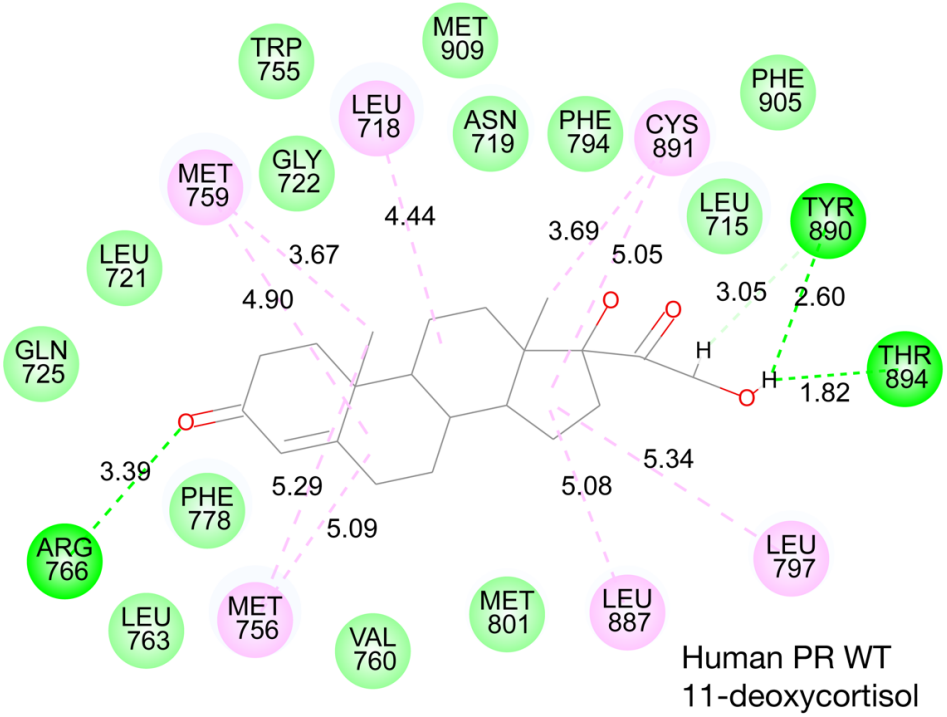
TRP 755
MET 909
LEU 718
ASN 719
PHE 794
CYS 891
PHE 905
MET 759
GLY 722
LEU 715
TYR 890
LEU 721
GLN 725
THR 894
ARG 766
PHE 778
LEU 763
MET 756
VAL 760
MET 801
LEU 887
LEU 797
4.44
3.69
5.05
3.67
4.90
3.05
2.60
1.82
3.39
5.29
5.08
5.34
5.09
Human PR WT
11-deoxycortisol

D.

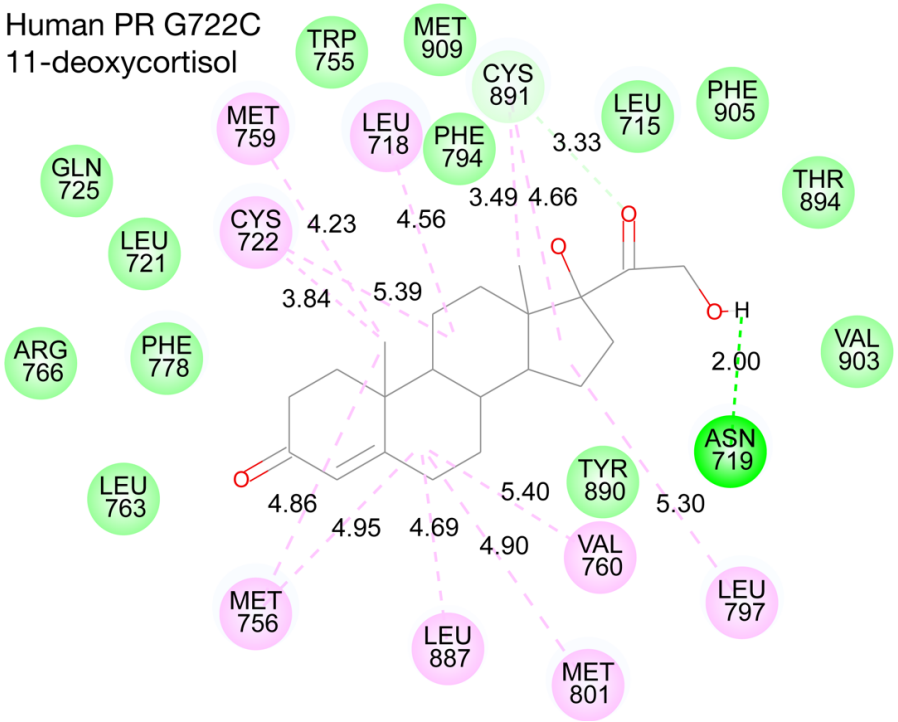
Human PR G722C
11-deoxycortisol
TRP 755
MET 909
CYS 891
LEU 715
PHE 905
MET 759
LEU 718
PHE 794
3.33
GLN 725
THR 894
3.49
4.66
CYS 722
4.23
4.56
LEU 721
3.84
5.39
ARG 766
PHE 778
VAL 903
2.00
ASN 719
LEU 763
TYR 890
4.86
5.40
5.30
4.95
4.69
4.90
VAL 760
MET 756
LEU 797
LEU 887
MET 801

Figure 2-6. Docking poses of 11-deoxycortisol bound to wild-type and mutant PRs from elephant shark and human.

Residues interacting with 11-deoxycortisol when bound to wild-type elephant shark PR (A), elephant shark PR-Cys528Gly (B), wild-type human PR (C), human PR-Gly722Cys (D). Residues in green represent amino acids that bind to ligand through hydrogen-bond. Residues in light green represent amino acids that have van der Waal's contact with a ligand. Residues in pink indicate amino acids that interact with ligand through hydrophobic interaction including Alkyl-Alkyl or Pi-Alkyl interactions. Numbers on the lines connecting residues and ligand show the distance (Å).

Figure 2-7

A.

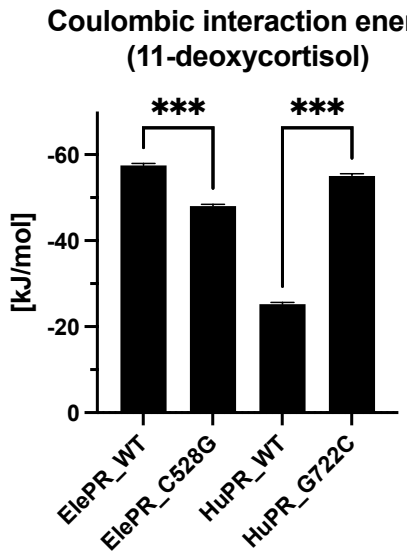

B.

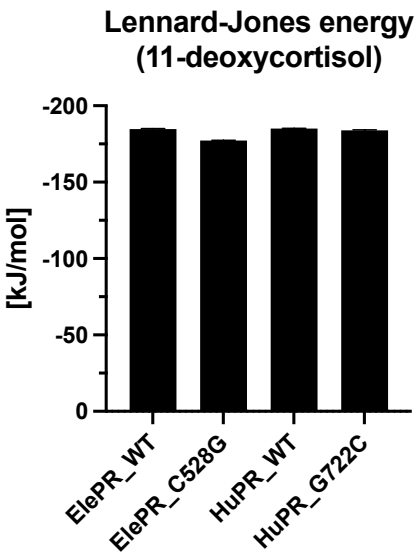

C.

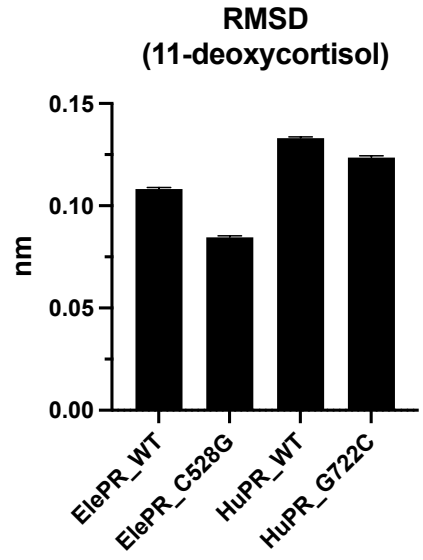

D.

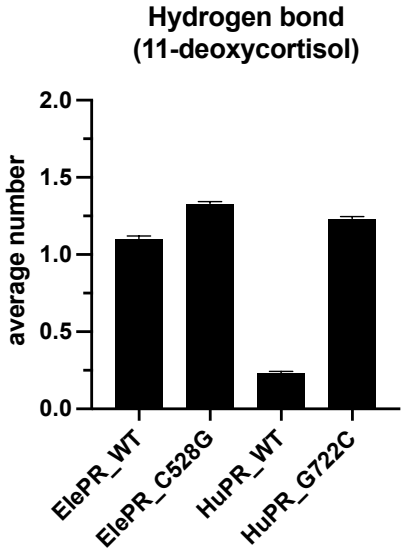

E.

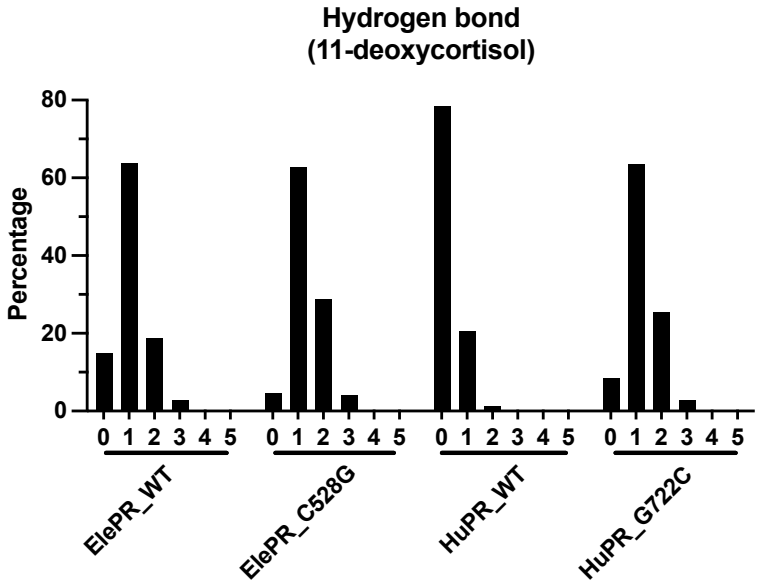
Hydrogen bond
(11-deoxycortisol)
Percentage
80
60
40
20
0
0 1 2 3 4 5
0 1 2 3 4 5
0 1 2 3 4 5
0 1 2 3 4 5
ElePR_WT
ElePR_C528G
HuPR_WT
HuPR_G722C

F

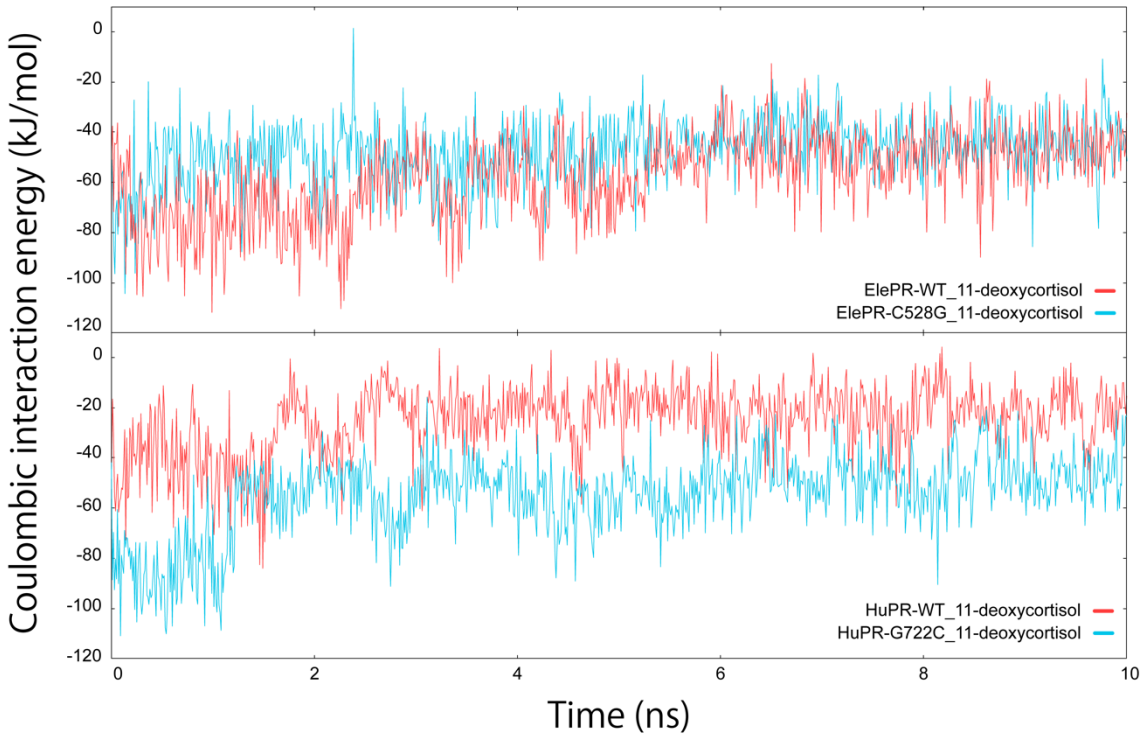
Coulombic interaction energy (kJ/mol)
0
-20
-40
-60
-80
-100
-120
ElePR-WT_11-deoxycortisol
ElePR-C528G_11-deoxycortisol
HuPR-WT_11-deoxycortisol
HuPR-G722C_11-deoxycortisol
0
2
4
6
8
10
Time (ns)

G.

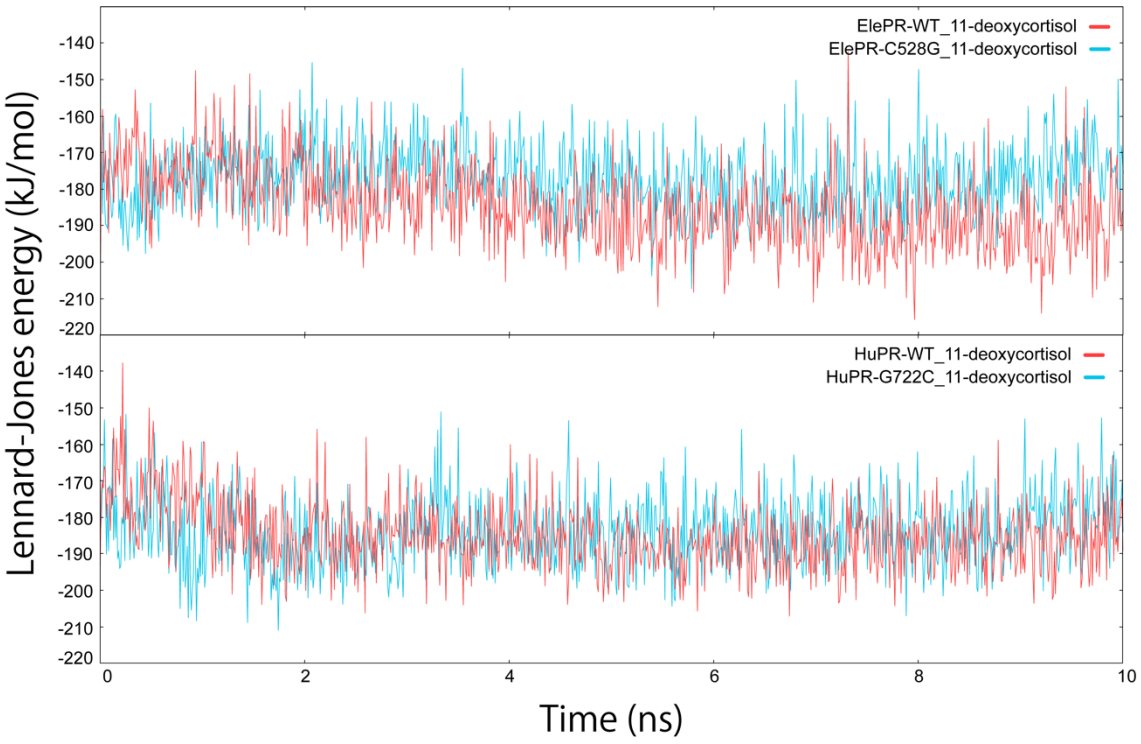
ElePR-WT_11-deoxycortisol
ElePR-C528G_11-deoxycortisol
HuPR-WT_11-deoxycortisol
HuPR-G722C_11-deoxycortisol
Lennard-Jones energy (kJ/mol)
-140
-150
-160
-170
-180
-190
-200
-210
-220
0
2
4
6
8
10
Time (ns)

H.

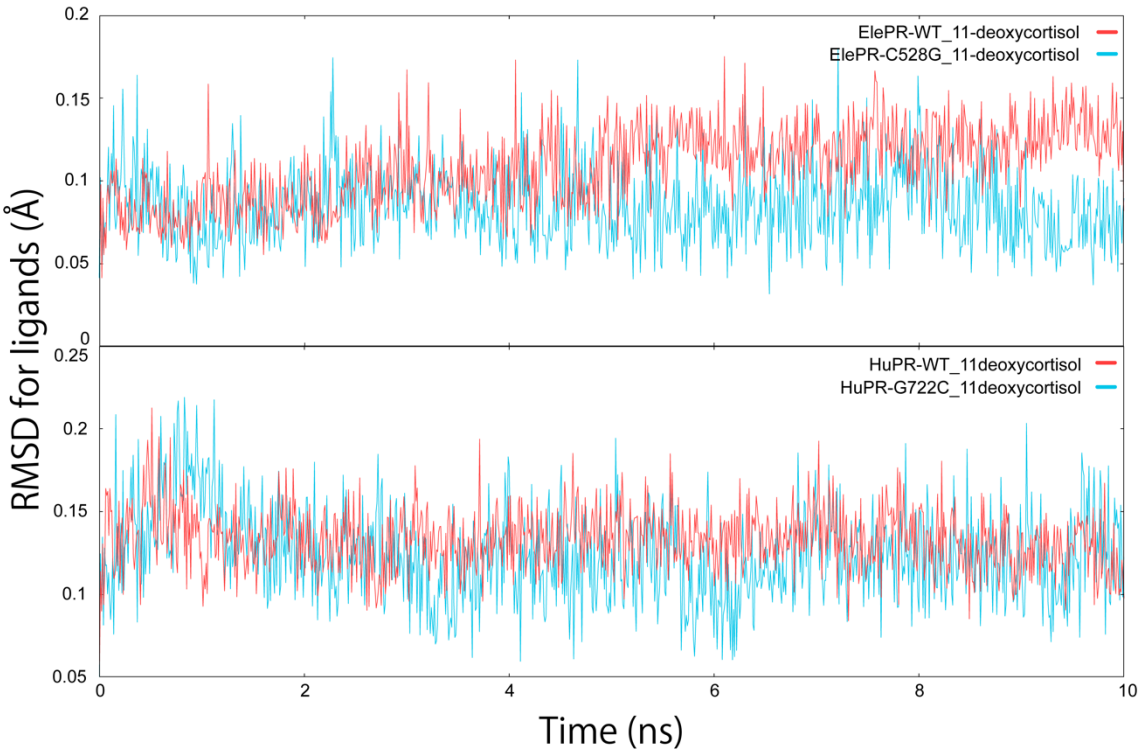
ElePR-WT_11-deoxycortisol
ElePR-C528G_11-deoxycortisol
HuPR-WT_11deoxycortisol
HuPR-G722C_11deoxycortisol
RMSD for ligands (Å)
0.2
0.15
0.1
0.05
0
0.25
0.2
0.15
0.1
0.05
0
2
4
6
8
10
Time (ns)

Figure 2-7. Receptor-ligand interaction analysis by MD simulation.

(A-C) Average values of Coulombic interaction energy, Lennard-Jones potential energy and RMSD values of 11-deoxycortisol in wild-type and mutant PRs from elephant shark and human.

(D, E) Average values of hydrogen-bond numbers and their percentages during 10 ns MD simulation.

(F, G) Fluctuation of Coulombic interaction energy and Lennard-Jones potential energy values of 11-deoxycortisol in wild-type and mutant PRs from elephant shark and human during 10 ns MD simulations.

(H) Fluctuation of RMSD value of 11-deoxycortisol in wild-type and mutant PRs from elephant shark and human during 10 ns MD simulations.

The comparison between 2 groups was analyzed with ordinary one-way ANOVA multiple comparison. Statistical significance was shown as: $P<0.05$, *; $P<0.01$, **; $P<0.001$, ***.

Figure 2-8

A.

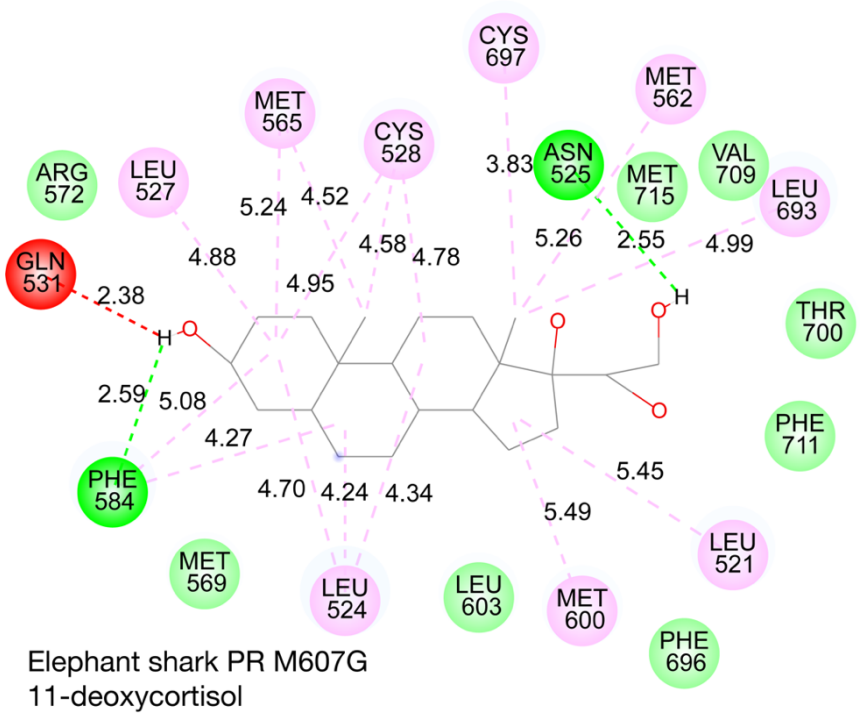

Elephant shark PR M607G
11-deoxycortisol

B.

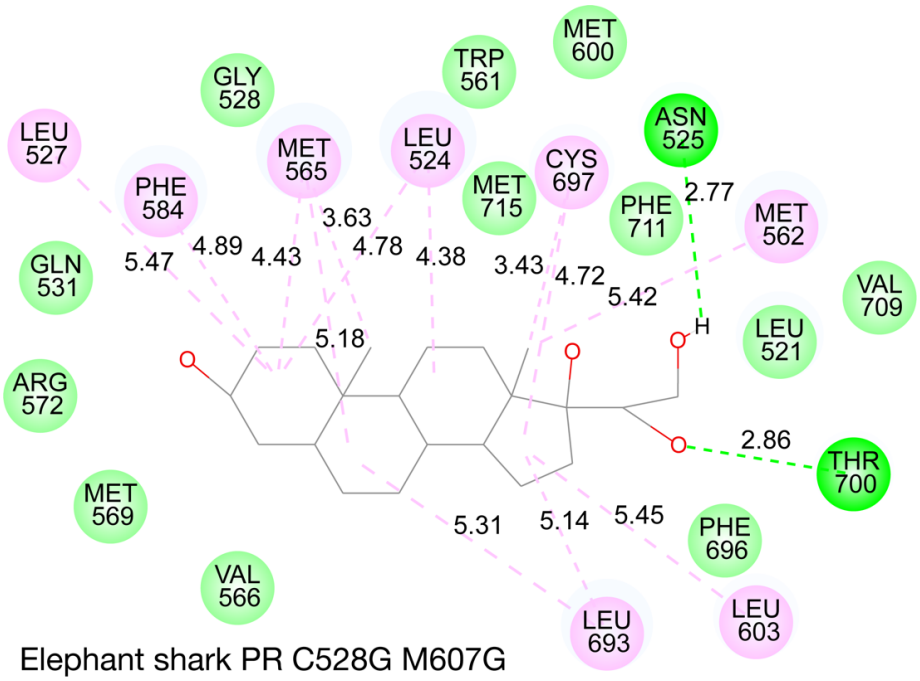

Elephant shark PR C528G M607G
11-deoxycortisol

C.

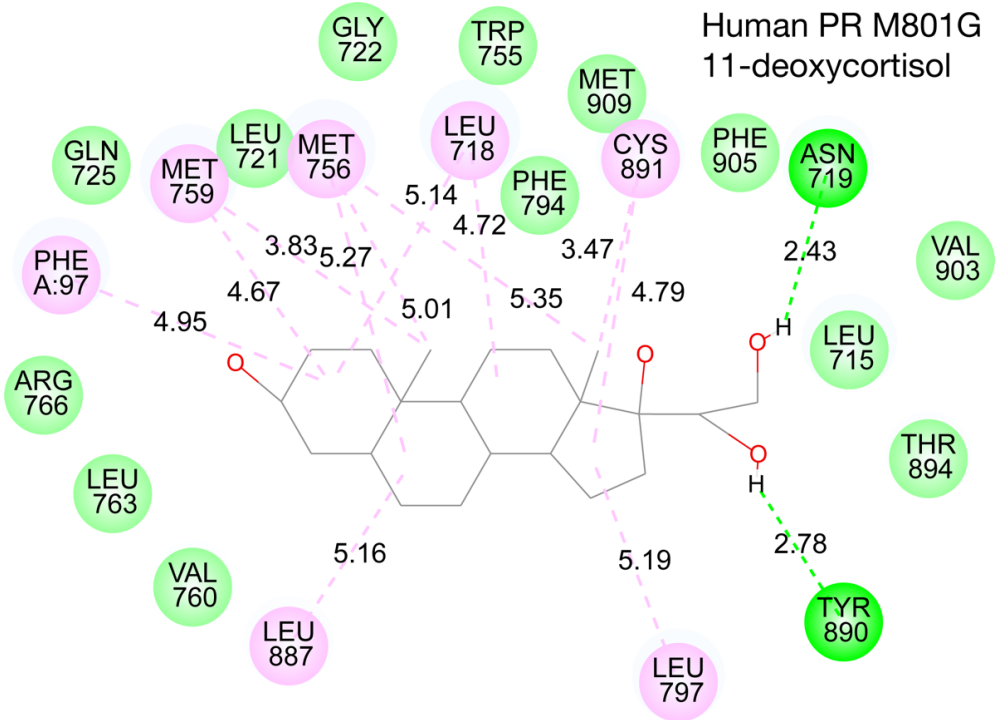
Human PR M801G
11-deoxycortisol
GLY 722
TRP 755
MET 909
LEU 721
MET 756
LEU 718
CYS 891
PHE 905
ASN 719
GLN 725
MET 759
PHE 794
PHE A:97
VAL 903
LEU 715
ARG 766
THR 894
LEU 763
VAL 760
LEU 887
LEU 797
TYR 890
5.14
4.72
3.83
5.27
3.47
2.43
4.67
5.01
5.35
4.79
4.95
H
5.16
5.19
2.78

D.

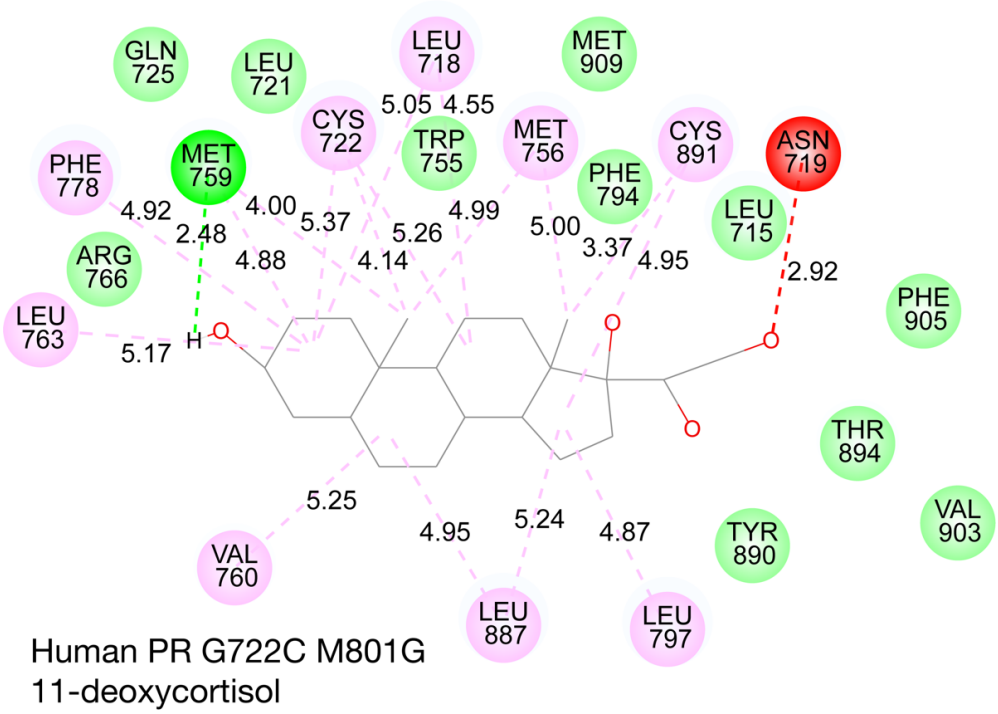
GLN 725
LEU 721
LEU 718
MET 909
CYS 722
TRP 755
MET 756
CYS 891
ASN 719
PHE 778
MET 759
PHE 794
LEU 715
ARG 766
PHE 905
LEU 763
THR 894
VAL 903
TYR 890
VAL 760
LEU 887
LEU 797
5.05
4.55
4.92
4.00
2.48
5.37
5.26
4.99
5.00
3.37
4.95
2.92
4.88
4.14
5.17
H
5.25
4.95
5.24
4.87
Human PR G722C M801G
11-deoxycortisol

Figure 2-8. Docking poses of 11-deoxycortisol bound to PRs from elephant shark and human with methionine to glycine mutation on helix-7.

Residues interact with 11-deoxycortisol when bound to elephant shark PR-Met607Gly (A), elephant shark PR-Cys528Gly- Met607Gly (B), human PR-Met801Gly (C), human PR-Gly722Cys-Met801Gly (D). Residues in green represent amino acids that bind to ligand through hydrogen-bond. Residues in light green represent amino acids that have van der Waal's contact with a ligand. Residues in pink indicate amino acids that interact with ligand through hydrophobic interaction including Alkyl-Alkyl or Pi-Alkyl interactions. Residues in red show amino acids that have unfavorable linkage with ligand. Numbers on the lines connecting residues and ligand show the distance (Å).

Figure 2-9

A.

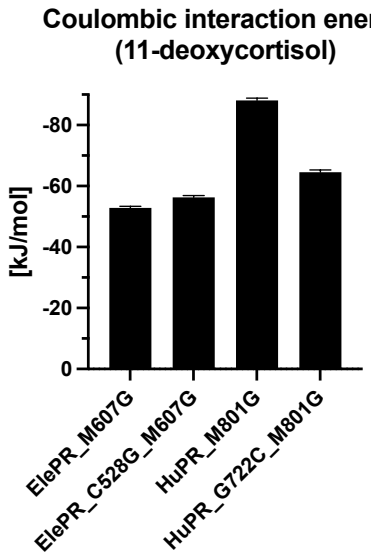

B.

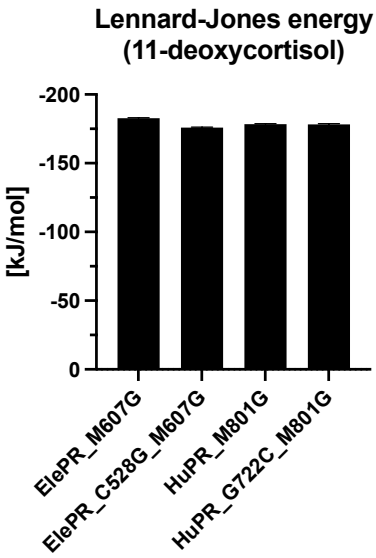

C.

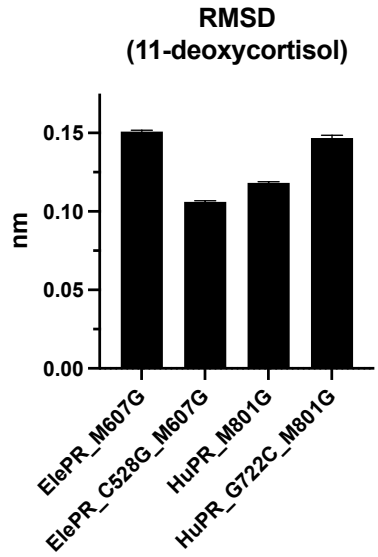

D.

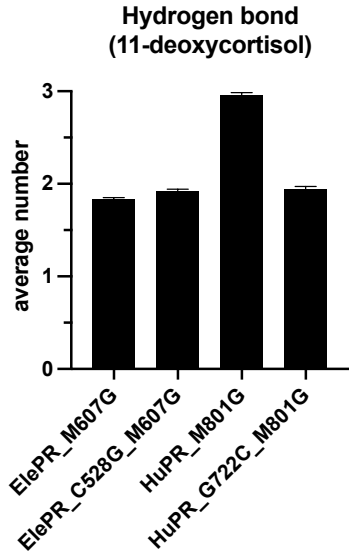

E.

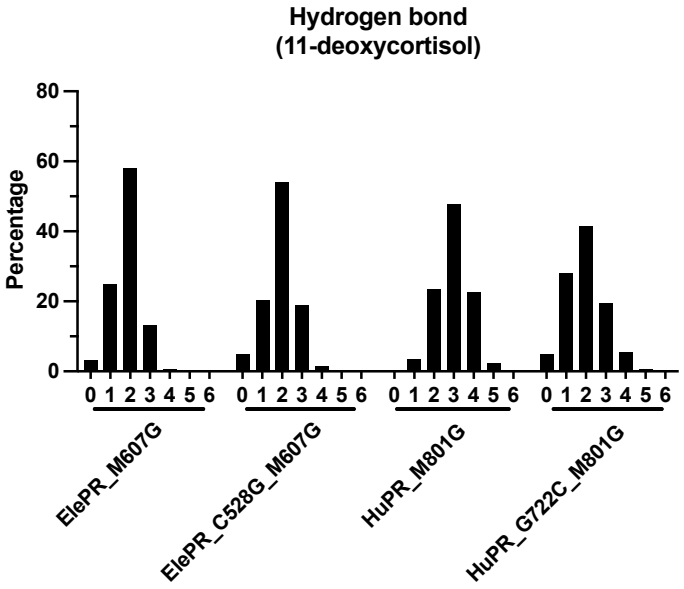
Hydrogen bond
(11-deoxycortisol)
Percentage
80
60
40
20
0
0 1 2 3 4 5 6
ElePR_M607G
ElePR_C528G_M607G
HuPR_M801G
HuPR_G722C_M801G

F.

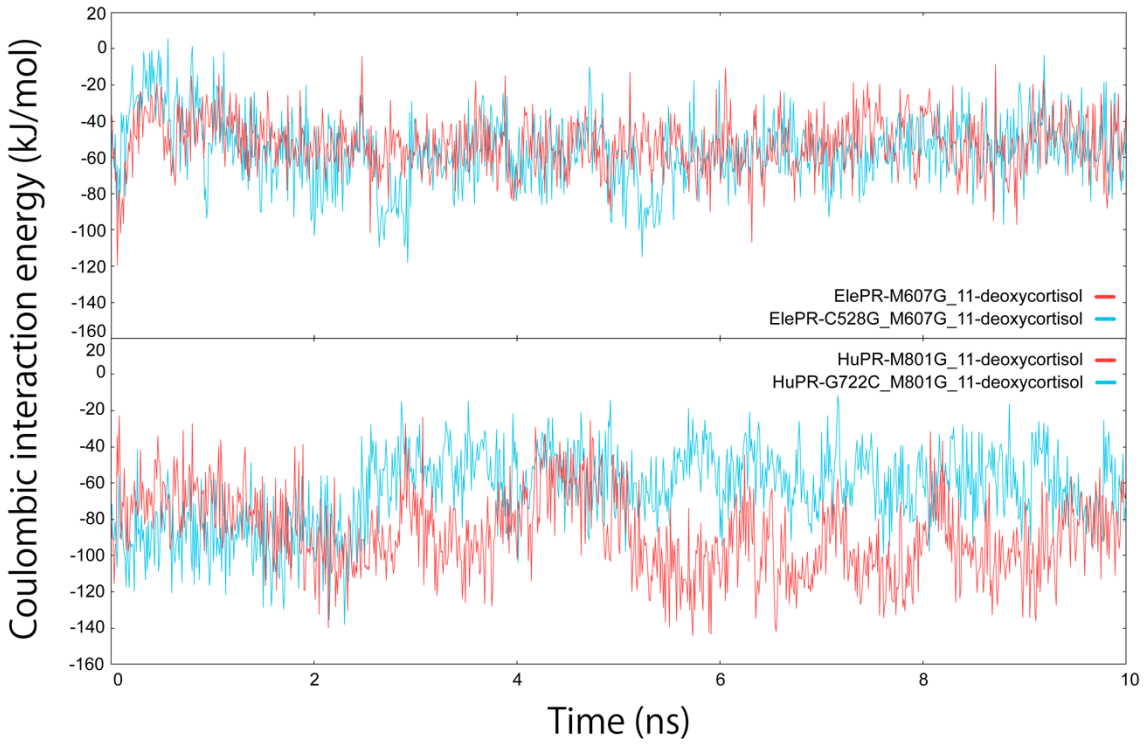
Coulombic interaction energy (kJ/mol)
ElePR-M607G_11-deoxycortisol
ElePR-C528G_M607G_11-deoxycortisol
HuPR-M801G_11-deoxycortisol
HuPR-G722C_M801G_11-deoxycortisol
Time (ns)

G.

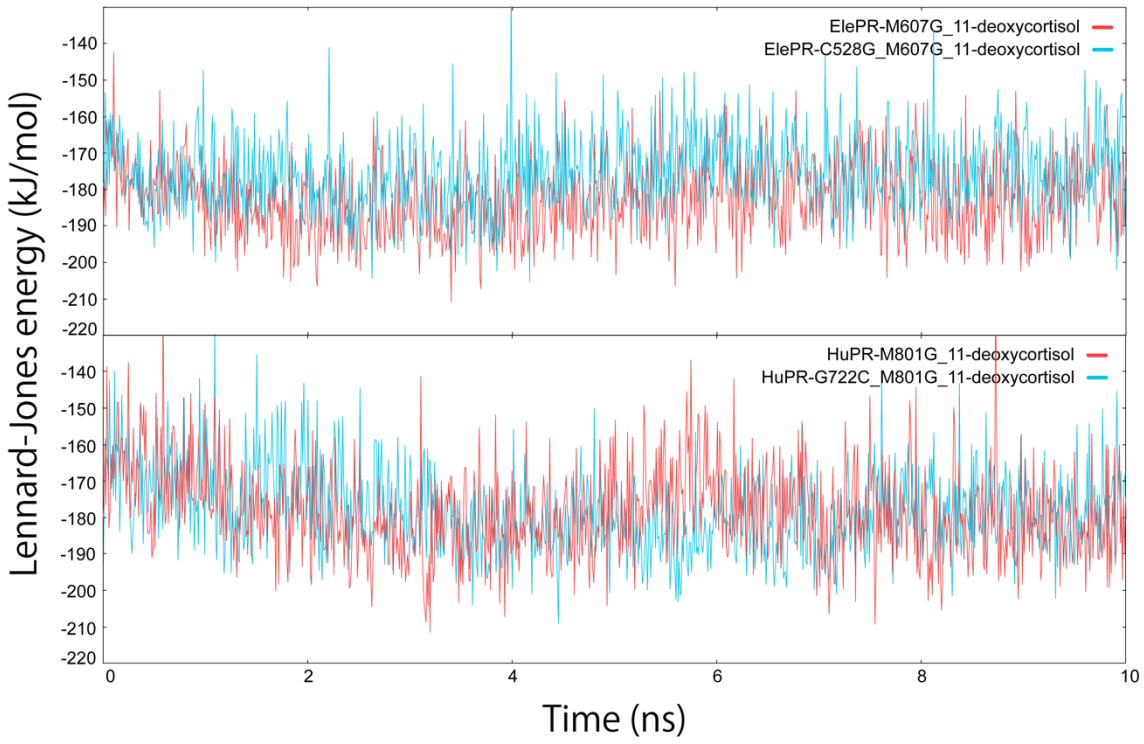
ElePR-M607G_11-deoxycortisol
ElePR-C528G_M607G_11-deoxycortisol
HuPR-M801G_11-deoxycortisol
HuPR-G722C_M801G_11-deoxycortisol
Lennard-Jones energy (kJ/mol)
-140
-150
-160
-170
-180
-190
-200
-210
-220
0
2
4
6
8
10
Time (ns)

H.

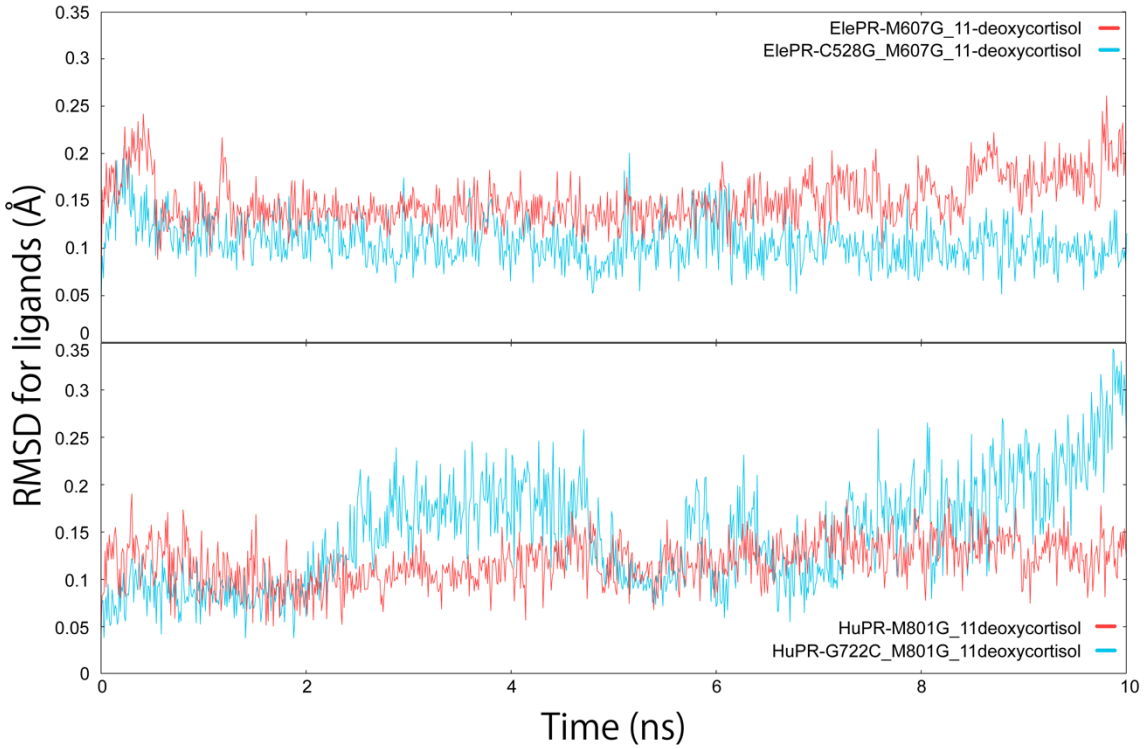
ElePR-M607G_11-deoxycortisol
ElePR-C528G_M607G_11-deoxycortisol
HuPR-M801G_11deoxycortisol
HuPR-G722C_M801G_11deoxycortisol
RMSD for ligands (Å)
0.35
0.3
0.25
0.2
0.15
0.1
0.05
0
0
2
4
6
8
10
Time (ns)

Figure 2-9. Receptor-ligand interaction analysis by MD simulation.

(A-C) Average values of Coulombic interaction energy, Lennard-Jones potential energy and RMSD values of 11-deoxycortisol in single or double mutated PRs from elephant shark and human.

(D, E) Average values of hydrogen-bond numbers and their percentages during 10 ns MD simulation.

(F, G) Fluctuation of Coulombic interaction energy and Lennard-Jones potential energy values during 10 ns MD simulations.

(H) Fluctuation of RMSD value during 10 ns MD simulations.

Figure 2-10

A.

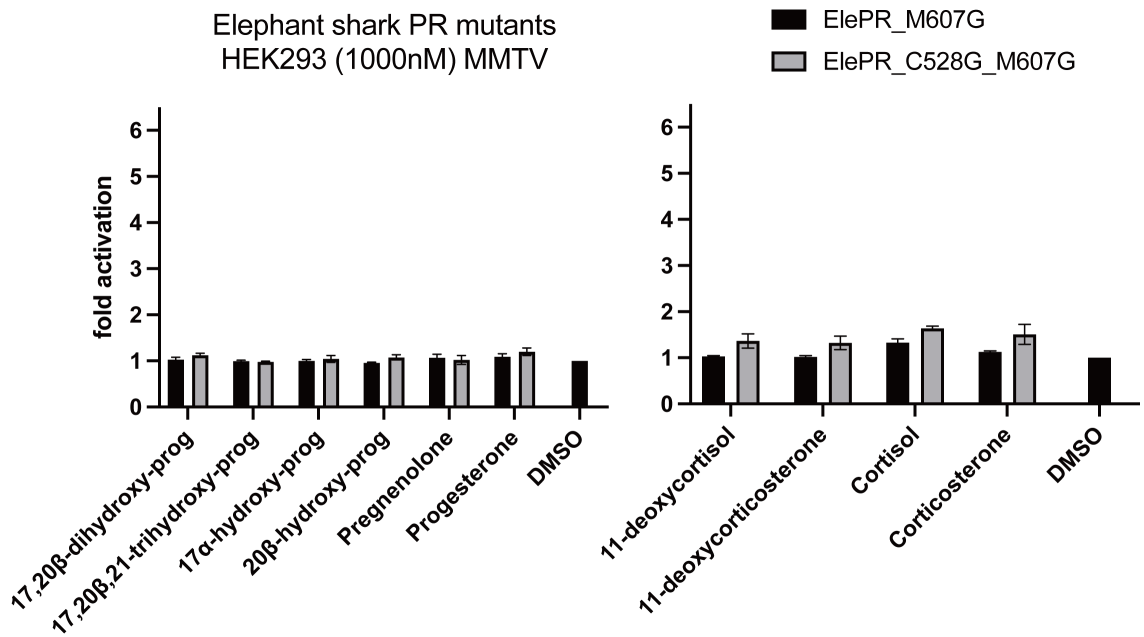

B.

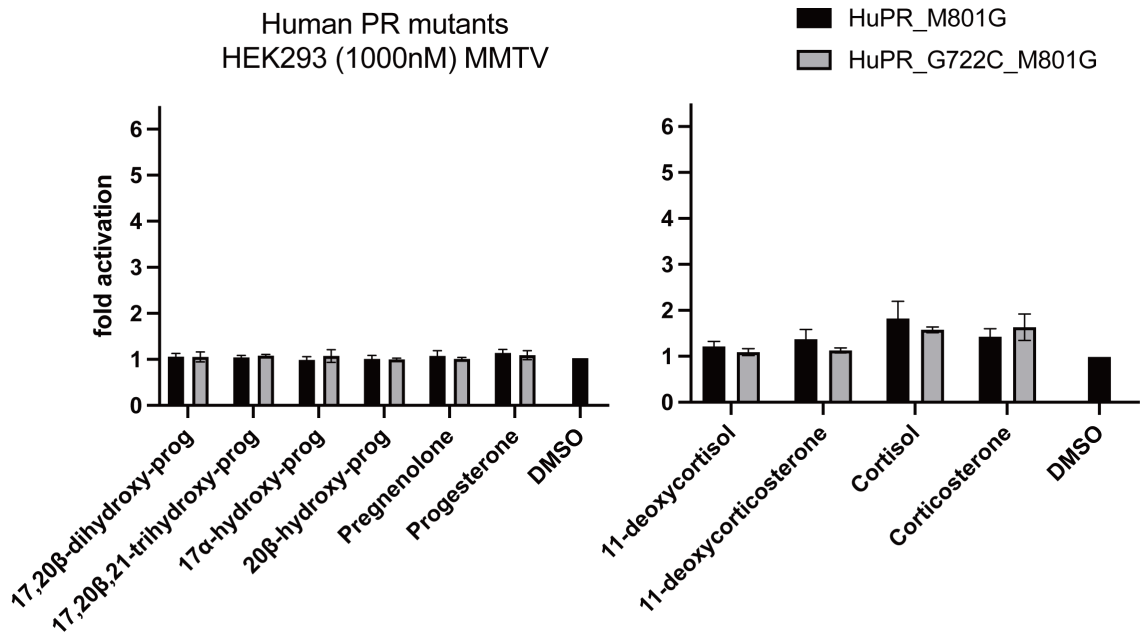

C.

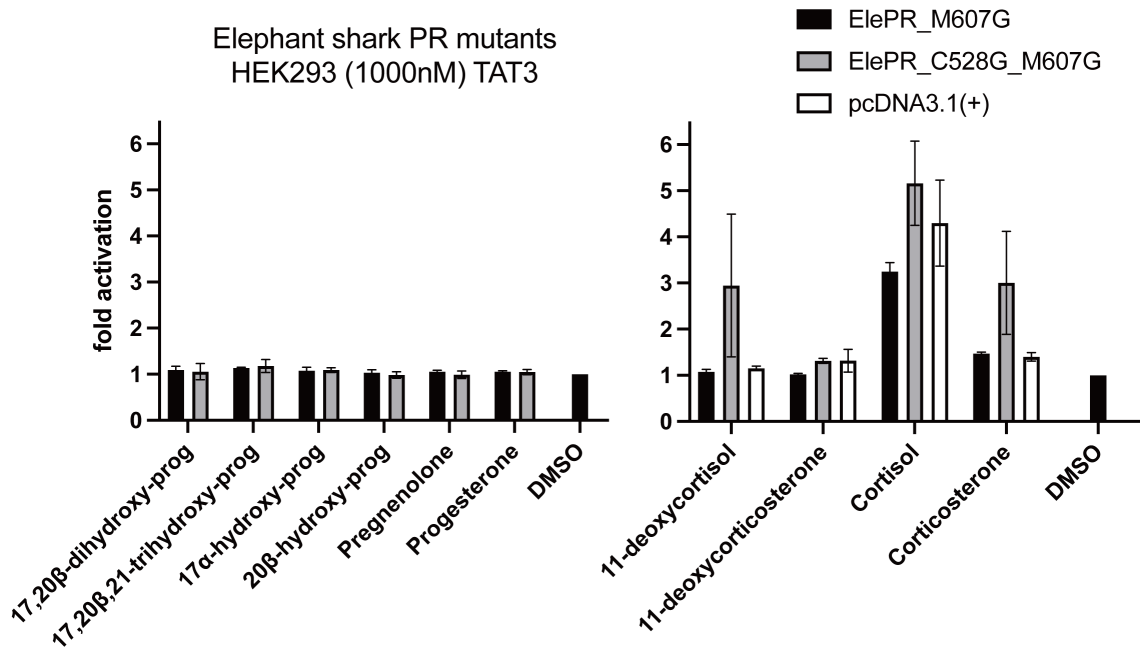
Elephant shark PR mutants
HEK293 (1000nM) TAT3
ElePR_M607G
ElePR_C528G_M607G
pcDNA3.1(+)
fold activation
0
1
2
3
4
5
6
17,20β-dihydroxy-prog
17,20β,21-trihydroxy-prog
17α-hydroxy-prog
20β-hydroxy-prog
Pregnenolone
Progesterone
DMSO
11-deoxycortisol
11-deoxycorticosterone
Cortisol
Corticosterone
DMSO

D.

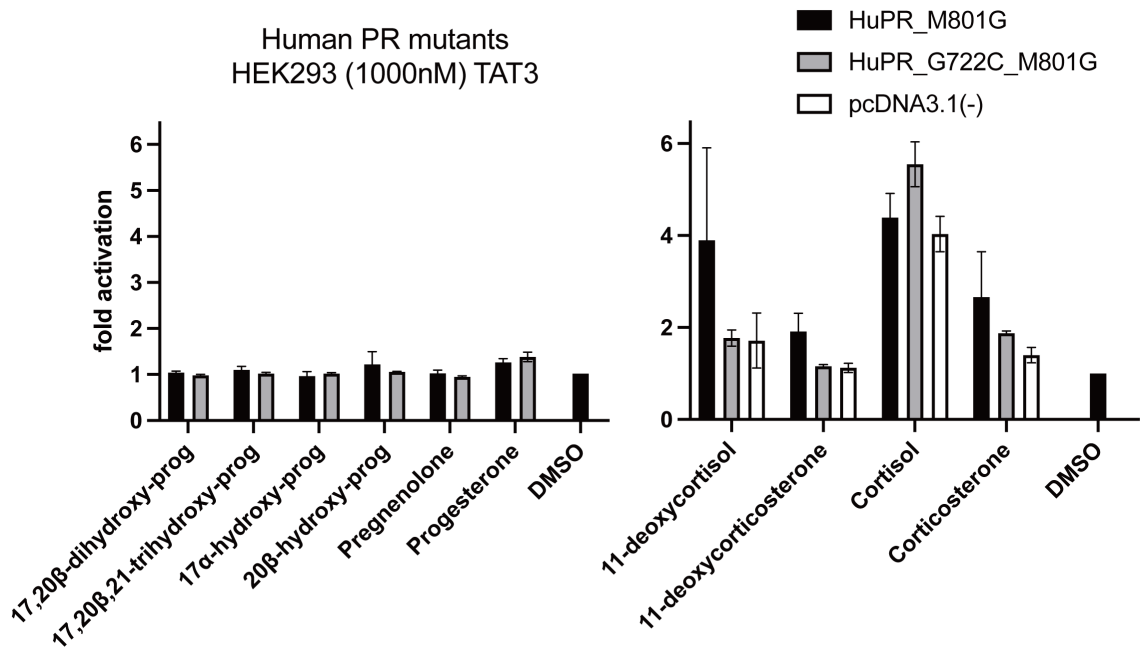
Human PR mutants
HEK293 (1000nM) TAT3
HuPR_M801G
HuPR_G722C_M801G
pcDNA3.1(-)
fold activation
0
1
2
3
4
5
6
17,20β-dihydroxy-prog
17,20β,21-trihydroxy-prog
17α-hydroxy-prog
20β-hydroxy-prog
Pregnenolone
Progesterone
DMSO
11-deoxycortisol
11-deoxycorticosterone
Cortisol
Corticosterone
DMSO

Figure 2-10. Comparison of hormone responses between elephant shark PR-Met607Gly and elephant shark PR-Cys528Gly-Met607Gly (A, C), and between human PR-Met801Gly and human PR-Gly722Cys-Met801Gly (B, D).

Plasmids with the full coding region of PRs with a single or double amino acid mutation from elephant shark and human were transfected to HEK293 cells with an MMTV-luc or TAT3 reporter vector. Cells were treated with the indicated concentration (10^{-6} M) of steroid hormones or vehicle alone (DMSO) for 44 hours before the activity of the reporter gene was measured. Data are means ± SEM of 3 independent experiments and expressed as fold activation compared to the activity of cells expressing the same vectors (expressing vector, reporter vector, and control vector) that treated with vehicle (DMSO) alone, which was set as 1. The comparison between 2 groups was analyzed with 2way ANOVA multiple comparisons. Statistical significance was shown as: $P < 0.05$, *; $P < 0.01$, **; $P < 0.001$, ***.

Figure 2-11

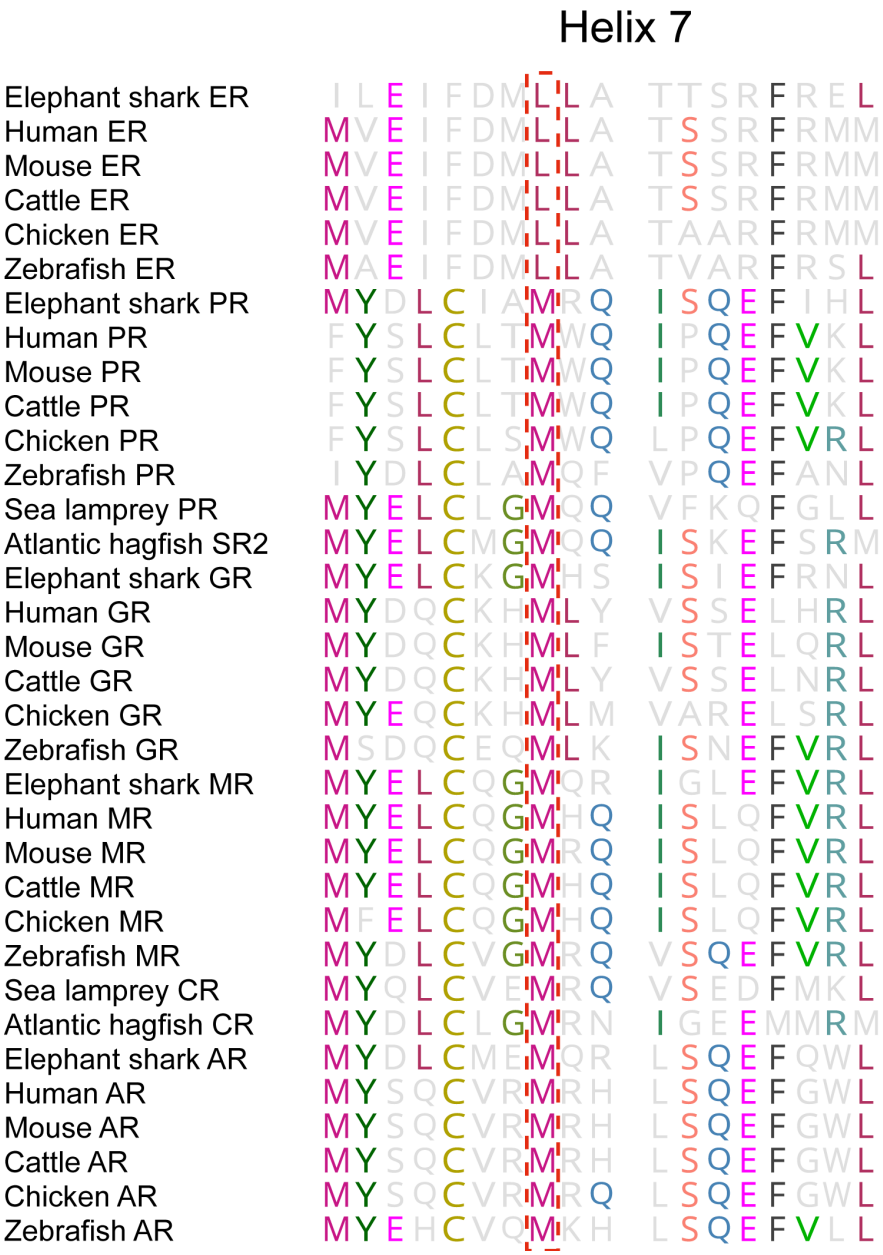

Figure 2-11. Alignment of residues around helix 7 in vertebrate SHRs.

Alignment of amino acid sequences around helix 7 of all elephant shark SHRs including PR, MR, GR, ER and AR with various vertebrate PRs. Met-607 in elephant shark PR corresponding to Met-801 in human PR is on helix 7 within the ligand-binding domain.

Figure 2-12

A.

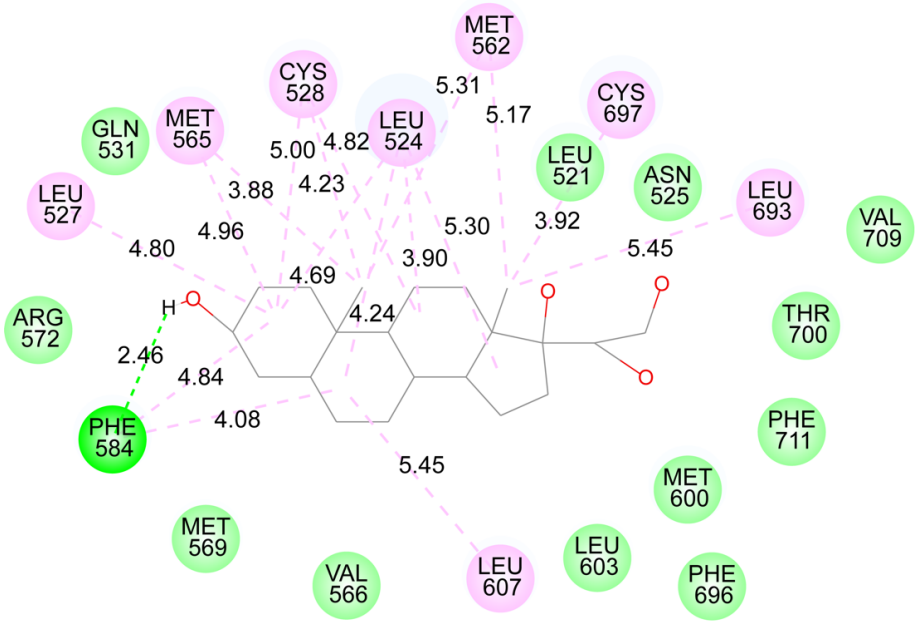

B.

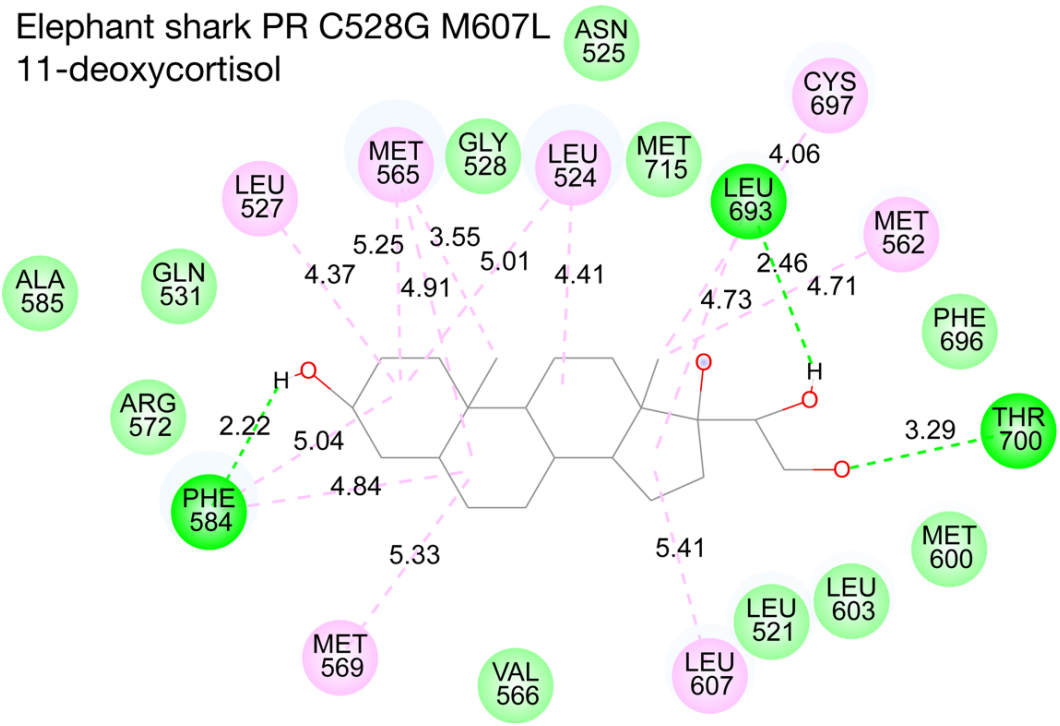

C.

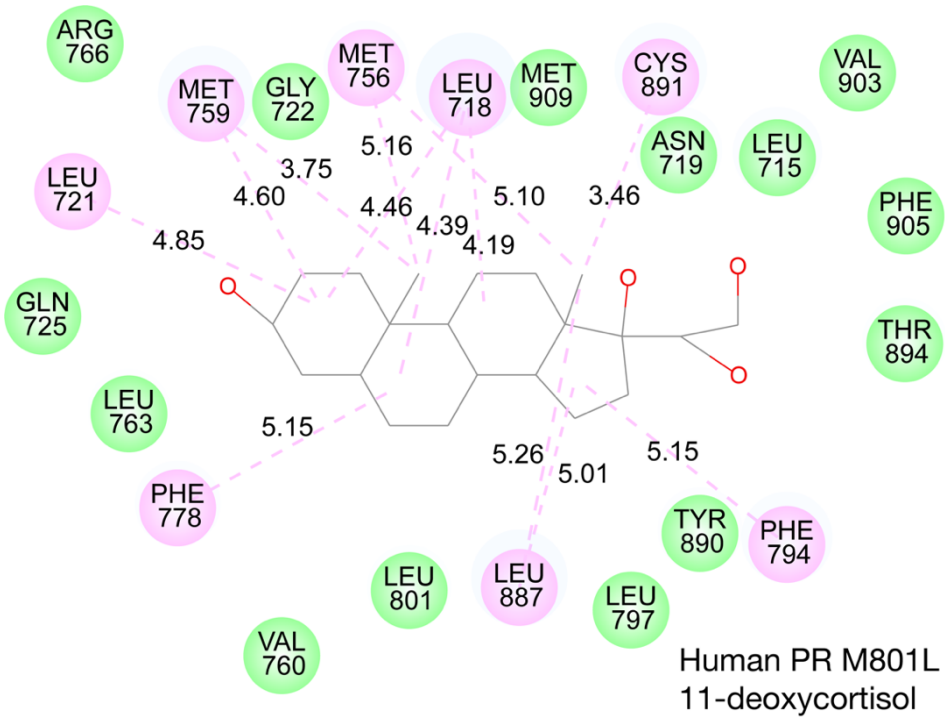
ARG 766
MET 759
GLY 722
MET 756
LEU 718
MET 909
CYS 891
VAL 903
ASN 719
LEU 715
LEU 721
PHE 905
GLN 725
THR 894
LEU 763
PHE 778
TYR 890
PHE 794
LEU 801
LEU 887
LEU 797
VAL 760
5.16
3.75
4.60
4.46
4.39
4.19
5.10
3.46
4.85
5.15
5.26
5.01
5.15
Human PR M801L
11-deoxycortisol

D.

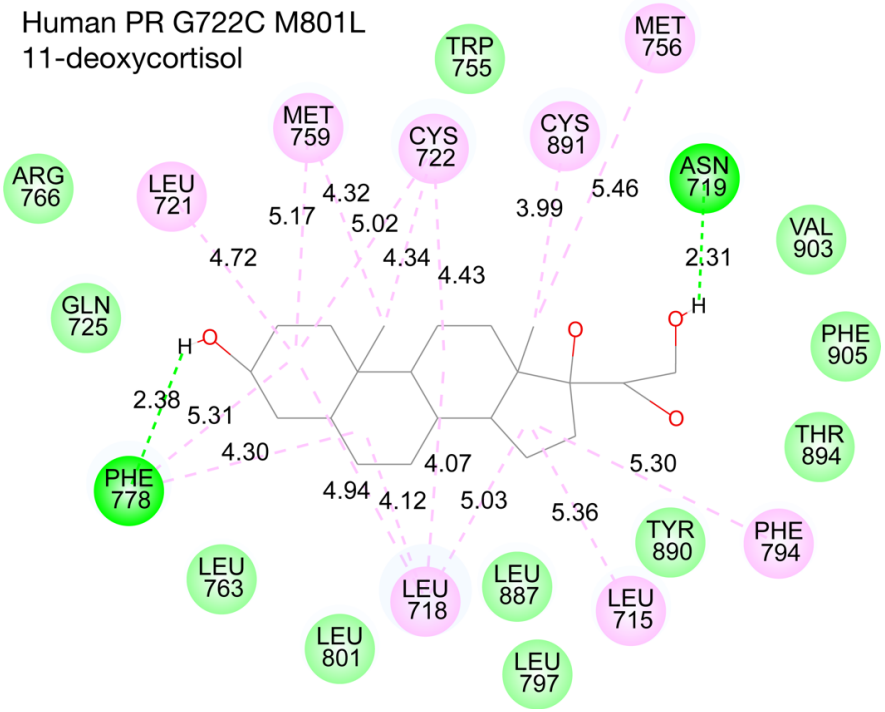
Human PR G722C M801L
11-deoxycortisol
TRP 755
MET 756
MET 759
CYS 722
CYS 891
ASN 719
ARG 766
LEU 721
VAL 903
GLN 725
PHE 905
THR 894
PHE 778
TYR 890
PHE 794
LEU 763
LEU 718
LEU 887
LEU 715
LEU 801
LEU 797
4.32
5.17
5.02
3.99
5.46
4.72
4.34
4.43
2.31
H
H
2.38
5.31
4.30
4.07
5.30
4.94
4.12
5.03
5.36

Figure 2-12. Docking poses of 11-deoxycortisol bound to PRs from elephant shark and human with methionine to leucine mutation on helix 7.

Residues interacting with 11-deoxycortisol when bound to elephant shark PR-Met607Leu (A), elephant shark PR-Cys528Gly- Met607Leu (B), human PR-Met801Leu (C), human PR-Gly722Cys-Met801Leu (D). Residues in green represent amino acids that bind to ligand through hydrogen-bond. Residues in light green represent amino acids that have van der Waal's contact with ligand. Residues in pink indicate amino acids that interact with ligand through hydrophobic interaction including Alkyl-Alkyl or Pi-Alkyl interactions. Numbers on the lines connecting residues and ligand show the distance (Å).

Figure 2-13

A.

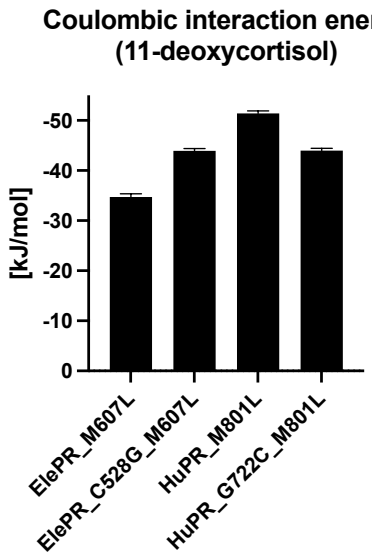

B.

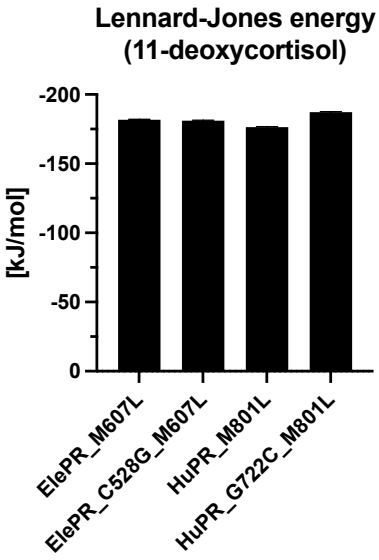

C.

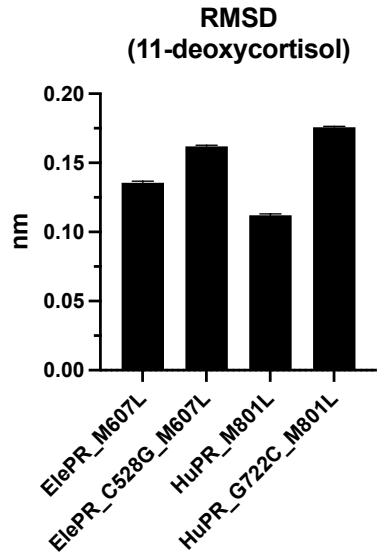

D.

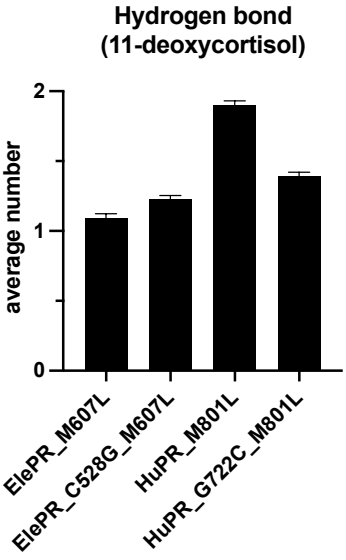

E.

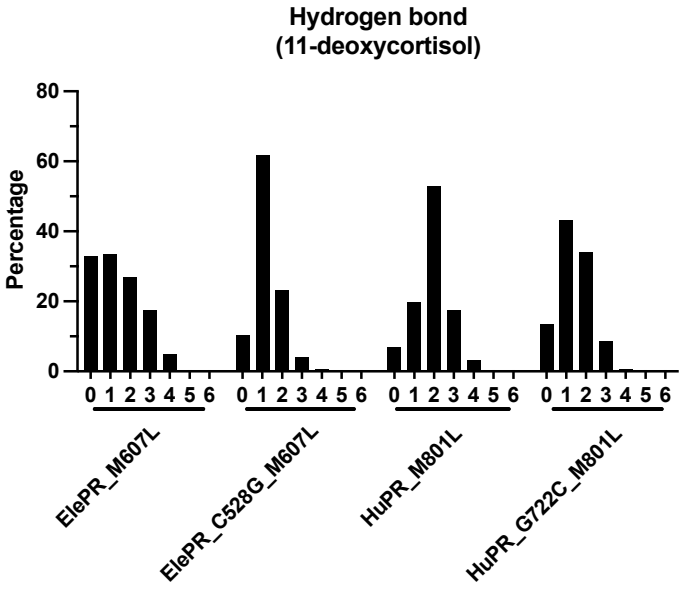
Hydrogen bond
(11-deoxycortisol)
Percentage
80
60
40
20
0
0 1 2 3 4 5 6
ElePR_M607L
ElePR_C528G_M607L
HuPR_M801L
HuPR_G722C_M801L

F.

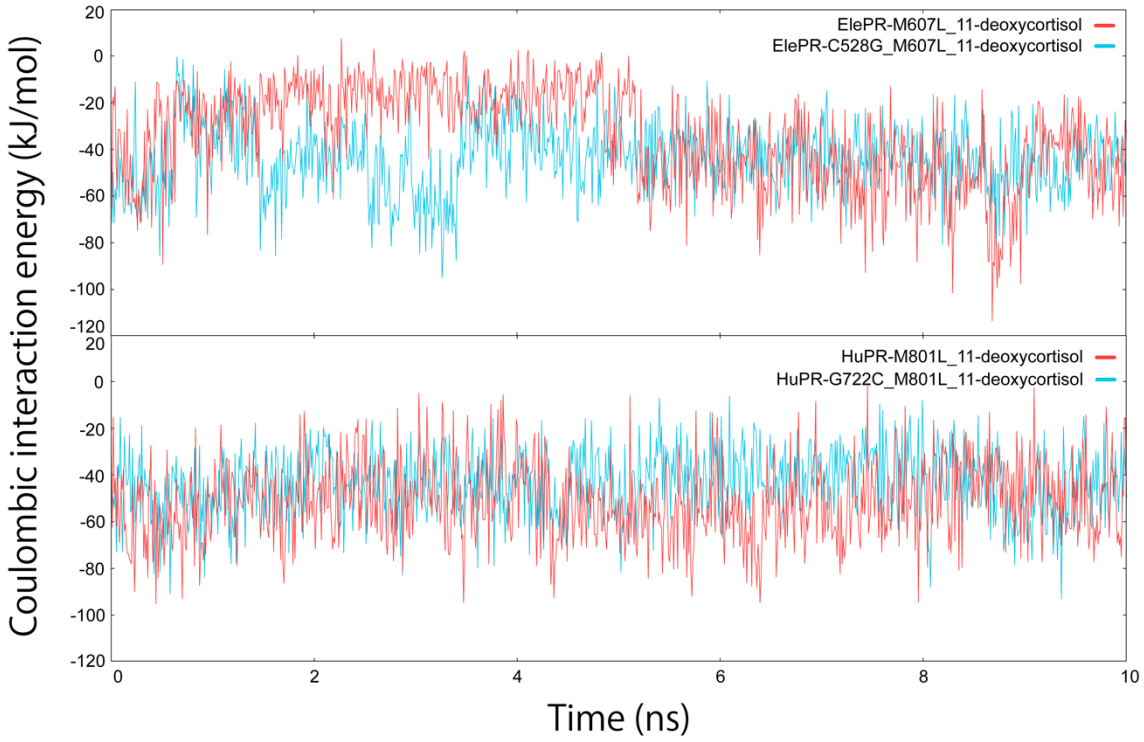
Coulombic interaction energy (kJ/mol)
ElePR-M607L_11-deoxycortisol
ElePR-C528G_M607L_11-deoxycortisol
HuPR-M801L_11-deoxycortisol
HuPR-G722C_M801L_11-deoxycortisol
20
0
-20
-40
-60
-80
-100
-120
0
2
4
6
8
10
Time (ns)

G.

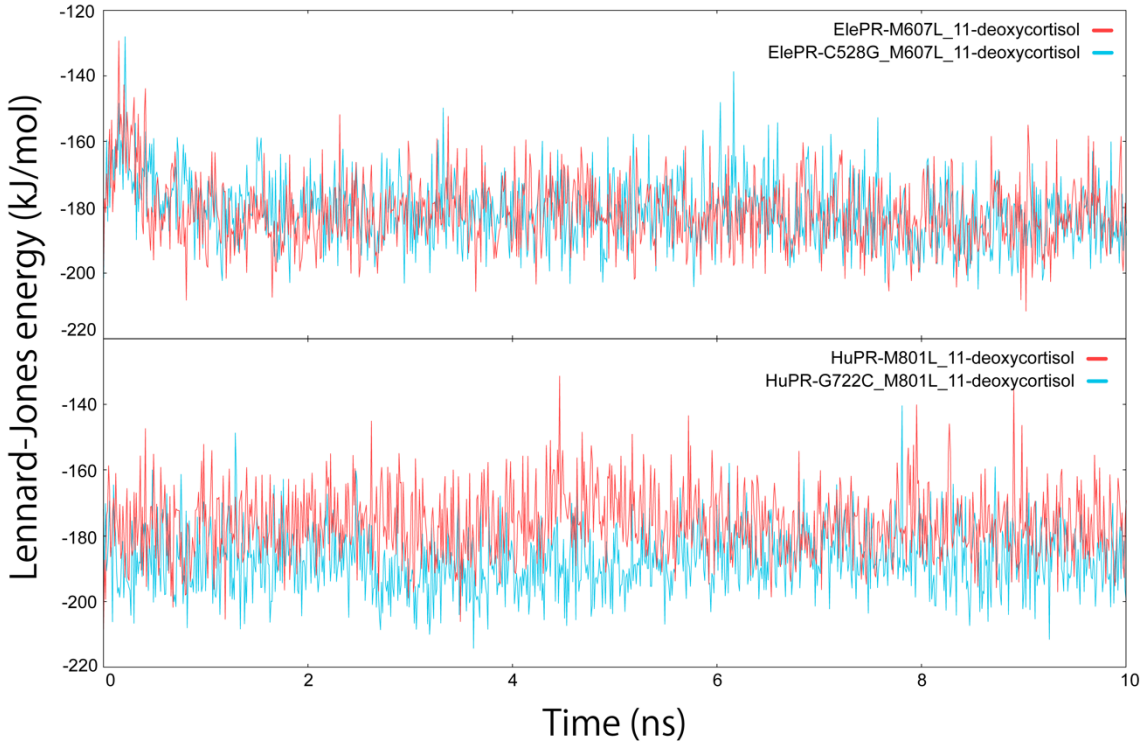
ElePR-M607L_11-deoxycortisol
ElePR-C528G_M607L_11-deoxycortisol
HuPR-M801L_11-deoxycortisol
HuPR-G722C_M801L_11-deoxycortisol
Lennard-Jones energy (kJ/mol)
-120
-140
-160
-180
-200
-220
0
2
4
6
8
10
Time (ns)

H.

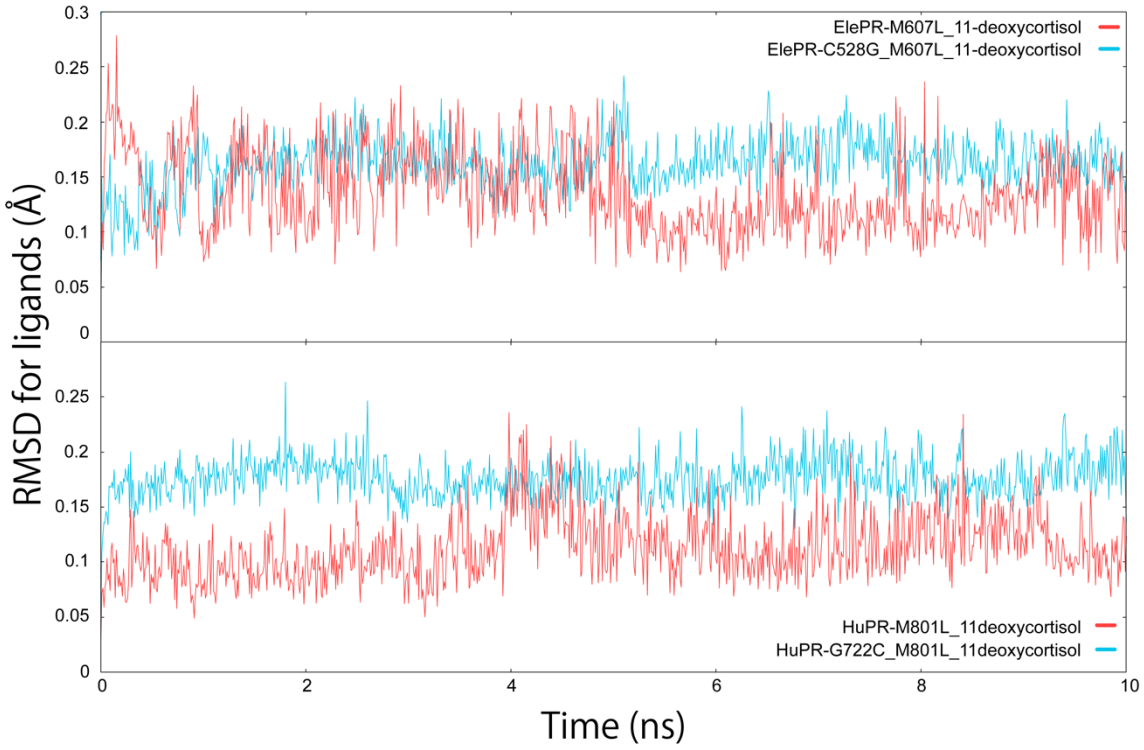
ElePR-M607L_11-deoxycortisol
ElePR-C528G_M607L_11-deoxycortisol
HuPR-M801L_11deoxycortisol
HuPR-G722C_M801L_11deoxycortisol
RMSD for ligands (Å)
0.3
0.25
0.2
0.15
0.1
0.05
0
0
2
4
6
8
10
Time (ns)

Figure 2-13. Receptor-ligand interaction analysis by MD simulation.

(A-C) Average values of Coulombic interaction energy, Lennard-Jones potential energy, and RMSD values of 11-deoxycortisol in single or double mutated PRs from elephant shark and human.

(D, E) Average values of hydrogen-bond numbers and their percentages during 10 ns MD simulation.

(F, G) Fluctuation of Coulombic interaction energy and Lennard-Jones potential energy values during 10 ns MD simulations.

(H) Fluctuation of RMSD value during 10 ns MD simulations.

Figure 2-14

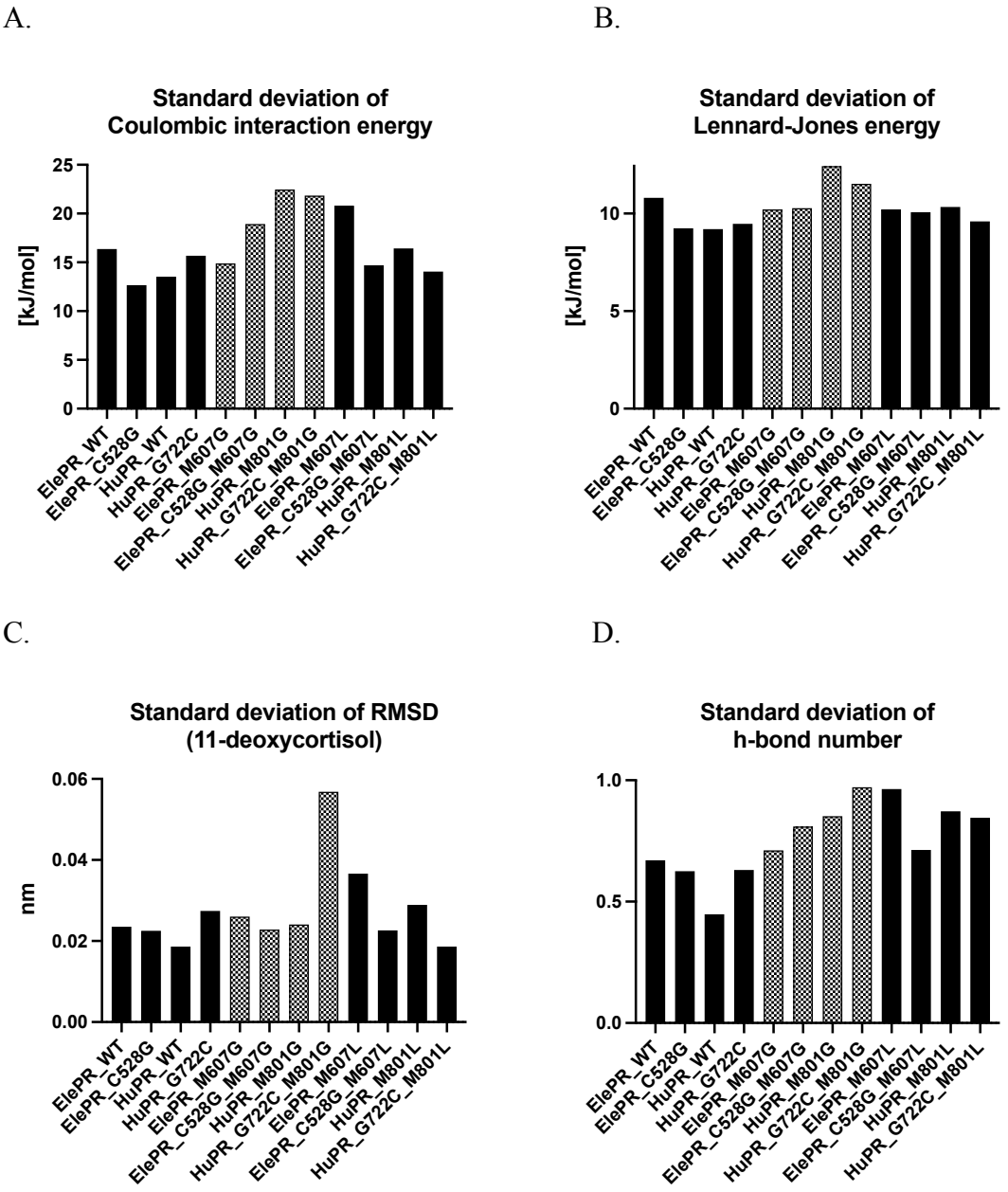

Figure 2-14. Standard deviation of MD simulation results.

Standard deviation of Coulombic interaction energy (A), Lennard-Jones potential energy (B), RMSD values (C) and hydrogen-bond numbers (D) during 10 ns MD simulations.

Figure 2-15

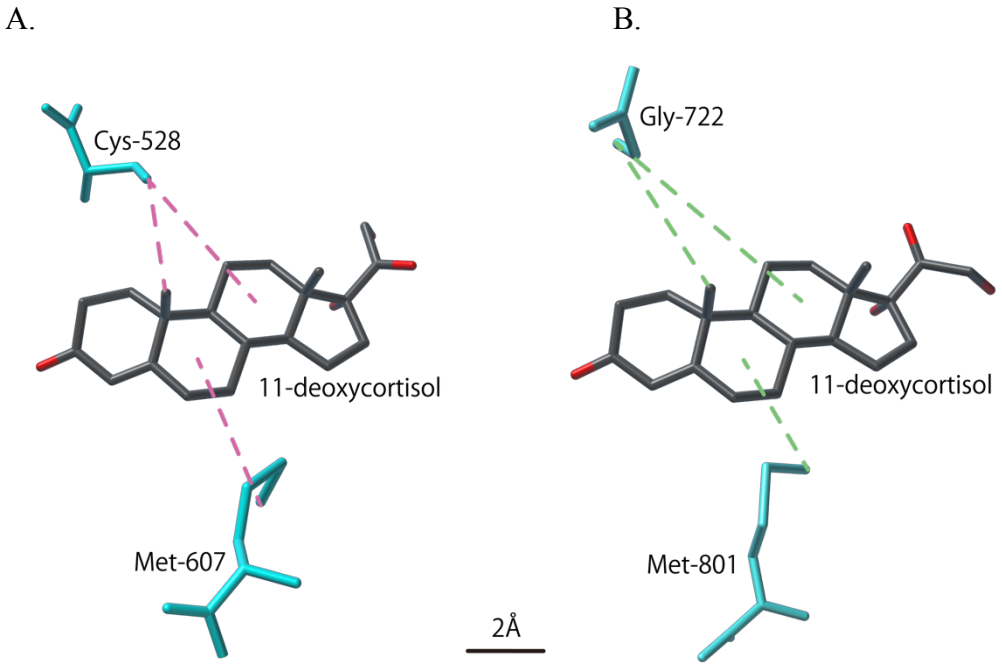

Figure 2-15. Interaction of 11-deoxycortisol with key residues on helix 3 and helix 7.

(A) Interaction of 11-deoxycortisol with Cys-528 and Met-607 of elephant shark PR.

(B) Interaction of 11-deoxycortisol with Gly-722 and Met-801 of human PR.

Pink line indicates hydrophobic interaction including Alkyl-Alkyl or Pi-Alkyl interactions. Green line indicates van der Waal's contact.

General discussion

Steroid hormones regulate a variety of physiological processes including reproduction, growth, immunity and metabolism [4,5]. Since the first molecular cloning of steroid hormone receptor (SHR) in the 1980s [7], a large amount of studies on the functional characterization and molecular mechanism of SHRs have been published, including in our laboratory. Previous studies on SHRs are mostly on receptors from common species, and only a few research groups have been focusing on species from cartilaginous fish. Considering the special evolutionary position of cartilaginous fishes in vertebrates [42], our research group have put our eyes on the nuclear receptors from elephant shark, which may provide an interesting insight into the molecular evolution of SHRs.

The first Chapter exhibited the steroid hormone response-ability of full-length and truncated elephant shark PR compared to human and zebrafish. However, the results are a little bit controversial as I compared luciferase results gained from different cell lines. During the investigation of the steroid hormone response, I found that both HEK293 and CHO-K1 cells cannot be used in the luciferase assay for both full-length and truncated PRs. To understand how the PR constructs response to steroids in various cells, I examined their hormone responses in cell lines including HEK293, CHO-K1, COS-7, and HepG2 (Table 1-3). As a result, all three full-length PRs can be stimulated by steroid hormones in HEK293, COS-7, and HepG2 cells, but not in CHO-K1 cells. On the other hand, truncated PRs only showed transcriptional activation to steroids in CHO-K1 cells.

In a normal situation, nuclear receptors will recruit coactivators and form a nuclear receptor-coactivator (NCoA) complex, after the release of corepressors and the conformational change of AF-2 domain triggered by the interaction with the steroid hormone [18-21]. The coactivators involved in this process belong to the SRC (steroid receptor coactivator) family, which consists of SRC-1, TIF2/GRIP1, and

RAC3/ACTR/pCIP/AIB-1 [85]. The transcriptional activation is enhanced through histone acetylation/methylation and additional recruitment of additional cofactors.

From the results of full-length PRs in HEK293, COS-7, and HepG2 cells, we can consider the receptor protein expressed by the plasmid construct should be available for recruitment of coactivators and for enhancement transcriptional activation after binding with hormones. A similar conclusion may also be available for the enhanced transactivation observed in CHO-K1 cells using truncated elephant shark and human PR. Ligand-response diversity of full-length and truncated PR observed in different cell lines indicated that full-length PR and truncated PR can improve transcriptional activation by recruiting different coactivators or cofactors. Another possible reason is that the loss of the N-terminal domain may result in difficulty of conformational change in AF-2 domain after ligand-binding, resulting in disability of coactivator recruitment. In the case of CHO-K1 cells, truncated PR may be available to enhance transcriptional activation through some kind of intracellular signal transduction without the recruitment of common coactivators. However, many experiments are still needed to clarify this hypothesis.

To date, still no kind of clinical result of single or multi amino acid mutation of progesterone receptor has been described [86]. Therefore, to study the role of an amino acid in PR, we need to focus on the residues that exhibit some kind of switch during evolution.

In Chapter 2, despite observing the inverted antagonistic effect of RU486 to PRs after the glycine/cysteine switch on helix 3, I also found that PRs with cysteine on the corresponding position in helix 3 showed higher transcriptional activation on 11-deoxycortisol compared with those with glycine. These results provided interesting insight that the evolution of this residue on PR, from cysteine (non-mammalian) to

glycine (mammalian), can result in changes in ligand responses that result in different physiological effects. *In silico* methods have been applied to investigate the molecular basis under this phenomenon. Results from docking simulations indicated that the interaction between 11-deoxycortisol and cysteine/glycine on helix 3 could directly affect its interaction with methionine on helix 7, Met-607 in elephant shark PR corresponding to Met-801 in human PR (Fig. 2-15). The results of MD simulation indicated methionine-to-glycine mutation on helix 7, meaning loss of contact with the residue on helix 7, could result in destabilized ligand-binding with 11-deoxycortisol. By comparing the standard deviation of the observed values during 10 ns MD simulation, the construct with methionine on helix 7 showed the highest binding stability. After the methionine on helix 7 is replaced by glycine, the receptor-ligand interaction became comparatively unstable. Even though the simulation results just became unstable in a comparative form, the *in vitro* experiments displayed a complete loss of transcriptional activation to all common progestins and corticoids after this methionine to glycine mutation.

These findings elucidated the importance of preserving interaction when trying to study the role of single amino acid in nuclear receptor function via mutation. Therefore, a methionine to leucine mutation on helix 7 was committed and evaluated by *in silico* methods. Then, the values of the standard deviation during 10 ns MD simulation are closer to the original methionine compared with the mutant with glycine at this position (Table 2-2).

All these *in silico* and *in vitro* results showed the importance of the interaction between steroid hormone and helix 7 in steroid activation of PR. These findings provided us with some further understanding into the role of interaction with helix 7 in the ligand-binding stability of PR, which has never been described previously.

Acknowledgement

I wish to express my grateful acknowledgement to Professor Yoshinao Katsu for his kind scientific and technical instruction, positive encouragements and such meaningful advices in this study. Thanks to his supports, I could experience such a full-filling laboratory time for 5 years. I am deeply grateful to Professor Masakane Yamashita, Associate Professor Atsushi P. Kimura and Associate Professor Katsueki Ogiwara for reviewing this dissertation, their various advices and discussion on this study. I am also very thankful to Professor Michael E. Baker at University of California, San Diego, for his useful suggestion, technical support in the publication of my paper. I would like to show deep appreciation to all the teachers and students I met during my laboratory life in Hokkaido University for their kindness. I particularly wish to thank Assistant Professor Shuhei Mizushima, Dr. Yui Satoh, Dr. Kai Otsuka, Dr. Atthanayake Mudiyanselage Thusitha Kosala Bandara, Mr. Josei Sato and all former and present members of Katsu Laboratory for their great discussion, daily communication and kindness in my laboratory life.

Reference

1. Graham, J. D. & Clarke, C. L. Physiological action of progesterone in target tissues. Endocr. Rev. 18, 502–19 (1997).
2. Venkatesh, B. *et al*. Elephant shark genome provides unique insights into gnathostome evolution. Nature 505, 174–179 (2014).
3. Benhamou, B. *et al*. A single amino acid that determines the sensitivity of progesterone receptors to RU486. Science. 255, 206–209 (1992).
4. Miller, W. L. & Auchus, R. J. The Molecular Biology, Biochemistry, and Physiology of Human Steroidogenesis and Its Disorders. Endocr. Rev. 32, 81–151 (2011).
5. MILLER, W. L. Molecular Biology of Steroid Hormone Synthesis*. Endocr. Rev. 9, 295–318 (1988).
6. KENDALL, E. C. Hormone of the adrenal cortex. Bull. N. Y. Acad. Med. 29, 91–100 (1953).
7. Gustafsson, J.-A. Historical overview of nuclear receptors. J. Steroid Biochem. Mol. Biol. 157, 3–6 (2016).
8. Hanukoglu, I. Steroidogenic enzymes: Structure, function, and role in regulation of steroid hormone biosynthesis. J. Steroid Biochem. Mol. Biol. 43, 779–804 (1992).
9. Chung, B. C., Matteson, K. J., Voutilainen, R., Mohandas, T. K. & Miller, W. L. Human cholesterol side-chain cleavage enzyme, P450scc: cDNA cloning, assignment of the gene to chromosome 15, and expression in the placenta. Proc. Natl. Acad. Sci. U. S. A. 83, 8962–8966 (1986).
10. Turcu, A. F. & Auchus, R. J. Adrenal Steroidogenesis and Congenital Adrenal Hyperplasia. Endocrinol. Metab. Clin. North Am. 44, 275–296 (2015).
11. Tremblay, J. J. Molecular regulation of steroidogenesis in endocrine Leydig cells. Steroids 103, 3–10 (2015).

12. Christenson, L. K. & Devoto, L. Cholesterol transport and steroidogenesis by the corpus luteum. Reprod. Biol. Endocrinol. 1, 1–9 (2003).
13. Cui, J., Shen, Y. & Li, R. Estrogen synthesis and signaling pathways during aging: from periphery to brain. Trends Mol. Med. 19, 197–209 (2013).
14. Okeigwe, I. & Kuohung, W. 5-Alpha reductase deficiency: A 40-year retrospective review. Curr. Opin. Endocrinol. Diabetes Obes. 21, 483–487 (2014).
15. Germain, P., Staels, B., Dacquet, C., Spedding, M. & Laudet, V. Overview of nomenclature of nuclear receptors. Pharmacol. Rev. 58, 685–704 (2006).
16. Huang, P., Chandra, V. & Rastinejad, F. Structural Overview of the Nuclear Receptor Superfamily: Insights into Physiology and Therapeutics. Annu. Rev. Physiol. 72, 247–272 (2010).
17. Rastinejad, F., Huang, P., Chandra, V. & Khorasanizadeh, S. Understanding nuclear receptor form and function using structural biology. J. Mol. Endocrinol. 51, T1–T21 (2013).
18. Wagner, R. L. *et al*. A structural role for hormone in the thyroid hormone receptor. Nature 378, 690–697 (1995).
19. Renaud, J.-P. *et al*. Crystal structure of the RAR-γ ligand-binding domain bound to all-trans retinoic acid. Nature 378, 681–689 (1995).
20. Brzozowski, A. M. *et al*. Molecular basis of agonism and antagonism in the oestrogen receptor. Nature 389, 753–758 (1997).
21. Bourguet, W., Ruff, M., Chambon, P., Gronemeyer, H. & Moras, D. Crystal structure of the ligand-binding domain of the human nuclear receptor RXR-α. Nature 375, 377–382 (1995).
22. Khorasanizadeh, S. & Rastinejad, F. Visualizing the architectures and interactions of

nuclear receptors. Endocrinology 157, 4212–4221 (2016).

23. Mueck, A. O., Ruan, X., Seeger, H., Fehm, T. & Neubauer, H. Genomic and non-genomic actions of progestogens in the breast. J. Steroid Biochem. Mol. Biol. 142, 62–67 (2014).
24. Contrò, V., R. Basile, J. & Proia, P. Sex steroid hormone receptors, their ligands, and nuclear and non-nuclear pathways. AIMS Mol. Sci. 2, 294–310 (2015).
25. Mani, S., Mermelstein, P., Tetel, M. & Anesetti, G. Convergence of Multiple Mechanisms of Steroid Hormone Action. Horm. Metab. Res. 44, 569–576 (2012).
26. Dooley, R., Harvey, B. J. & Thomas, W. Non-genomic actions of aldosterone: From receptors and signals to membrane targets. Mol. Cell. Endocrinol. 350, 223–234 (2012).
27. Quaynor, S. D. *et al*. Delayed Puberty and Estrogen Resistance in a Woman with Estrogen Receptor α Variant. N. Engl. J. Med. 369, 164–171 (2013).
28. Smith, E. P. *et al*. Estrogen Resistance Caused by a Mutation in the Estrogen-Receptor Gene in a Man. N. Engl. J. Med. 331, 1056–1061 (1994).
29. Bouligand, J. *et al*. Familial glucocorticoid receptor haploinsufficiency by non-sense mediated mRNA decay, adrenal hyperplasia and apparent mineralocorticoid excess. PLoS One 5, 1–9 (2010).
30. Charmandari, E., Kino, T., Ichijo, T. & Chrousos, G. P. Generalized glucocorticoid resistance: Clinical aspects, molecular mechanisms, and implications of a rare genetic disorder. J. Clin. Endocrinol. Metab. 93, 1563–1572 (2008).
31. Nicolaides, N. C. & Charmandari, E. Chrousos syndrome: From molecular pathogenesis to therapeutic management. Eur. J. Clin. Invest. 45, 504–514 (2015).
32. Zennaro, M. C. & Lombès, M. Mineralocorticoid resistance. Trends Endocrinol.

Metab. 15, 264–270 (2004).

33. Geller, D. S. Mineralocorticoid resistance. Clin. Endocrinol. (Oxf). 62, 513–520 (2005).
34. Infante, J. B., Alvelos, M. I., Bastos, M., Carrilho, F. & Lemos, M. C. Complete androgen insensitivity syndrome caused by a novel splice donor site mutation and activation of a cryptic splice donor site in the androgen receptor gene. J. Steroid Biochem. Mol. Biol. 155, 63–66 (2016).
35. Brinkmann, A. O. Molecular basis of androgen insensitivity. Mol. Cell. Endocrinol. 179, 105–109 (2001).
36. Bulun, S. E. *et al*. Progesterone resistance in endometriosis: Link to failure to metabolize estradiol. Mol. Cell. Endocrinol. 248, 94–103 (2006).
37. Li, X., Feng, Y., Lin, J. F., Billig, H. & Shao, R. Endometrial progesterone resistance and PCOS. J. Biomed. Sci. 21, 1–7 (2014).
38. Bernard, V. *et al*. Familial multiplicity of estrogen insensitivity associated with a loss-of-function ESR1 mutation. J. Clin. Endocrinol. Metab. 102, 93–99 (2017).
39. Vitellius, G. *et al*. Three Novel Heterozygous Point Mutations of NR3C1 Causing Glucocorticoid Resistance. Hum. Mutat. 37, 794–803 (2016).
40. Forest, D. et al. RNA expression in a cartilaginous fish cell line reveals ancient 3' noncoding regions highly conserved in vertebrates. Proc. Natl. Acad. Sci. U. S. A. 104, 1224–1229 (2007).
41. Gottlieb, B., Beitel, L. K., Nadarajah, A., Paliouras, M. & Trifiro, M. The androgen receptor gene mutations database: 2012 update. Hum. Mutat. 33, 887–894 (2012).
42. Nelson, J. S., Grande, T. C. & Wilson, M. V. H. Fishes of the World. (John Wiley & Sons Inc., 2016).

43. Proietti, C. J., Cenciarini, M. E. & Elizalde, P. V. Revisiting progesterone receptor (PR) actions in breast cancer: Insights into PR repressive functions. Steroids 133, 75–81 (2018).
44. Grindstad, T. *et al*. Progesterone Receptors in Prostate Cancer: Progesterone receptor B is the isoform associated with disease progression. Sci. Rep. 8, 11358 (2018).
45. Jacobsen, B. M. & Horwitz, K. B. Progesterone receptors, their isoforms and progesterone regulated transcription. Mol. Cell. Endocrinol. 357, 18–29 (2012).
46. Oka, K. *et al*. Allosteric role of the amino-terminal A/B domain on corticosteroid transactivation of gar and human glucocorticoid receptors. J. Steroid Biochem. Mol. Biol. 154, 112–119 (2015).
47. Katsu, Y., Oka, K. & Baker, M. E. Evolution of human, chicken, alligator, frog, and zebrafish mineralocorticoid receptors: Allosteric influence on steroid specificity. Sci. Signal. 11, eaao1520 (2018).
48. Katsu, Y., Kohno, S., Oka, K. & Baker, M. E. Evolution of corticosteroid specificity for human, chicken, alligator and frog glucocorticoid receptors. Steroids 113, 38–45 (2016).
49. Saitou, N. & Nei, M. The neighbor-joining method: a new method for reconstructing phylogenetic trees. Mol. Biol. Evol. 4, 406–425 (1987).
50. Kumar, S., Stecher, G. & Tamura, K. MEGA7: Molecular Evolutionary Genetics Analysis Version 7.0 for Bigger Datasets. Mol. Biol. Evol. 33, 1870–1874 (2016).
51. Jones, D. T., Taylor, W. R. & Thornton, J. M. The rapid generation of mutation data matrices from protein sequences. Comput. Appl. Biosci. 8, 275–82 (1992).
52. Felsenstein, J. Confidence limits on phylogenies: an approach using the bootstrap. Evolution. 39, 783-791 (1985).

53. Li, B. & Dewey, C. N. RSEM: accurate transcript quantification from RNA-Seq data with or without a reference genome. BMC Bioinformatics 12, 323 (2011).
54. Langmead, B. & Salzberg, S. L. Fast gapped-read alignment with Bowtie 2. Nat. Methods 9, 357–359 (2012).
55. Sandor, T., Lehoux, J.-G. & Mehdi, A. Z. Comparative enzymology of steroid-hydroxylating enzyme systems of nonmammalian vertebrate adrenal tissue. Gen. Comp. Endocrinol. 3, 279–288 (1972).
56. Zhang, Y. *et al*. The White-Spotted Bamboo Shark Genome Reveals Chromosome Rearrangements and Fast-Evolving Immune Genes of Cartilaginous Fish. iScience vol. 23 (Elsevier Inc., 2020).
57. Najafpour, B., Cardoso, J. C. R., Canário, A. V. M. & Power, D. M. Specific Evolution and Gene Family Expansion of Complement 3 and Regulatory Factor H in Fish. Front. Immunol. 11, (2020).
58. Dale, S. L., Chattoraj, S. C., Biswas, A., Gajewski, A. & Nuzzo, P. Identification of 19-norprogesterone in pregnant rat urine. Steroids 56, 472–476 (1991).
59. Gomez-Sanchez, C. E., Gomez-Sanchez, E. P., Shackleton, C. H. L. & Milewich, L. Identification of 19-Hydroxydeoxycorticosterone, 19-Oxo-deoxycorticosterone, and 19-Oic-deoxycorticosterone as products of deoxycorticosterone metabolism by rat adrenals. Endocrinology 110, 384–389 (1982).
60. Awruch, C. A. Reproductive endocrinology in chondrichthyans: The present and the future. Gen. Comp. Endocrinol. 192, 60–70 (2013).
61. Benhamou, B. *et al*. A single amino acid that determines the sensitivity of progesterone receptors to RU486. Science. 255, 206–209 (1992).
62. Baker, M. E. & Uh, K. Y. Evolutionary analysis of the segment from helix 3 through

helix 5 in vertebrate progesterone receptors. J. Steroid Biochem. Mol. Biol. 132, 32–40 (2012).

63. Williams, S. P. & Sigler, P. B. Atomic structure of progesterone complexed with its receptor. Nature 393, 392–396 (1998).
64. Zhang, J., Simisky, J., Tsai, F. T. F. & Geller, D. S. A critical role of helix 3-helix 5 interaction in steroid hormone receptor function. Proc. Natl. Acad. Sci. 102, 2707–2712 (2005).
65. Geller, D. S. Activating Mineralocorticoid Receptor Mutation in Hypertension Exacerbated by Pregnancy. Science. 289, 119–123 (2000).
66. Rafestin-Oblin, M.-E. *et al*. The Severe Form of Hypertension Caused by the Activating S810L Mutation in the Mineralocorticoid Receptor Is Cortisone Related. Endocrinology 144, 528–533 (2003).
67. Huyet, J., Pinon, G. M., Fay, M. R., Fagart, J. & Rafestin-Oblin, M.-E. Structural Basis of Spirolactone Recognition by the Mineralocorticoid Receptor. Mol. Pharmacol. 72, 563–571 (2007).
68. Guex, N. & Peitsch, M. C. SWISS-MODEL and the Swiss-Pdb Viewer: An environment for comparative protein modeling. Electrophoresis 18, 2714–2723 (1997).
69. Bertoni, M., Kiefer, F., Biasini, M., Bordoli, L. & Schwede, T. Modeling protein quaternary structure of homo- and hetero-oligomers beyond binary interactions by homology. Sci. Rep. 7, 1–15 (2017).
70. Studer, G. *et al*. QMEANDisCo—distance constraints applied on model quality estimation. Bioinformatics 36, 1765–1771 (2020).
71. Guex, N., Peitsch, M. C. & Schwede, T. Automated comparative protein structure

modeling with SWISS-MODEL and Swiss-PdbViewer: A historical perspective. Electrophoresis 30, S162–S173 (2009).

72. Waterhouse, A. *et al*. SWISS-MODEL: Homology modelling of protein structures and complexes. Nucleic Acids Res. 46, W296–W303 (2018).
73. Bienert, S. *et al*. The SWISS-MODEL Repository—new features and functionality. Nucleic Acids Res. 45, D313–D319 (2017).
74. Trott, O. & Olson, A. J. AutoDock Vina: Improving the speed and accuracy of docking with a new scoring function, efficient optimization, and multithreading. J. Comput. Chem. 31, (2009).
75. Páll, S., Abraham, M. J., Kutzner, C., Hess, B. & Lindahl, E. Tackling Exascale Software Challenges in Molecular Dynamics Simulations with GROMACS. in 3–27 (2015).
76. Hess, B., Kutzner, C., van der Spoel, D. & Lindahl, E. GROMACS 4: Algorithms for Highly Efficient, Load-Balanced, and Scalable Molecular Simulation. J. Chem. Theory Comput. 4, 435–447 (2008).
77. Berendsen, H. J. C., van der Spoel, D. & van Drunen, R. GROMACS: A message-passing parallel molecular dynamics implementation. Comput. Phys. Commun. 91, 43–56 (1995).
78. Pronk, S. *et al*. GROMACS 4.5: a high-throughput and highly parallel open source molecular simulation toolkit. Bioinformatics 29, 845–854 (2013).
79. Van Der Spoel, D. *et al*. GROMACS: Fast, flexible, and free. J. Comput. Chem. 26, 1701–1718 (2005).
80. Lindahl, E., Hess, B. & van der Spoel, D. GROMACS 3.0: a package for molecular simulation and trajectory analysis. J. Mol. Model. 7, 306–317 (2001).

81. Abraham, M. J. *et al*. GROMACS: High performance molecular simulations through multi-level parallelism from laptops to supercomputers. SoftwareX 1–2, 19–25 (2015).

82. Vanommeslaeghe, K. *et al*. CHARMM general force field: A force field for drug-like molecules compatible with the CHARMM all-atom additive biological force fields. J. Comput. Chem. 31, NA-NA (2009).

83. Brooks, B. R. *et al*. CHARMM: The biomolecular simulation program. J. Comput. Chem. 30, 1545–1614 (2009).

84. Yu, W., He, X., Vanommeslaeghe, K. & MacKerell, A. D. Extension of the CHARMM general force field to sulfonyl-containing compounds and its utility in biomolecular simulations. J. Comput. Chem. 33, 2451–2468 (2012).

85. Leo, C. & Chen, J. D. The SRC family of nuclear receptor coactivators. Gene 245, 1–11 (2000).

86. Ramos, N. & Lombès, M. Résistances aux hormones stéroïdes: physiologie et pathologie. Ann. Endocrinol. (Paris). 77, S1–S10 (2016).

87. Nunez, B. S. & Trant, J. M. Characterization of adrenal cytochrome P450c21 from the blacktip shark (Carcharhinus limbatus). J. Exp. Zool. 272, 291–298 (1995).

88. 88. Parton, A. et al. Cell and molecular biology of SAE, a cell line from the spiny dogfish shark, Squalus acanthias. Comp. Biochem. Physiol. - C Toxicol. Pharmacol. 145, 111–119 (2007).

89. Poyer, J. C. & Hartmann, J. X. Establishment of a cell line from brain tissue of the silky shark, Carcharhinus falciformis. Vitr. Cell. Dev. Biol. - Anim. 28, 682–684 (1992).

90. Duff, M. O. et al. Genome-wide identification of zero nucleotide recursive splicing

in Drosophila. Nature 521, 376–379 (2015).

91. Hutchinson, K. A., Matić, G., Czar, M. J. & Pratt, W. B. DNA-binding and non-DNA-binding forms of the transformed glucocorticoid receptor. J. Steroid Biochem. Mol. Biol. 41, 715–718 (1992).

92. Kauppi, B. et al. The three-dimensional structures of antagonistic and agonistic forms of the glucocorticoid receptor ligand-binding domain: RU-486 induces a transconformation that leads to active antagonism. J. Biol. Chem. 278, 22748–22754 (2003).